Ecological Monographs, 66(1), 1996, pp. 1–43

FOREST MODELS DEFINED BY FIELD MEASUREMENTS: ESTIMATION, ERROR ANALYSIS AND DYNAMICS[1]

STEPHEN W. PACALA
Department of Ecology and Evolutionary Biology, Princeton University, Princeton, New Jersey 08544 USA

CHARLES D. CANHAM
Institute of Ecosystem Studies, Millbrook, New York 12454 USA

JOHN SAPONARA
Department of Ecology and Evolutionary Biology, Princeton University, Princeton, New Jersey 08544 USA

JOHN A. SILANDER JR., RICHARD K. KOBE, AND ERIC RIBBENS
Department of Ecology and Evolutionary Biology, The University of Connecticut, Storrs, Connecticut 06268 USA

Abstract. A spatial and mechanistic model is developed for the dynamics of transition oak–northern hardwoods forests in northeastern North America. The purpose of the model is to extrapolate from measurable fine-scale and short-term interactions among individual trees to large-scale and long-term dynamics of forest communities. Field methods, statistical estimators, and model structure were designed simultaneously to ensure that parameters could be estimated from data collected in the field.

This paper documents eight aspects of a three-year study to calibrate, test, and analyze the model for the nine dominant and subdominant tree species in transition oak–northern hardwoods forests:

1) Design and structure of the model. The model makes population dynamic forecasts by predicting the fate of every individual tree throughout its life. Species-specific functions predict each tree's dispersal, establishment, growth, mortality, and fecundity. Trees occupy unique spatial positions, and individual performance is affected by the local availability of resources. Competition is mechanistic; resources available to each tree are reduced by neighbors. Although the model was developed to include light, water, and nitrogen, the version described here includes only competition for light (shading and light-dependent performance) because the field data provide little evidence of competition for nitrogen and water over the range of sites examined.

2) Estimates of the model's parameters for each species. The estimates reveal a variety of "strategic trade-offs" among the species. For example, species that grow quickly under high light tend to cast relatively little shade, have low survivorship under low light, and have high dispersal. In contrast, species that grow slowly under high light tend to cast relatively dark shade, and to have high survivorship under low light and low dispersal. These trade-offs define one of two dominant "axes" of strategic variation.

3) Community level predictions of the model. The model predicts succession from early dominance by species such as *Quercus rubra* and *Prunus serotina,* to late dominance by *Fagus grandifolia* and *Tsuga canadensis,* with *Betula alleganiensis* present as a gap phase species in old-growth stands. The model also predicts that old-growth communities will have intraspecifically clumped and interspecifically segregated spatial distributions.

4) An error analysis that identifies community level predictions that are robust given the level of sampling uncertainty in the study. This analysis translates the statistical uncertainty associated with each parameter estimate into statistical uncertainty in the model's predictions. The robust predictions include those mentioned in aspect (3) above.

5) Sensitivity of the model to changes in initial conditions and to changes in the three parameters not included in the error analysis. For example, the model predicts that initial abundances continue to affect community composition well into succession (>300 yr for some species).

6) Tests of the system- and community-level predictions of the model against independent data gleaned from other studies. These tests support the predictions found to be robust in the error analysis, including those predictions mentioned in aspect (3) above.

[1] Manuscript received 10 August 1994; revised 22 January 1995; accepted 30 January 1995; final version received 17 March 1995.

7) Modeling experiments that determine which aspects of individual performance and inter-neighbor competition are responsible for each of the robust predictions identified in aspect (4) above and tested in aspect (6) above. This analysis reveals a wide variety of causal relationships, with most parameters contributing to at least one community level phenomenon.

8) An explanation of the diversity of individual level causes identified in aspect (7). The two "axes" describing most of the strategic variation among the species (see [2]), provide a simple explanation of community level pattern in terms of individual level processes.

Key words: error analysis; forest dynamics; interspecific trade-offs; sapling growth and mortality; seedling recruitment; sensitivity analysis; SORTIE; spatially-explicit models; species-specific light extinction.

Introduction

Following explosive growth during the 1960s and 1970s, community ecology entered a difficult period in the 1980s. The pioneering work of theoreticians such as Robert MacArthur and Robert May in defining the important issues was replaced by widespread uncertainty about the connection between simple models and available data (Connor and Simberloff 1979, Connell 1980, Simberloff and Boecklin 1981, Strong and Simberloff 1981). Paradoxically, this uncertainty caused waning interest in community ecology, and yet catalyzed significant advances in physiological, population, and ecosystem ecology.

During the 1980s, physiological, population, and ecosystem ecologists tightened the coupling between empirical studies and models. Their achievements include a useful and highly developed theory of multiple resource limitation and plant performance (i.e., Landsberg 1986, Chapin et al. 1987, Gross 1989, Mooney 1991), explanatory and predictive population dynamic models of host–parasite systems (i.e., Anderson and May 1991), intertidal invertebrates (i.e., Roughgarden et al. 1985, 1988), and dispersing animals (i.e., Kareiva 1984, Kareiva and Odell 1987, Kareiva and Anderson 1988), and predictive ecosystem models of carbon and nitrogen dynamics that perform well at local, regional, and global scales (i.e., Parton et al. 1987, 1988, 1993, Potter et al. 1993).

In contrast, community ecologists were faced with a seemingly intractable methodological problem. How does one develop a minimal model of a community from data when the number of interspecific interactions grows as the square of the number of species? Tilman (1982) recognized that mechanistic (resource-based) models offered a possible resolution to this problem, because the number of parameters in a mechanistic model grows only linearly with the number of species. Over the next 10 yr, he and his colleagues mounted an extensive effort to develop simple mechanistic models of terrestrial vegetation and to test insights from these in a nitrogen-limited community of herbaceous species (i.e., Tilman 1987, 1993, Inouye and Tilman 1988, Wedin and Tilman 1990, Tilman and Wedin 1991, Gleeson and Tilman 1992). Their success demonstrates that an integrated program of modeling and empirical work can yield the same dividends to community ecology as it has to the other ecological sub-disciplines. The community dynamics predicted by Tilman's uncalibrated models have generally been tested through direct observation of the dynamics of experimentally-manipulated communities. However, this effectively limits application of the approach to communities with rapid dynamics.

Most plant communities have dynamics that are slow relative to the lifetime of an investigator, let alone the lifetime of a typical research grant. Forest succession takes hundreds of years and yet forests dominate the terrestrial biosphere (e.g., majority of primary productivity and biomass). In studies of communities with slow dynamics, models can do more than supply insights. Models provide the means to extrapolate from the short-term and small-scale measurements that are possible in the field, to the long-term and large-scale dynamics of interest. Of course, models used to scale-up empirical measurements must be calibrated by the measurements, and must contain sufficient biological realism to capture the critical features of the system under study. Moreover, such models must remain relatively simple if they are to be analyzed and understood. This leaves us with three, sometimes conflicting, design criteria: simplicity, observability, and biological realism.

In this paper, we report results of three years of field work and modeling of transition oak–northern hardwoods forests in northeastern North America. The overall goal of the study was to understand the processes controlling the structure and dynamics of the tree community across the range of spatial and temporal scales from the few square metres relevant to interactions among competing individuals to the hundreds of hectares relevant to community dynamics, and from the small number of years of empirical inquiry to the hundreds of years that characterize dynamics. An unusual feature of the study is that field methods, statistical estimators, and models were designed *simultaneously,* in an attempt to optimize jointly the three design criteria. The model is spatial and mechanistic. Individual trees occupy unique spatial positions and compete by depleting resources of neighbors. The model makes population dynamic forecasts by predicting the birth, dispersal, growth, survivorship, and repro-

duction of every individual in the community using simple submodels that are defined by data collected in the field.

This paper documents the following eight features of the study:

1) Design and structure of the model.

2) Estimates of the model's parameters for the nine dominant tree species in the system together with an overview of the empirical and statistical methods used to obtain these.

3) Community level predictions of the model in the "baseline" case of no disturbance except for the single-tree gaps created by random adult mortality (cases involving more extreme disturbance will be treated elsewhere).

4) An error analysis that translates sampling uncertainty about parameter estimates into uncertainty about the model's community level predictions. This analysis identifies predictions about community dynamics and structure that are robust given the level of sampling uncertainty in the study.

5) A sensitivity analysis evaluating the sensitivity of the model's predictions to changes in the values of the relatively few parameters not included in the error analysis.

6) Comparison of the robust predictions identified in (4) to published data on community composition and dynamics.

7) Modeling experiments that determine which aspect(s) of individual performance and inter-individual interactions cause each of the robust community level predictions identified in (4) and tested in (6).

8) Documentation of interspecific trade-offs among the different aspects of performance that provide a simple explanation for the diversity of results obtained in (7).

In addition, we compare the conclusions of the study to published views about the dynamics and structure of forest communities and the relationship of our model to the widely studied JABOWA-FORET forest simulation models (e.g., Shugart 1984, Botkin 1992).

Previous papers (Canham et al. 1994, Ribbens et al. 1994, Kobe et al. 1995, Pacala et al. 1995) describe, in detail, the data and methods used to estimate the components of the model and report estimates. We include an overview of this work here because of the close coupling between the model and data—an understanding of the model requires an understanding of the underlying data. We have also published a preliminary report (Pacala et al. 1993) on (2) and (3), but for a subset of the nine species, an early version of the model, and a small number of small-scale runs.

METHODS

Study sites and species

The primary study sites are located in and around Great Mountain Forest (GMF) in northwestern Connecticut (41°57′ N, 73°15′ W) at elevations of 450–510 m. These sites contain second-growth stands that are predominantly 80–120 yr in age, and are found on sandy, acidic inceptisols and spodsols on glacial till derived from schist/gneiss bedrock. Data were collected in 1990, 1991, and 1992.

The nine species described in this paper include all of the dominant and subdominant species found in mid- and late-successional stands in our study sites. The species are (in roughly decreasing order of a traditional classification of shade tolerance; Baker 1949): *Fagus grandifolia* Ehrh. (beech, Be), *Tsuga canadensis* (L.) Carr. (eastern hemlock, Hm), *Acer saccharum* Marsh. (suger maple, SM), *Acer rubrum* L. (red maple, RM), *Betula alleghaniensis* (yellow birch, YB), *Pinus strobus* L. (white pine, WP), *Quercus rubra* L.(red oak, RO), *Prunus serotina* Ehrh. (black cherry, BC), and *Fraxinus americana* L. (white ash, WA).

Design and structure of the model SORTIE

The model SORTIE contains a record of every individual's diameter (at 10 cm height), species identity, and x- and y-coordinates, and uses four submodels to determine the fate of each individual throughout its life. Although we originally developed the model and field methods to consider three resources (light, water, and nitrogen), light is the only resource included in the version described in this paper.

Rationale for including only light limitation.—Our field data show little evidence of limitation of seedling and sapling growth by water or nitrogen. Pacala et al. (1995) showed that growth of naturally established saplings was significantly related to light availability (assessed by fish-eye photography), but not to whole-season soil moisture. A. C. Finzi and C. D. Canham (*unpublished manuscript*) show that sapling growth is not related to net nitrogen mineralization rates, and that nitrogen mineralization rates are not correlated with light availability in natural vegetation, indicating that light was not a surrogate for nitrogen mineralization rate in the Pacala et al. (1995) study. We have also performed a 3-yr experiment (C. D. Canham, J. D. Hill, and A. F. Finzi, *unpublished manuscript*) in which we planted six species of tree seedlings in a full factorial combination of (1) trenching to eliminate uptake of water and nutrients by surrounding vegetation, and (2) clipping of surrounding herbaceous vegetation. Trenching had no significant effect on seedling growth or survival. Collectively, these results provide strong evidence of light limitation, but very little evidence of water or nitrogen limitation in our study sites. We recognize that both nitrogen and water are thought to be limiting resources in northeastern forests (e.g., Rastetter et al. 1991), and anticipate that we would observe effects of both resources in a study encompassing a broader range of sites and/or years.

Resource submodel.—The resource submodel calculates the light available to an individual from char-

acteristics of the individual's neighborhood. It consists of four parts: (1) species-specific equations relating tree height, crown diameter, and crown depth to stem diameter that are used to construct cylindrical crowns for each of the modeled trees, saplings, and seedlings, (2) species-specific light extinction coefficients that determine the attenuation of light as it passes through a crown, (3) a spatial distribution of sky brightness that accounts for the diurnal and seasonal movements of the sun throughout the growing season at the latitude of our sites, and (4) the mix of diffuse and beam radiation in our sites. These attributes are used to compute a measure of whole-season photosynthetically active radiation (in units of percentage of full sun) at the top of each individual's crown. The measure (global light index [GLI]; Canham 1988*a*) is calculated in the model in exactly the same way as it is obtained in the field—by digitizing a fish-eye photograph taken above the individual.

The algorithm for taking fish-eye photographs in the model is highly optimized because >90% of the computation time is devoted to this task. Briefly, an efficient sorting routine identifies all neighbors within a fish-eye photograph (restricted to zenith angles within 45° of vertical because very little illumination comes from angles closer to the horizon [Canham et al. 1990]). The algorithm then determines the suite of zenith and azimuth angles that are blocked by each neighbor's crown and uses the species-specific light extinction coefficients to determine how much light is intercepted at each angle. It thus assembles, neighbor by neighbor, a table of the fraction of light remaining at each zenith and azimuth angle. Each element in the table is then multiplied by the corresponding element in the distribution of sky brightness, and the results are summed to yield GLI. The neighbor-by-neighbor calculation of GLI is many orders of magnitude more efficient than the angle-by-angle alternative (in which neighbors intercepted by an angle are identified separately for each angle). Fish-eye photographs were partitioned into 720 pixels representing unique combinations of zenith and azimuth angles in all runs described in this paper (20 zenith and 36 azimuth angles). A preliminary analysis of the model showed no difference among runs with greater than 10 zenith and greater than 18 azimuth angles.

We selected this resource submodel rather than a simpler alternative, such as Beer's Law, because numerous studies have established that understory plants are affected critically by non-vertical shading and illumination. For example, in temperate latitudes, a gap 15 m north of a sapling has virtually no effect on the plant, but a gap 15 m south may have a dramatic effect (Canham 1988*b*, Canham et al. 1990). Very little light comes from within 10° of vertical in our sites simply because the sun is never located within this region of the sky. We use GLI in the field because it assesses the critical non-vertical shading and illumination. The model must also use GLI if it is to extrapolate from field measurements.

Growth submodels.—The growth submodels consist of species-specific equations that predict radial growth from diameter and GLI. Diameter is included as an independent variable simply because trees grow geometrically when small (annual diameter growth increases linearly with diameter), and grow progressively slower than geometrically as they become large (Pacala et al. 1995). Obviously, GLI is included because of light limitation.

Mortality submodels.—The mortality submodels include an equation for each species that gives an individual's probability of mortality as a function of its rate of growth over the previous five years. The rationale behind these functions is that growth reflects carbon balance, and carbon balance determines mortality (Kobe et al. 1995). Thus, the unfavorable carbon balance of heavily shaded understory plants (reflected in their slow growth) increases their risk of starvation and reduces their ability to withstand stresses such as disease, herbivory, and unfavorable weather. Similar functions have been shown to predict mortality in previous studies (reviewed in Kobe et al. 1995). It is important to understand that processes such as herbivory, predation, and disease are not included explicitly in this version of the model. Thus, the model does not include any density-dependent regulation of community structure caused by these agents (e.g., Janzen 1970, Connell 1971).

The mortality submodels also include purely random disturbance. Each individual has a constant probability of dying from density independent factors, in addition to its growth-dependent mortality. Individuals that die leave single tree gaps; we do not include severe disturbances such as windthrow or fire in runs described in this paper.

Recruitment submodels.—The recruitment submodels consist of species-specific equations that predict the number and spatial locations of seedlings produced by a maternal tree as a function of the tree's size (diameter) and location. The function determining the spatial locations of a tree's progeny is a radially symmetric probability density centered on the tree (with a different such function for each species of tree). It gives the probability that each seedling will disperse to any location given the coordinates of the maternal tree. This version of the model does not include safe sites for germination or spatially variable survivorship of seeds. All spatial heterogeneity in the distribution of new seedlings is the result of spatial heterogeneity in fecundity and finite dispersal.

The community level model SORTIE.—A run of the community level model proceeds from an initial condition consisting of the location, species identity, and size of each individual. Unless otherwise stated, individuals present at the start of a run are assigned positions at random. The modeled plot is wrapped onto

a torus to avoid edge effects. Each iteration has a duration of 5 yr (forecasts the state of the forest 5 yr into the future). Experiments with intervals of 2.5 and 1 yr produced results indistinguishable from 5 yr. At the beginning of an iteration, SORTIE computes a GLI for each seedling, sapling, and adult. SORTIE then computes each plant's growth rate from its GLI and diameter using the appropriate species-specific growth submodel. Competition occurs whenever individuals are shaded by taller neighbors. Following growth, SORTIE calculates each individual's probability of mortality from its growth rate, using the mortality submodels. Pseudorandom coin tosses determine which plants are killed. Finally, SORTIE uses the recruitment submodels to determine the number and spatial positions of all new recruits produced by every tree. Each recruit's spatial position is drawn randomly from the dispersal function centered on its mother. This completes one iteration. By repeated iterations, SORTIE forecasts long-term changes in the abundance, age and size structure, and spatial distribution of all species.

The algorithm is implemented in C and versions run on UNIX workstations, personal computers and supercomputers. The UNIX version includes a graphical interface, written in "X11," that allows one to choose maps of the current state of the plot and graphs summarizing the chronosequence of previous states from a menu while an application is running. Runs covering 1 km^2 and 1000 yr average $\approx$2 d on a fast UNIX workstation. Such runs contain hundreds of thousands of individuals $\geq$5 yr of age at any one time. Experiments with different plot sizes revealed little difference between plots of 9, 25, and 100 ha over a duration of 1000 yr, but greater stochastic variation among plots of 1 ha. Unless otherwise specified, the plot size of runs described in this paper is 9 ha.

In SORTIE, the growth and resource models are deterministic, while the mortality and recruitment submodels are stochastic. Nevertheless, the growth and resource submodels are estimated by regression methods. Like all such methods, these yield both a deterministic function and a probabilistic distribution of the data about the function (a distribution of residuals). For example, the method for the growth submodels yields an equation for radial growth as a function of GLI and radius, and a normal distribution of actual growth about this mean. In this paper, we use the estimated functions as the submodels and omit the stochastic distributions. Thus, all individuals of the same species that share the same GLI and size have the same growth rate in SORTIE. However, in the field, these growth rates would be normally distributed about the value predicted by SORTIE. We thus assume for growth, crown shape, and light transmission, that all individuals sharing identical independent variables will function precisely like the *mean* individual sharing these independent variables in nature. This is a common and often unstated assumption of models and we make it here for the following reason. Residual variation is presumably caused by mechanisms other than those in the version of SORTIE described here. Such mechanisms might include heterogeneous nutrient availability, herbivory, genetic variation among individuals, etc. A principal purpose of the study is to determine if the suite of mechanisms in the model is sufficient to produce pattern observed in nature. The inclusion of additional and unnamed mechanisms as phenomenological noise in the submodels would work against this purpose.

Parameter estimation

Resource submodel.—Regression equations predicting tree height from radius were developed from measurements of 47–125 individuals per species. These individuals ranged in size from 25 cm tall to canopy height and up to 60 cm diameter. The equation for each species was:

$$h = H_1(1 - e^{-(H_2/H_1)2r}), \quad (1)$$

where h is height (in metres), r is radius (in centimetres), H_1 is the asymptotic height, and $2H_2$ is the slope at 0 radius. In addition, we estimated: C_1 = canopy radius (in metres)/stem diameter (in centimetres), and C_2 = canopy depth (in metres)/tree height (in metres), from a subsample of 16–23 individuals per species ranging in diameter from 10 to 60 cm. See Canham et al. (1994) and Pacala et al. (1995) for additional details.

To estimate species-specific light extinction coefficients, Canham et al. (1994) mapped nine circular stands (30–50 m diameter), each dominated by a different species but all containing a mix of the nine species. They used the regression equations described to construct a cylindrical crown for each mapped tree. They took 10 fish-eye photographs at 1 m height in each stand, and 10 additional photographs at heights of 2, 4, 6, and 7.5 m in each of six of the stands. After digitizing the photographs, they divided each into 480 regions representing different zenith and azimuth angles and determined the percentage of sky visible in each region. Consider the ray emanating from the location of a fish-eye photograph and extending through the center of 1 of the 480 regions. Using the reconstructed map of the canopy, Canham et al. (1994) determined the number of crowns and length of crown of each species intercepted by each such ray. After discarding rays that exited the stand below canopy height, they were left with 2782 lines of data, each containing canopy openness (percentage of sky visible in the region) and the numbers and path lengths of each species intercepted.

Finally, Canham et al. (1994) developed a maximum likelihood estimator, based on the β distribution, to regress canopy openness against numbers and path lengths of crowns intercepted. They selected a function based on the numbers of crowns intercepted for use in

SORTIE, rather than path lengths, because the former provided better fits than the latter. The function was:

$$\text{Openness} = e^{-\sum_{i=1}^{9} E_i[\text{Number of crowns of species } i \text{ intercepted}]}, \quad (2)$$

where E_i is the light extinction coefficient for species i. See Canham et al. (1994) for additional details about the method, including the alternative functions examined, a discussion of the role of sun flecks and beam enrichment, and a validation of the method involving a comparison of predicted GLI's, actual GLI's, and direct measures of photosynthetically active radiation obtained from quantum sensors.

Growth submodels.—to estimate the growth submodels, Pacala et al. (1995) took fish-eye photographs above 570 saplings in midsummer (range of 49–110 saplings per species), and then harvested these after leaf fall in late October and November. The saplings ranged in stem radius from 2 to 50 mm (at 10 cm height) and in height from 15 to 750 cm. They measured soil moisture (gravimetrically in September for five species and on a series of dates with time domain reflectometry for four) at the base of each sapling and radial (most recent five annual growth increments with a computerized tree ring measuring device) and extension growth. After an extensive regression analysis detailed in Pacala et al. (1995), they estimated the following radial growth function for each species:

$$\text{Annual Radial Increment} = \text{Radius}\frac{G_1\text{GLI}}{\frac{G_1}{G_2} + \text{GLI}}, \quad (3)$$

where G_1 is the asymptotic growth rate at high light and G_2 is the slope at 0 light.

Although Pacala et al. (1995) show that saplings ≤750 cm in height grow geometrically as in Eq. 3 (note that radial growth is proportional to radius), this relationship clearly does not extend to canopy trees. The current version of SORTIE thus assumes the Constant Area Increment Law (as in Phipps 1967). The cross-sectional area of a growth ring cannot exceed a constant G_3, and radial growth is given by the smaller of the ring widths predicted by Eq. 3 and the Constant Area Increment Law. Although we went to considerable lengths to estimate G_1 and G_2, we did not measure the radial growth of canopy trees during the study, but rather obtained G_3 from the literature (Teck and Hilt 1991). We focused the sampling on seedling and sapling growth because an individual's success at reaching the canopy depends largely on its performance as a sapling (Canham 1988*a*, Clark and Clark 1992). Unless stated otherwise, the value of G_3 in all runs corresponds to an annual radial increment of 1.5 mm for a tree 100 cm in diameter. However, we also report results for a range of values of G_3 to document the sensitivity of the model's behavior to changes in this parameter.

Mortality submodels.—The most direct way to measure the probability of mortality as a function of growth rate is to measure the growth of a sample of saplings and then wait to determine which live and die over some subsequent interval. One can then perform a simple Bernouli regression. However, because saplings in the understory may have very low death rates (e.g., suppressed hemlock saplings may live for 100 years), this direct approach requires either an enormous sample, a long interval of time, or a restriction to species or stages (e.g., seedlings) that die rapidly (see Monserud 1976, Buchman 1983, Buchman and Lentz 1984, Hamilton 1986, 1990, for examples).

For this reason, Kobe et al. (1995) developed an alternative that requires considerably less sampling effort. The following data were collected from a site for each species: 5-yr average radial growth rates for each of 30–60 standing dead and 30–60 live saplings, and a count of live and standing dead saplings along transects. Twig suppleness characters were used to restrict the sampling of dead individuals to those that had died within the previous 22–33 mo (see Kobe et al. 1995 for details). Saplings were defined as individuals >25 cm in height and lacking any foliage reaching the canopy (6, 8, or 10 cm diameter depending on the stand).

Suppose that $m(g)$ is the probability of mortality for a sapling with 5-yr average growth rate g. If mortality increases as g decreases, then a sample of dead individuals will contain more low values of g than a sample of live individuals. Let $f(g)$ be the distribution of sapling growth rates. Then the distribution (probability density) of growth rates for dead individuals is:

$$f_d(g) = \frac{m(g)f(g)}{\int_{-\infty}^{\infty} m(g)f(g)\,dg}, \quad (4)$$

and the distribution of live individuals is:

$$f_a(g) = \frac{[1 - m(g)]f(g)}{\int_{-\infty}^{\infty} [1 - m(g)]f(g)\,dg}. \quad (5)$$

Kobe et al. (1995) derived a maximum likelihood estimator based on the conditional densities (Eqs. 4 and 5) and the binomial distribution (for the transect data), and used this to estimate the parameters of $f(g)$ and $m(g)$ for each species. The method works by finding the mortality function that best reshapes the growth distribution, $f(g)$, into the growth distributions of dead and live saplings (Eqs. 4 and 5). Monte Carlo studies with simulated data showed that the method is approximately non-biased, despite its non-standard nature and despite the use of growth as a surrogate for carbon balance—the independent variable hypothesized to control competitive mortality in nature. Moreover, Kobe et al. (1995) obtained similar estimates for sites in Michigan and Connecticut, indicating that the relationship between growth and mortality is geographically consistent.

After considering a number of alternatives, including dependence of m on both size and growth, and growth averages over intervals other than 5 yr, Kobe et al. (1995) selected a γ-density for $f(g)$ and the exponential mortality function:

$$m(g) = M_1 e^{-M_2 g}. \quad (6)$$

Because a sapling's radial growth increases with its size if light is held constant (Eq. 3), growth-dependent mortality in SORTIE generally decreases with sapling size. Also, because the probability of mortality given by Eq. 6 corresponds to a period of ≈2.5 yr, this function is applied twice during each 5-yr iteration of SORTIE (recall that the twig suppleness character restricted sampling to individuals that died within ≈2.5 yr).

Runs described in this paper correspond to a baseline scenario of low disturbance. Each individual has a constant annual probability of mortality of 0.01 in addition to the growth-dependent mortality specified by Eq. 6. This additional mortality yields an average gap-to-gap interval (100 yr) representative of natural low-disturbance stands (e.g., Runkle 1985).

Together, the growth function (Eq. 3) and mortality function (Eq. 6) capture mortality of saplings caused by shading. Canopy trees growing in full sun generally have growth rates large enough to make $m(g)$ negligible. However, because of the Constant Area Increment Law, very large trees do grow slowly. To prevent mortality characteristic of saplings from affecting these large trees, SORTIE does not implement (Eq. 6) for trees >20 m in height if they are growing in full sun.

Recruitment submodels.—to estimate the recruitment submodels Ribbens et al. (1994) mapped adults >10 cm in diameter in stands totaling >10 ha. They then located 2047 1-m^2 quadrats within these stands and determined the number of new recruits in each (totaling >6000). New recruits were defined as seedlings that had germinated during the current year for all species except for beech and sugar maple. Beech reproduces almost exclusively by root sprouting in GMF, and so beech recruits were defined as sprouts <25 cm in height. Also, because sample sizes of new sugar maple seedlings were inadequate, all sugar maple individuals <25 cm in height were included in the analysis. Finally, the sex of each white ash adult was determined because white ash is dioeceous, and males were excluded from the analysis.

Suppose that the mean density of recruits produced by an adult decreases with distance as:

$$\text{Seedling Density} = \left[R_2\left(\frac{\text{Diameter}}{100}\right)^2\right]\left[\frac{e^{-R_1 \text{Distance}^3}}{N}\right]$$

$$N = \int_0^\infty e^{-R_1 \text{Distance}^3} 2\pi \text{Distance}\, d\text{Distance}, \quad (7)$$

where "Diameter" is the diameter (in centimetres) of the adult, N is a normalizer, R_1 is a constant governing the distance decay of dispersal (inversely related to mean dispersal distance), and R_2 is the number of 5-yr-old recruits produced by an adult 100 cm in diameter. The first term in brackets is the total number of recruits produced as a function of the adult's diameter. The second term in brackets is a dispersal function (probability density) describing the probability that a recruit disperses an amount Distance from its mother in any given direction (assuming equiprobable dispersal in any direction). Thus, if d_{ij} is the distance between the ith adult and the center of the jth 1-m^2 quadrat, then the mean number of seedlings in the quadrat *produced by all adults* is obtained simply by summing Eq. 7 over all adults:

$$\lambda_j = \text{Total Density of Quadrat } j = \sum_{i=1}^{\text{No adults}} R_2\left(\frac{\text{Diameter}_i}{100}\right)^2 \frac{e^{-R_1 d_{ij}^3}}{N}. \quad (8)$$

Ribbens et al. (1994) developed a maximum likelihood estimator in which the mean of a Poisson random variable for the jth quadrat was λ_j, and used this to estimate values of R_1 and R_2 for each species. The method works by finding the values of R_1 and R_2 that bring the recruitment "shadows" of the mapped adults into optimal congruence with the spatial distribution of conspecific recruits. The exponent of 2 in the first bracketed term in Eq. 7 and the exponent of 3 in the second term were chosen because these values yielded consistently better fits than other integers.

Ribbens et al. (1994) validated the method in several ways. First, plots of predicted vs. actual mean density per quadrat and predicted vs. actual fraction of empty quadrats showed close agreement between predicted and actual values. Second, estimates from one data set predicted the spatial distribution of recruits in replicate data sets (eight comparisons employing the t test adjusted for spatial autocorrelation as described in Clifford et al. 1989; $P < 0.05$ in each case). Third, cross-validation analyses (estimating the submodel using two-thirds of the quadrats and testing it against the remaining one-third) were used to check the method for species lacking a replicate data set ($P < 0.05$ in all such tests). Fourth, estimates of R_1 were highly consistent across replicates (including sites in Michigan), indicating that dispersal functions were approximately constant across sites and years. However, estimates of R_2 revealed considerable inter-site and inter-year variation in fecundity (e.g., masting) and/or pre-establishment mortality. Fifth, seed addition experiments and data from seed traps demonstrated that the spatial distribution of recruits in nature reflected limited dispersal and heterogeneous spatial distributions of parents rather than solely an underlying template of microsite quality affecting establishment. These data effectively eliminate the hypothesis that conspecific adults and recruits occur in close proximity, not because of finite

dispersal, but because each species is able to establish only in a highly restricted portion of the habitat.

The current version of SORTIE uses estimates of R_1 from GMF, but does not use estimates of R_2. The problem is that we do not yet have a sufficient time series of data to estimate mean fecundity, in the face of the enormous temporal variability in tree seed production. In particular, fecundities in mast years may be four orders of magnitude higher than in non-mast years for several of the species (e.g., Bjorkbom 1979, Graber and Leak 1992, Sork et al. 1993). Also, preliminary data from our current studies of seed and seedling predation and herbivory on all size classes (together with R. Ostfeld, *unpublished data*) imply large temporal heterogeneity in the survivorship of individuals <5 yr of age (the age at which recruits enter SORTIE). Predation of seeds and seedlings by microtines and insects is intense, and populations of these consumers are known to exhibit large fluctuations (Baker 1968, Rose and Birney 1985). Thus, our estimates of R_2 cannot be considered reliable until we acquire more data.

Values of R_2 used in this paper were set by systematically varying the R_2's across a preliminary set of runs of SORTIE. We chose values that produced juvenile abundances similar to those in natural stands. This analyses is described in subsequent sections of the paper.

Interspecific trade-offs among the tree species

It is sometimes difficult to predict how an individual in SORTIE will perform, solely by examining the parameter estimates. For example, the outcome of competition among saplings in a gap depends primarily on growth in height. In SORTIE, height growth is governed by parameters G_1, G_2, H_1, and H_2. How does one combine estimates of these four parameters to understand relative abilities of species to capture gaps? Similarly, the level of shade produced by a canopy tree, with any given diameter, depends of its crown geometry and light extinction coefficient. How does one combine a species' H's, C's, and E_t to understand its relative ability to deprive neighboring saplings of light?

To clarify the competitive strategies of species in SORTIE, we calculated five simple metrics that quantify aspects of performance likely to be important to competitive dynamics. First, for each species, we calculated the total amount of shade cast by a 30 cm diameter tree (approximate average size of canopy individuals in GMF). Total shade was defined as the absolute value of the difference between the spatial integral of ln(GLI) over the individual's shadow and the corresponding integral for full sun (GLI = 100). Second, we computed, for each species, the amount of time necessary to grow from the seedling stage (diameter = 2 mm) to 3 m in height at a low light level representative of conditions in GMF (GLI = 1%) and in full sun (GLI = 100%). These times are labeled t_1 and t_{100}, respectively. Note that t_1 is a measure of a species' ability to gain a head start over competitors in the understory, while t_{100} is a measure of competitive ability within gaps. We obtained similar results for t_{100} (in terms of the ordering of species) using final heights from 3 to 20 m and using GLI's from 20 to 100%. Third, we used the mortality function (Eq. 6) and radial growth function (Eq. 3) to compute the 5-yr survivorship of a 1 cm diameter sapling of each species growing in 1% light. This metric describes a species ability to persist in the understory. Together with t_1, it quantifies a species' strategy of advance regeneration. Finally, recall that R_1 is the only parameter governing species-specific differences in dispersal. To clarify the meaning of this parameter, we calculated the mean dispersal distance (MDD) corresponding to each estimate of R_1.

We are thus left with five species-specific metrics, each describing a different aspect of individual performance. We plotted these values against one another to explore interspecific trade-offs among them.

Dynamics of SORTIE and sensitivity and error analyses

Dynamical baseline of the calibrated model.—We performed 100 2000-yr runs of the model containing the maximum likelihood estimates of all parameters (the species-specific estimates of the C's, H's, E's, G's, M's, and R_1). Also, we set $R_2 = 5$ for all species except beech (Be), whose value was set at 2. The smaller value for Be reflects the vegetative reproduction of this species at GMF. Individuals of white ash (WA, the sole dioeceous species) were assigned a gender at random when born (50:50 sex ratio). Each run was initiated with a different random number seed, a random spatial distribution, and a density of 25 1 cm diameter saplings of each species/ha. New recruits had an initial diameter of 2 mm. The range of community level predictions from the series of runs reflects the inherent stochasticity of the model at a scale of 9 ha.

Community level consequences of uncertainty about parameter values.—Error analyses are used to translate statistical uncertainty in parameter estimates into statistical uncertainty in a model's predictions. In an error analysis, one estimates the *sampling distribution* of the parameters. A sampling distribution specifies the distribution (probability density) of parameter estimates about the "true" parameter values (Mood et al. 1974). Repeated runs of a model, each for a different random draw of the parameters from the sampling distribution, thus produces a distribution of model output that reflects the uncertainty in the parameter estimates.

We estimated the sampling distribution for the maximum likelihood estimates of the C's, H's, E's, G's, M's, and R's by inverting the Fisher's information matrix (Mood et al. 1974, Kendall and Stuart 1977). This asymptotic method is commonly used to estimate confidence limits for parameters and is the source of all confidence limits reported in this paper. It yields a mul-

tivariate normal sampling distribution for the estimates. The variance–covariance matrix of the distribution is obtained by inverting a matrix, whose elements are negative one times the second partial derivatives of the likelihood function with respect to each parameter. The derivatives are evaluated at the likelihood estimates (Mood et al. 1974).

In practice, one estimates the sampling distribution in segments, corresponding to different independent data sets. For example, consider the data set used to estimate the growth submodel (Eq. 3) of Be. To estimate the sampling distribution of G_1 and G_2 for this species, we first calculated the 4×4 matrix containing the second partial derivatives of Be's growth likelihood function with respect to G_1, G_2, and the two additional parameters governing the variance of observed growth rates about the mean given in Eq. 3 (see Pacala et al. 1995 for a description of the two parameters governing variance in Be's growth). After multiplying these elements by negative one and inverting, we obtained a 4×4 variance–covariance matrix, including the variances and covariance for the estimates of Be's G_1 and G_2. Because Be's growth data set was independent of all other data sets, there was zero covariance between estimates of Be's growth parameters and all other maximum likelihood estimates in SORTIE.

After repeating this procedure for all data sets, we obtained the complete variance–covariance matrix (and thus the sampling distribution) for all parameters in the model. The error analysis of SORTIE then required two steps. First, the multivariate normal sampling density may be written as:

$$\frac{1}{[(2\pi)^Q|\mathrm{V}|]^{1/2}}\exp\left[-\frac{1}{2}(\Theta^* - \Theta)^T\mathrm{V}^{-1}(\Theta^* - \Theta)\right], \quad (9)$$

where V is the variance-covariance matrix, Θ^* is the column vector of maximum likelihood estimates, Θ is the column vector of "true" parameter values, Q is the number of parameters, and T signifies transpose. We randomly drew 100 sets of parameters from Eq. 9, yielding 100 different Θ's. These 100 sets of parameters represented 100 different possible manifestations of the "true" parameter values. Second, we used each of the 100 sets of parameters for a 2000-yr run of the SORTIE. The 100 initial conditions in these runs were the same as the 100 initial conditions in the baseline runs described. We compared the distributions of community level predictions obtained in the baseline and error analyses to separate variability in SORTIE's predictions caused by sampling uncertainty in the parameter values from variability caused by the inherent stochasticity of the model at 9-ha scales.

Error analyses are uncommon in the ecological literature (but see Pacala and Silander 1990), simply because few studies have estimated the majority of parameters in a dynamic model with statistical methods. More common are sensitivity analyses, in which one *assumes* a range of values for each parameter and then evaluates the model's behavior for parameter values spanning the specified ranges. The number of parameters in a model typically limits sensitivity analyses to three values for each parameter: a best value and upper and lower bounds. Parameters are varied one at a time, with all other parameters at their best values. Note that 10 parameters would otherwise require 3^{10} runs.

We performed sensitivity analyses for the three parameters, R_2, G_3, and the initial diameter of new recruits, not estimated statistically from our field data. We completed three replicate 2000-yr runs with G_3 = 63 cm^2, three with G_3 = 126 cm^2, three with recruit diameter = 1 mm, and three with recruit diameter = 4 mm (G_3 = 94 cm^2 and initial recruit diameter = 2 mm in the baseline runs). All species shared the same value of G_3 and recruit diameter. Also, prior to the baseline runs and error analysis, we completed 12 runs involving the following values of R_2: 1:2.5, 2:5, 4:10, and 8:20 (R_2 for Be:R_2 for all other species, with three replicates per combination). The two intermediate combinations (2:5 and 4:10) yielded densities of juveniles most consistent with published information (see *Results*). We selected 2:5 for the baseline runs and error analysis because 4:10 would have required nearly double the computer time. In addition, we performed 27 runs in which we quadrupled the baseline value of a single species' R_2, and kept all other species at their baseline values (three replicates for each of the nine species). This set of runs investigated the competitive advantage conferred by increased fecundity and/or preestablishment survivorship. Finally, we investigated the sensitivity of SORTIE's dynamics to changes in the initial densities of 1 cm diameter saplings. We completed 27 runs in which a single species was initiated at 250 saplings/ha, and all others at 25 saplings/ha (three replicates for each of nine species). Note that total initial densities in these runs were twice as large as in the baseline runs (450 saplings/ha vs. 225 saplings/ha). Finally, we performed three replicates each with initial densities 12 saplings/ha and 250 saplings/ha of each species.

Statistical concerns.—The error analysis in this paper must be interpreted in light of the statistical assumptions behind it. In particular, the error analysis relies on all of the assumptions behind the estimators of each submodel (e.g., normally distributed radial growth rates about the mean given by Eq. 3, statistically independent observations, β-distributed crown openness about the mean given by Eq. 2, etc.). In addition, it relies on an asymptotic (large sample) approximation for the sampling distribution (Kendall and Stuart 1977). Because of the large number of assumptions involved, we do not view the error analysis as a rigorous statistical evaluation of SORTIE's behavior, but rather as an objective and qualitative means to identify predictions of the model that appear most robust to sampling uncertainty, as well as predictions that evaporate because of sampling uncertainty.

In this section, we offer our statistical concerns about each of the submodels. The methods behind the growth and mortality submodels and the methods used to estimate the C's and H's from the resource submodel are probably the most reliable in the study. To estimate the G's, C's, and H's, we employed standard methods (normal-based regression). The asymptotic sampling distributions of these parameters agree well with distributions obtained from a bootstrap. Although the method of estimating the parameters of the mortality submodels is non-standard, modeling studies imply that it is approximately unbiased. Recall that replicate sites yielded consistent estimates (see Kobe et al. 1995). In addition, we checked the asymptotic sampling distributions of the M's using a bootstrap.

We went to considerable lengths to ensure the reliability of the R's and E's from the recruitment and resource submodels, including tests against replicate data sets and seed addition experiments for the recruitment submodels, and tests against data from quantum sensors for the resource submodel (see Canham et al. 1994, Ribbens et al. 1994). However, we did not check the sampling distributions of the R's and E's against bootstrapped distributions because this would have required prohibitive computer time. We employed a slow but reliable method to maximize likelihoods (the Metropolis algorithm in Szymura and Barton 1986) because faster alternatives often failed to converge. We were able to test one of the assumptions behind our method of estimating sampling distributions for the R_1's and E's. Specifically, we used the Metropolis algorithm to explore the shapes of the likelihood surfaces (see Szymura and Barton 1986) and found that contours were indeed elliptical as required by our asymptotic methods.

Our concerns about the sampling distributions of the R_1's center on the presence of small-scale spatial clumping among residuals (positive autocorrelation at scales of typically ≤ 3 m) presumably caused by fine-scale safe sites for germination and establishment or by the tendency of seeds to roll into small depressions. In some of our recruitment sites, the 1-m^2 quadrats were arrayed sequentially along transects, and so were spaced at distances less than the scale of clumping. Although positive autocorrelation should not bias parameter estimates, it will inflate sampling variances (by reducing the effective sample sizes; Cliff and Ord 1981). Our method of estimating sampling distributions for the R_1's assumes no spatial autocorrelation. However, we suspect that any underestimation of the sampling variances of the R_1's is slight, because replicate samples produced estimates well within each other's 95% confidence limits in all cases but one (see Ribbens et al. 1994).

Our estimate of the sampling distribution of the E's is probably the least reliable part of the study for three reasons. First, the independent variables in Eq. 2 contain error not accounted for by our statistical methods. Recall that cylindrical crowns were constructed for the mapped stems on the resource submodel sites using allometric equations. Thus, the independent variables in Eq. 2 represent the numbers of cylinders intercepted, rather than the actual numbers of crowns intercepted. Second, when estimating the sampling distribution of the E's, we did not account for the possibility of non-zero covariance between estimates of the crown sizes and shapes (the H's and C's) and estimates of the E's. To do so would have required prohibitive amounts of computer time. Third, residuals of canopy openness are spatially autocorrelated (positively). We suspect that this autocorrelation is a consequence of the error in observations of the independent variables (error in the numbers of crowns of each species intercepted in the resource submodel estimation sites). Portions of some of the reconstructed cylindrical crowns in the mapped stands undoubtedly were placed in "wrong" places, thus creating too much shade in some regions and too little shade in others. Thus, all the statistical problems associated with the resource submodel arise because of the simple assumptions about crown sizes, shapes, and placement. Resolution of these problems will require a more realistic representation of crown architecture.

Because of our statistical concerns about the sampling distributions of the R_1's and E's, we expanded the sensitivity analysis. We performed 15 2000-yr runs in which the R_1's and E's were set at values well outside their 95% confidence limits. There were three replicates with the R_1's at twice or one-half the estimated values and three replicates with the canopy openesses (e^{-Et}) at one-fourth, one-half, and one and one-half times the estimated values (twice the estimated value of canopy openness would have produced a value >1 for RO). In the few cases when this displacement produced a value within the 2.5 standard errors of the estimate, we used the estimate plus or minus 2.5 standard errors. Initial densities and plot size were the same as in the baseline runs.

Spatial distribution produced by the model

To assess spatial distributions produced by the model, we performed three runs identical to the baseline runs, but with a plot size of 1 km^2. At 100-yr intervals, we overlayed a 10×10 m grid and recorded the basal area of each species in each square. We then computed semivariograms for each species. We also calculated the covariance spectrum for the two species showing substantial spatial clumping (Hm and Be). The pattern documented in these runs also occurred in every run of the baseline and error analyis that contained substantial late-successional abundances of Hm and Be.

Tests of the SORTIE's dynamical predictions

Five robust predictions about community dynamics and structure emerged from the error and sensitivity

TABLE 1. Definitions of parameters in the model SORTIE.

Submodel	Symbol	Description
Resource	H_1	Asymptotic tree height (m) (Eq. 1)
	H_2	Initial slope of height–diameter relationship (m/cm) (Eq. 1)
	C_1	Tree crown radius/stem diameter ratio (m/cm)
	C_2	Crown depth/tree height ratio (m/m)
	E_t	Light extinction coefficient (Eq. 2)
Growth	G_1	Asymptotic high-light growth rate of saplings (yr^{-1}) (Eq. 3)
	G_2	Slope of sapling growth rate at low light (yr^{-1} GLI^{-1})* (Eq. 3)
	G_3	Maximum allowed growth of adult stem area (cm^2)
Mortality	M_1	Probability of mortality at zero growth (2.5 yr^{-1}) (Eq. 6)
	M_2	Decay of growth dependent mortality function (cm^{-1}) (Eq. 6)
	—	Probability of mortality due to random disturbance (yr^{-1})
Recruitment	R_1	Distance decay of recruitment shadow (m^{-3}) (Eq. 7)
	R_2	Number of recruits produced by a tree 100 cm in diameter (Eq. 7)
	—	Initial radius of new recruits

* GL1 = Global light index.

analyses (*Results*). We compared the non-spatial predictions of SORTIE to data on species abundances and total basal area in transition oak–northern hardwoods stands as reported in Nichols (1913), Hough and Forbes (1943), Potzger (1946), Stephens and Waggoner (1980), Kelty (1984, 1986), and G. R. Stephens (*unpublished data*). We also compared the spatial predictions to spatial palynological records of stands in upper Michigan (Davis et al. 1992, 1994, Frelich et al. 1993).

Tests of hypotheses explaining the community-level predictions

We developed hypotheses to explain the five robust predictions of SORTIE in terms of attributes of the submodels. Each hypothesis traced the cause of a community level phenomenon to one or more aspects of individual performance. We tested these hypotheses with a series of runs in which we experimentally altered the submodels. Most experiments involved replacing one or more submodels of one species with the corresponding submodels of another. For example, to test the hypothesis that Be and Hm were predicted to be late-successional dominants because they had distinctive mortality submodels, we showed that any species receiving the mortality submodel of either Be or Hm became a late successional dominant, and that Be and Hm did not become late-successional subdominants if they received any other species' mortality submodel (see *Results*). All tests were replicated three times and had the initial densities, parameter values, and plot size used in the baseline runs.

RESULTS

Submodel estimates

Table 1 contains a list of definitions for all parameters of SORTIE. Parameter estimates and 95% confidence limits for all parameters are found in Table 2. Estimated submodels are illustrated in Figs. 1–4.

Resource submodel.—The two late successional dominants (Hm and Be) had the densest crowns, with estimated opennesses (e^{-E_t}) of 6.4%. Red oak had the least dense crowns (56.6%), while all others were intermediate (39.9%). Although our method provided separate estimates of E_t for each species, pooling the species into three classes yielded a nonsignificantly poorer fit, while pooling into fewer than three classes yielded significantly poorer fits (likelihood ratio tests; Pacala et al. 1993, Canham et al. 1994).

The shade cast by a tree is determined both by its canopy openness and by the size and shape of its crown (given by the H's and C's). Fig. 1 integrates these measures, by showing the size and shape of 30 cm diameter trees in SORTIE. The striping pattern in the figure shows the estimated canopy openness (e.g., the white stripes for Hm and Be occupy 6.4% of the crown). Note that the relatively high opennesses of BC, RO, WA, and WP are augmented by relatively shallow and open crowns. In addition, WA and WP have the narrowest crowns of the nine species. In contrast, the low opennesses of Hm and Be are augmented by either extremely deep (Hm) or broad and deep (Be) crowns. SM, RM, and YB are intermediate in all respects. Together, these estimates specify a close relationship between the total shade cast by an individual tree and a traditional classification of shade tolerance. The order, in decreasing shade cast (first column of Table 3), is Be > Hm > SM > YB > RM > BC > WA > RO > WP.

Growth submodels.—Estimated patterns of radial and height growth conform less well to traditional assignments of shade tolerance than do patterns of shade cast (Table 2 and Fig. 2; Pacala et al. 1995). For example, YB had an extremely large radial growth rate at low light (G_2) and a relatively small radial growth rate at high light (G_1) despite its traditional assignment as a relatively intolerant species. Also, the traditional shade tolerant Hm had a relatively small G_2 and large G_1. Estimates for SM, WP, WA, and RO were in better agreement with conventional wisdom (small G_2 and large G_1 for WP, WA, and RO, and the opposite for SM). Although these patterns are supported by the confidence limits in Table 2 and other analyses in Pacala et al. (1995), the radial growth regressions explained

TABLE 2. Estimates and 95% confidence intervals of parameters produced by maximum likelihood methods. Numbers in parentheses indicate the coefficients of determination (R^2) for normal-based regressions used to estimate the G's and H's.

Species					
American beech (Be)	Eastern hemlock (He)	Sugar maple (SM)	Red maple (RM)	Yellow birch (YB)	White pine (WP)
H_1 (m)					
34.6 ± 7.1 (0.96)	29.6 ± 8.9 (0.92)	24.8 ± 2.9 (0.93)	25.7 ± 2.4 (0.97)	23.2 ± 2.2 (0.96)	38.4 ± 7.4 (0.97)
H_2 (m/cm)					
1.06 ± 0.06	0.73 ± 0.06	1.87 ± 0.11	1.89 ± 0.11	1.89 ± 0.15	1.00 ± 0.09
C_1 (m/cm)					
0.152 ± 0.014	0.100 ± 0.011	0.107 ± 0.011	0.108 ± 0.007	0.109 ± 0.013	0.087 ± 0.010
C_2 (m/m)					
0.664 ± 0.061	0.846 ± 0.043	0.580 ± 0.041	0.490 ± 0.057	0.540 ± 0.071	0.413 ± 0.063
e^{-E_t}					
0.064 ± 0.014	0.064 ± 0.014	0.399 ± 0.004	0.399 ± 0.004	0.399 ± 0.004	0.399 ± 0.004
G_1 (yr^{-1})					
0.152 ± 0.035	0.229 ± 0.037	0.125 ± 0.029	0.167 ± 0.064	0.169 ± 0.047	0.230 ± 0.048
G_2 ($yr^{-1} \cdot GLI^{-1}$)					
0.075 ± 0.052 (0.53)	0.051 ± 0.022 (0.50)	0.159 ± 0.077 (0.23)	0.027 ± 0.014 (0.24)	0.137 ± 0.071 (0.44)	0.019 ± 0.007 (0.78)
M_1 (2.5 yr^{-1})					
0.014 ± 0.020	0.077 ± 0.059	0.998 ± 0.172	0.912 ± 0.406	0.555 ± 0.337	0.268 ± 0.122
M_2 (cm^{-1})					
0.2 ± 43.9	59.7 ± 32.8	47.9 ± 11.4	68.8 ± 22.3	26.7 ± 10.8	46.7 ± 18.6
$R_1 \cdot 10^3 (m^{-3})$					
1.957 ± 1.266	5.991 ± 1.037	0.744 ± 0.416	0.363 ± 0.103	0.000 ± 0.010	0.103 ± 0.114

an average of only 51% of the variance (see the coefficients of determination in Table 2). Sources of unexplained error might include such factors as pathogens, herbivory, variation in unmeasured resources, genetic variation, and microclimate.

In contrast, the height–diameter regressions explained an average of 96% of the variation (Table 2). This result supports the use of a static relationship between height and diameter over the range of conditions typically found in GMF and suggests that substantial departures from a static allometry require atypically low densities.

The second and third columns in Table 3 combine estimates of the H's and G's for each species. The number of years required to reach 3 m in height in full sun (GLI = 100%) is determined primarily by estimates of G_1 and H_2. Note that the product, rG_1H_2 is precisely the annual change in height of small trees in the limit of infinite GLI (see Eqs. 1 and 3). The ordering of the values in the second column in Table 3 corresponds closely to traditional shade tolerance classifications. A similar ordering is obtained if a final height of 5, 7, 10, 15, and 20 m is substituted for the 3 m given in the table. Thus, the height–diameter relationships compensate for some of the surprises about estimates of G_1. In particular, the squat architecture of Hm (low H_2) ensures a relatively poor ability to overtop competitors in large gaps (a relatively long time to reach 3 m in height in full sun), despite its large estimate of G_1.

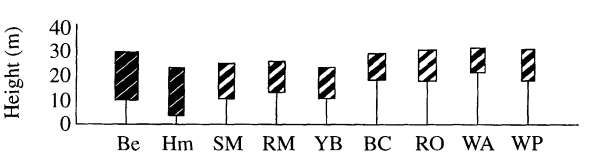

FIG. 1. Heights and crown shapes of 30 cm diameter trees in the model. The striping pattern shows crown openness. The total fraction of crown area that is light in the figure is equal to the estimated openness (the e^{-E_t} in Table 2).

The number of years required to reach 3 m in height at 1% light is determined primarily by estimates of G_2 and H_2. In the limit of low light and small radius, the annual change in height is simply $(GLI)rG_2H_2$ (Eqs. 1 and 3). Unlike patterns of high light height growth, patterns of low light height growth do not conform to traditional notions about shade tolerance. Note that the YB and BC are predicted to grow faster in 1% light than Be and Hm (Table 3).

Mortality submodels.—Estimates of M_1 and M_2 in Table 2 and the plots in Fig. 3 show striking interspecific variation in growth-dependent mortality. The functions predict interspecific differences in mortality of nearly two orders of magnitude at the low growth rates typical of suppressed saplings in GMF (0.0–0.2 mm radial increment). The 95% confidence limits in

TABLE 2. Continued.

Species		
Red oak (RO)	Black cherry (BC)	White ash (WA)
33.6 ± 3.1 (0.98)	30.8 ± 2.1 (0.98)	32.4 ± 2.5 (0.96)
1.26 ± 0.07	1.35 ± 0.11	1.68 ± 0.13
0.119 ± 0.009	0.116 ± 0.009	0.095 ± 0.010
0.413 ± 0.043	0.370 ± 0.059	0.319 ± 0.029
0.566 ± 0.042	0.399 ± 0.004	0.399 ± 0.004
0.266 ± 0.080	0.249 ± 0.069	0.225 ± 0.008
0.022 ± 0.011 (0.56)	0.064 ± 0.029 (0.59)	0.025 ± 0.008 (0.52)
0.985 ± 0.476	0.998 ± 0.282	0.999 ± 0.374
93.8 ± 27.7	48.5 ± 21.2	51.5 ± 15.5
0.607 ± 0.149	0.775 ± 0.353	0.092 ± 0.121

Table 2 and other analyses in Kobe et al. (1995) demonstrate that this variation is not a statistical artifact. The interspecific variation is particularly significant in light of the assumption of most JABOWA-FORET simulators that all species share a single function relating growth and mortality (Shugart 1984).

With the exception of the uniformly low mortalities predicted for Hm and Be, the functions in Fig. 3 are difficult to explain in isolation. Note, for example, that the traditional shade tolerant SM has a mortality function nearly coincident with that of the traditional intolerant WA. The interpretation of patterns of understory mortality is clarified considerably by the final column in Table 3, which gives the 5-yr survivorship of a 1-cm sapling at 1% light (using Eqs. 3 and 6 together with the estimated M's and G's). Note that the ordering of 5-yr survivorships corresponds almost exactly to a traditional ordering of shade tolerance. This result explains our difficulty in reconciling patterns of low light growth and patterns of growth-dependent mortality with shade tolerance. Evidently, different species achieve the same low light survivorship in different ways. For example, YB achieves a survivorship of 0.65 (Table 3) through rapid low-light growth but poor low-growth survivorship, while WP achieves an identical value through slower growth under low light growth but higher survivorship under low growth.

Recruitment submodels.—The estimates of R_1 in Table 2, mean dispersal distances in Table 3, and dispersal functions in Fig. 4 reveal some of the expected negative correlation between dispersal ability and shade tolerance, but with some important exceptions (Ribbens et al. 1994). First, RO and BC have relatively short mean dispersal distances despite their relatively early successional and shade intolerant status. Red oak and BC are the only animal-dispersed species in the study and our field methods are not designed to detect the occasional long distance dispersal event caused by foraging squirrels or birds. Thus, the mean dispersal distances for these species of between 8 and 9 m probably correspond to the fraction of seeds that escape the attention of animal dispersers. T. Coulson of Imperial College at Silwood Park has confirmed this suspicion for RO seeds in GMF (T. Coulson, *unpublished data*). Second, YB has by far the longest dispersal, despite its status as an only moderately shade intolerant species. Seeds of YB are dispersed in the winter and are capable of long distance secondary dispersal over snow

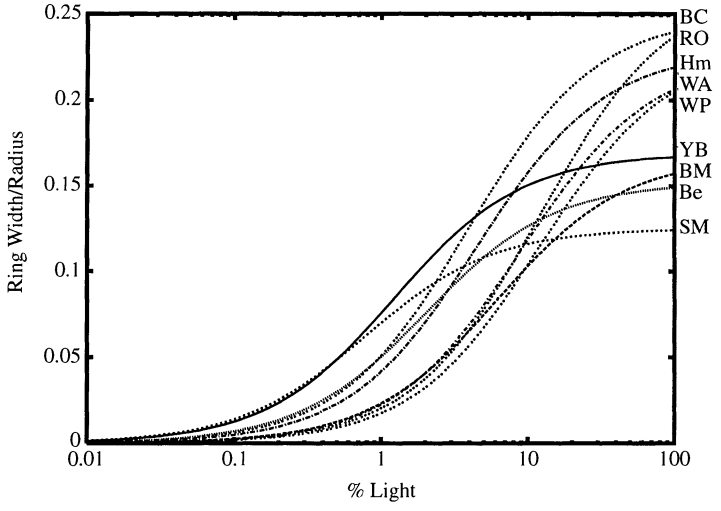

FIG. 2. Estimates of the radial growth functions (Eq. 3 in the text).

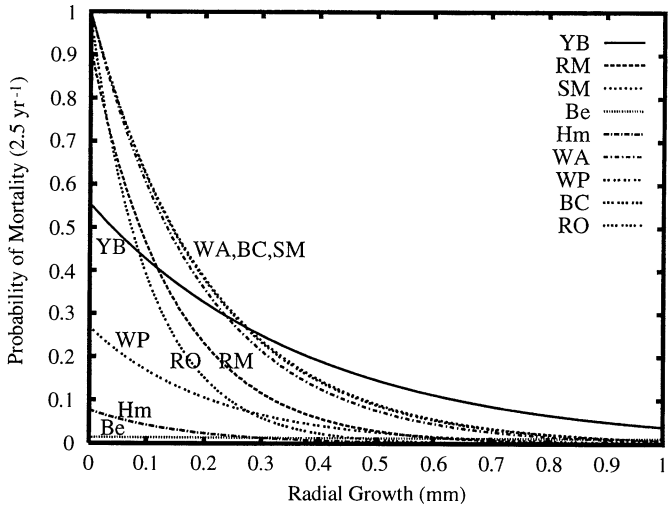

FIG. 3. Estimates of the growth-dependent mortality functions (Eq. 6 in the text).

(Matlack 1989). Finally, note the extremely short dispersal of Hm and Be. This is caused by the tendency of Hm seeds to fall within intact cones and by the dominance of clonal reproduction by Be at GMF.

Interspecific trade-offs

Fig. 5 shows the interspecific relationships among the five performance measures in Table 3. Fig. 5a and b are *five-dimensional.* In Fig. 5a, the thinness of the bars indicates mean dispersal distance (see the scale in the upper right hand corner), while the darkness of the striping pattern indicates years to 3 m in height at 1% light (see the scale at the bottom). Note that bars become generally shorter from the upper left hand corner to the lower right hand corner, thus illustrating interspecific trade-offs among shade cast, overtopping ability in gaps, and survivorship in the understory. The bars also tend to become narrower from the upper left to the lower right, indicting a further trade-off with mean dispersal distance, although this pattern would be considerably sharpened if the bars of animal-dispersed species (RO and BC) were narrower (as we suspect they should be). Finally, height growth at low light is not obviously correlated with high-light growth, low-light survivorship, or dispersal. For example, observe that the darkest striping pattern (WP) is directly next to the lightest striping pattern (YB). Thus, Fig. 5a shows rough colinearity among four different performance measures—as overtopping ability in gaps increases, understory survivorship decreases, shade cast decreases, and dispersal increases.

Spearman rank correlations provide some statistical support for these relationships. Let: A represent shade cast, B represent years to 3 m in height at 100% light, C represent mean dispersal distance, and D represent survivorship of a 1 cm diameter sapling in 1% light. Correlations $A \times D$ and $B \times D$ are significant ($P < 0.04$ for $A \times D$ and $P < 0.02$ for $B \times D$), while correlation $A \times B$ is marginally significant ($P < 0.07$). Even with the probable underestimation of the mean

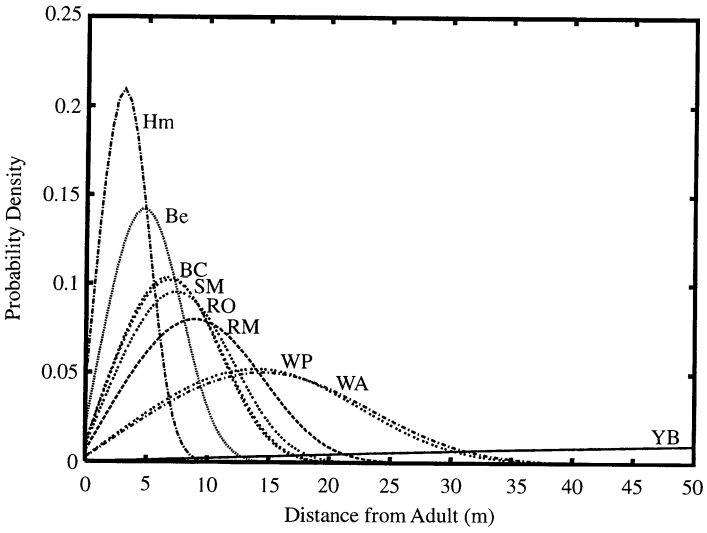

FIG. 4. Estimates of the dispersal functions. Each curve shows the probability that a seed will disperse any given distance (obtained by integrating Eq. 7 around the circle).

TABLE 3. Metrics summarizing interspecific variation among competitive strategies.

Species	Shade cast by a 30 cm diameter tree*	Time to 3 m in height in full sun (yr)	Time to 3 m height in 1% sun (yr)	Mean dispersal distance (m)	5-yr survivorship of a 1 cm diameter sapling in 1% sun
Be	78.5	19.4	55.0	5.9	0.92
He	46.0	15.5	75.3	4.1	0.91
SM	27.0	18.4	31.7	8.1	0.69
RM	25.7	14.6	92.8	10.6	0.35
YB	25.9	13.9	29.3	31.0†	0.65
WP	16.6	14.7	158.0	15.8	0.65
RO	19.5	11.9	125.4	8.7	0.38
BC	25.3	11.4	49.5	8.0	0.53
WA	19.5	11.9	100.6	16.3	0.20

* See *Methods: Interspecific trade-offs among tree species* for a description of the measurement of shade cast.
† This value is the lower 95% support limit (Edwards 1992). The estimated value was >65 m and our field plots were not sufficiently large to ensure reliability of estimates this large (see Ribbons et al. 1994).

dispersal distances of RO and BC, two of three correlations involving dispersal distances are marginally significant ($P < 0.08$ for $A \times C$, $P < 0.24$ for $B \times C$, and $P < 0.07$ for $C \times D$).

Comparisons $A \times B$ and $B \times D$ technically violate assumptions of the statistical test. First, estimates of H_1 and H_2 are used to calculate both the amount of shade cast by a 30 cm diameter tree (because the height of a tree influences its crown size) and the time needed to grow to any height. This violation of the Spearman Rank Test's independence assumption results in a conservative test. Species that grow slowly in high light tend to be shorter at 30 cm in diameter than fast-growing species (see Fig. 1). Thus, the appropriate null hypothesis is that A and B should be *negatively* correlated because they both rely on the same estimates of the H's. We obtained a marginally significant positive correlation between A and B under the conservative null hypothesis of zero correlation.

Second, the radial growth parameters are used to calculate both B and D. Although B is affected primarily by G_1 and D by G_2, estimates of the two growth parameters are themselves marginally correlated (negative covariance in the sampling distributions of G_1 and G_2). As a result, the appropriate null hypothesis is that B and D should be positively correlated. Because this violation of the independence assumption is in the same direction as the result, we performed an additional randomization test. We assigned each species the M's of a randomly chosen species (without replacement). After repeating this process 1000 times, we calculated the correlation between B and D in each of the 1000 randomly assembled sets. We then compared this distribution to the correlation between the actual measures of B and D, and obtained the same result as in the original Spearman Rank Test ($P < 0.02$). The randomization test shows that the association between the M's and the other parameters results in positive correlation between B and D, beyond that which is expected solely because estimates of the G's are used to calculate both B and D.

The final technical violation of the assumptions behind the Spearman Rank Test involves the light extinction coefficients used in calculating our measure of shade cast. All parameters, except for the E's, were estimated separately for each species from independent data sets. Because the E's were estimated collectively from the same data set, estimates of the E's are technically not independent. However, estimates of the sampling covariances among the E's are negligibly small (correlations <0.02 in all cases), probably because the light extinction data were obtained from a collection of separate and largely monodominant stands.

Fig. 5b provides another view of the relationships among the performance measures in Table 3. Now, shade cast is shown by the darkness of the striping pattern and low light growth is plotted on one of the horizontal axes. The figure shows the large interspecific variation in low-light growth about the approximately unidimensional trend in Fig. 5a. Spearman Rank and randomization tests show that this variation is not significantly correlated with three of the four remaininng performance measures (i.e., Spearman Rank correlation of low-light growth with A: $P < 0.04$, B: $P < 0.64$, C: $P < 0.70$, and D: $P < 0.23$).

Bars in the foreground represent species that grow faster *at both high and low light* than bars in the background. Because bars are often shorter in the foreground than in the background (compare Be or Hm with SM, Hm with RM or YB, and WP with RO and WA), the pattern in the figure is consistent with a trade-off between growth at any light level and understory survivorship. Kobe et al. (1995) hypothesized that this trade-off might be due to differences in allocation. Species allocating a large fraction of their photosynthate to internal stores or defenses would have relatively high survivorship, but would have relatively few remaining reserves to devote to growth. In contrast, species allocating most of their photosynthate to growth would grow relatively quickly, but at the price of low survivorship when resource-deprived.

Like Fig. 5a, Fig. 5b shows that there is not a clean trade-off between growth at low and high light. For

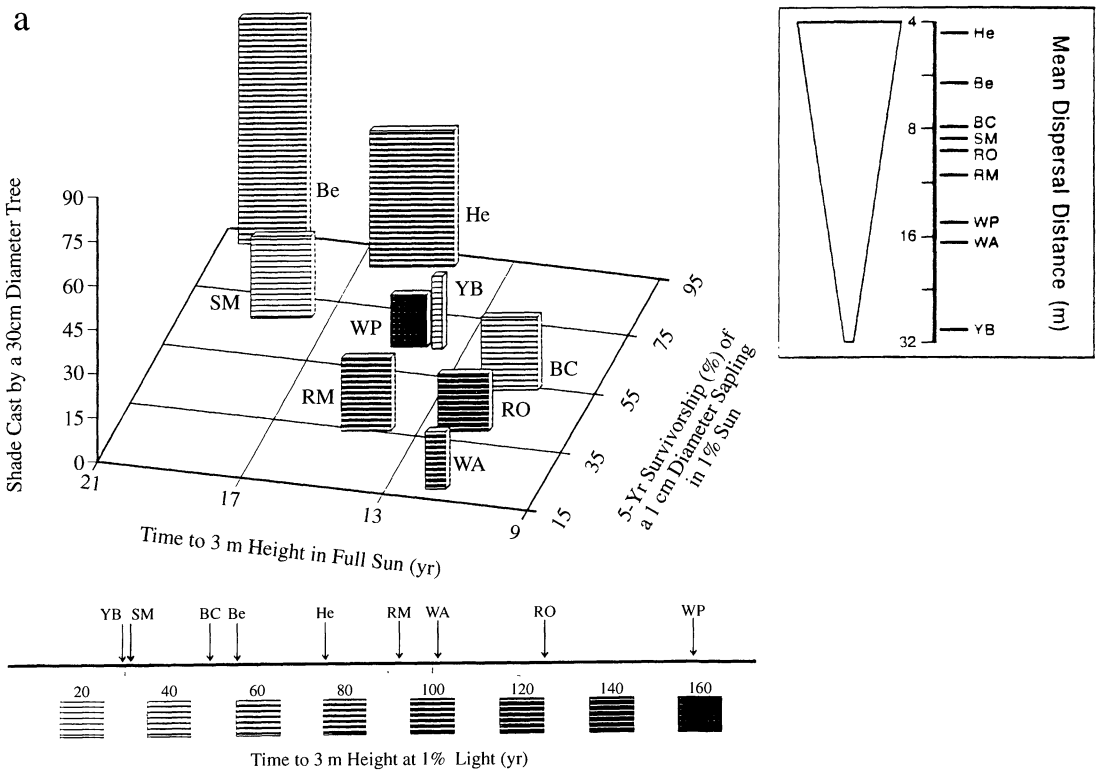
a
Shade Cast by a 30cm Diameter Tree
90
75
60
45
30
15
0
Be
He
SM
YB
WP
BC
RM
RO
WA
21
17
13
9
Time to 3 m Height in Full Sun (yr)
95
75
55
35
15
5-Yr Survivorship (%) of a 1 cm Diameter Sapling in 1% Sun
YB SM
BC Be
He
RM WA
RO
WP
20
40
60
80
100
120
140
160
Time to 3 m Height at 1% Light (yr)
Mean Dispersal Distance (m)
4
8
16
32
He
Be
BC
SM
RO
RM
WP
WA
YB

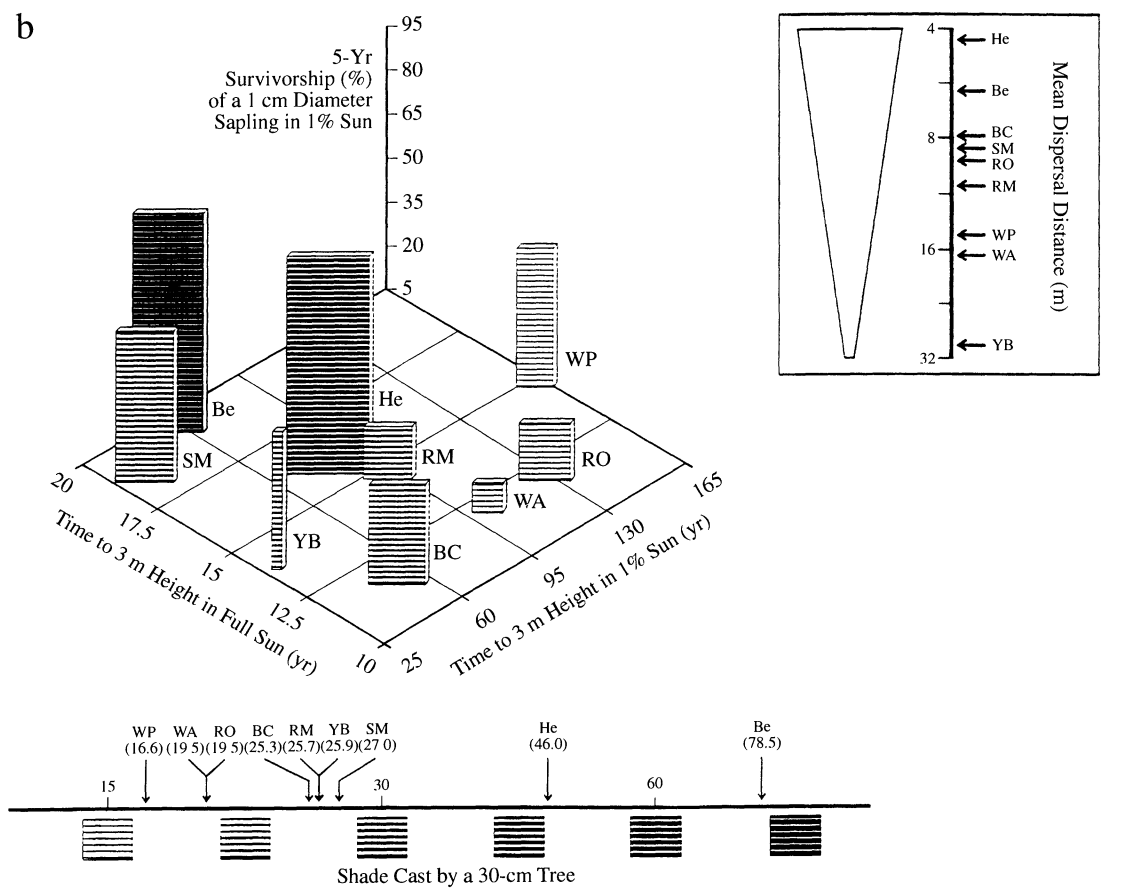
b
5-Yr Survivorship (%) of a 1 cm Diameter Sapling in 1% Sun
95
80
65
50
35
20
5
Be
He
WP
SM
RM
RO
WA
YB
BC
20
17.5
15
12.5
10
Time to 3 m Height in Full Sun (yr)
25
60
95
130
165
Time to 3 m Height in 1% Sun (yr)
WP WA RO BC RM YB SM
(16.6) (19 5) (19 5) (25.3) (25.7) (25.9) (27 0)
He
(46.0)
Be
(78.5)
15
30
60
Shade Cast by a 30-cm Tree
Mean Dispersal Distance (m)
4
8
16
32
He
Be
BC
SM
RO
RM
WP
WA
YB

example, BC and Be require approximately the same amount of time to reach 3 m in height at 1% light, but BC grows much faster in full sun. Similarly, YB and WP grow equally rapidly at high light, but YB grows considerably faster at low light.

In summary, although four of the performance metrics are correlated closely with traditional assignments of shade tolerance (Fig. 5a), there appears to be at least one other strategic dimension. This dimension may be explained as large "scatter" in low light growth along the approximately unidimensional trend in Fig. 5a, or as a trade-off between growth at any light level and low light survivorship (Fig. 5b).

Baseline and error analysis runs

Total basal area.—In the mean of the baseline runs, total basal area increased from near zero to a maximum of 60 m^2/ha at ≈200 yr, and then declined slowly to 42 m^2/ha at 2000 yr (Fig. 6a, b). Basal areas were approximately constant after year 1000. Stochastic variation among runs was relatively large; 94% of runs produced maxima between 40 and 80 m^2/ha and final values between 30 and 50 m^2/ha.

The mean of the error analysis runs shows a similar pattern up to year 200, but then predicts a smaller decline through year 2000 (from 63 to 54 m^2/ha; Fig. 6c, d). The mean of the error analysis runs differs from the mean of the baseline runs simply because SORTIE is a non-linear function of its parameters. In the suite of error analysis runs, the parameters are formally random variables (because of sampling uncertainty). Whenever a function of random variables is non-linear, the mean of the function will not generally equal the function evaluated at the random variables' means.

A substantial fraction of the error analysis runs showed monotonic increase to a rough steady state basal area rather than a hump at ≈200 yr, as evidenced by the monotonic 3 and 97% limits as well as the moderate declines in the mean and 25 and 75% limits (Fig. 6d). Thus, the hump in Fig. 6d is not particularly robust to our level of uncertainty about parameter values. Note also that the 25 and 75% limits in Fig. 6d are only slightly farther apart than the corresponding limits in Fig. 6b. This shows that, at the 50% level (the 50% of basal areas between the 25 and 75% limits), uncertainty about parameter values contributes little to variation in predicted basal areas. Most of the observed variation at the 50% level is caused by the inherent stochasticity of the model (present in both the baseline and error analysis runs), rather than statistical uncertainty about parameter values (present in only the error analysis runs). Similarly, the lower 3% limit in Fig. 6b, d are very similar. However, the upper 97% limit for the error analysis runs is substantially above the corresponding limit for the baseline runs, indicating a substantial impact of parameter uncertainty. The elevated 97% limit in Fig. 6d is caused primarily by nine of the error analysis runs in which YB remained the basal area dominant through year 2000 (rather than Hm or Be; see *Results: Community level predictions,* below). In these nine runs, YB "drew" G's and M's that permitted it to regenerate under closed canopy and thus become the late-successional dominant. Because YB trees cast less shade than Hm or Be trees (Table 3), YB-dominated communities in SORTIE may reach substantially higher steady-state basal areas than Hm-dominated or Be-dominated communities. This result illustrates how uncertainty about the parameter values of a single species may create seemingly disproportionate uncertainty in ecosystem level behavior.

Community level predictions.—The mean basal areas for each species from the baseline runs (Fig. 7a) show a familiar successional pattern, with shade intolerant species initially dominant, but declining after reaching peak abundances between years 100 (WA) and 400 (YB), and subsequent late successional codominance by Be and Hm. Note that the model apparently does not predict indefinite persistence of gap phase species at the low disturbance levels of the baseline runs, although all species persist through year 1000 in at least some runs (Fig. 8a). The one major surprise is the relatively rapid competitive exclusion and low dominance of the shade tolerant species SM.

The corresponding plot for the error analysis runs (Fig. 7b) shows a qualitatively similar pattern, except that competitive exclusions are less abrupt than in the baseline runs, and YB appears to persist, on average, as a subdominant through year 2000. Because of parameter uncertainty, some random "draws" in the error analysis runs enhance the ability of relatively shade intolerant species to persist late into succession.

Fig. 8a and b underscore this point. There, we plot persistence—the fraction of runs in which each species is present. Note in Fig. 8a that neither Hm nor Be goes extinct in any baseline run, and that YB, BC, and WP persist until year 2000 in at least some runs. A com-

←

FIG. 5. Five-dimensional plots of the performance measures in Table 3. (a) the horizontal axes show high-light growth in height (time from seedling to 3 m in height) and low-light survivorship (5-yr survivorship for a 1 cm diameter sapling). The vertical axis gives the amount shade cast by an individual tree (difference between the spatial integral of ln(GLI) over the individual's shadow and the corresponding integral for full sun (GLI = 100%). The thickness of the bars shows the mean dispersal distance (scale in the upper right; note that thickness is inversely related to mean dispersal distance). Finally, the striping pattern on the bars gives the low-light growth in height (scale shown at the bottom of the figure); (b) same as (a) except low-light growth is shown on one of the horizontal axes, low-light survivorship on the vertical axis, and shade cast by the striping pattern.

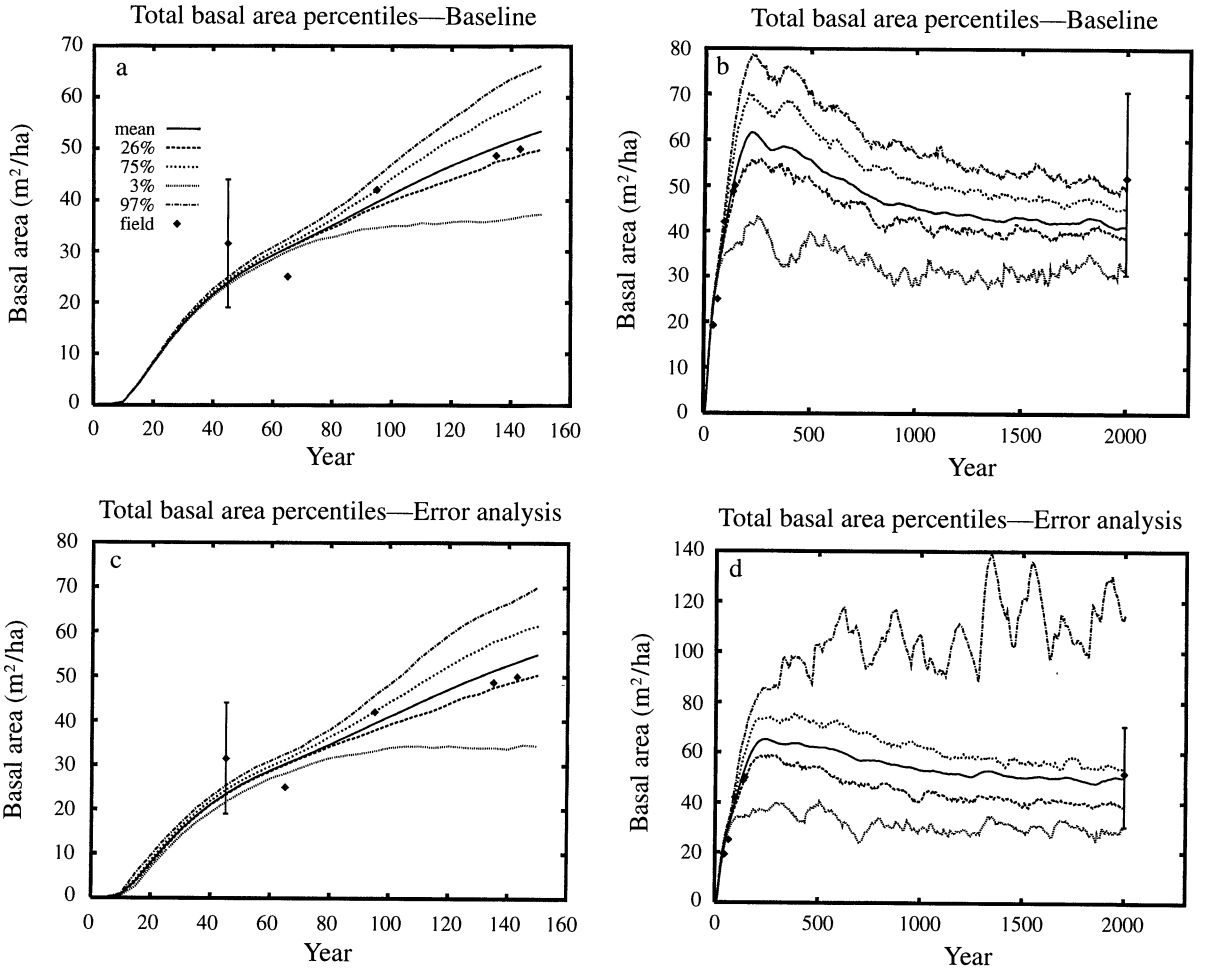

FIG. 6. Total basal areas predicted by the (a, b) 100 baseline and (c, d) 100 error analysis runs of SORTIE. The key in each panel is interpreted as follows. The mean is the mean basal area of the 100 runs. Ninety-seven of the basal areas produced by the 100 runs fall beneath the 97% curve, 75 of 100 beneath the 75% curve and so on. The diamonds show actual basal areas from natural stands of transition oak–northern hardwoods (citations in the text). The value at 2000 yr corresponds to stands reported to be "virgin" or "old-growth" in the literature. Other diamonds are located at the successional ages reported (years since catastrophic disturbance). The bars around the diamonds at 50 yr represent the range reported from 10 natural stands, and those around the diamonds at 2000 yr represent the range from 30 natural studies. (a) baseline runs from years 0–160; (b) baseline runs from years 0–2000; (c) error analysis runs from years 0–160; (d) error analysis runs from years 0–2000. The increased width between the 97% and 3% curves in the error analysis runs (compared to the baseline runs) shows the uncertainty produced by sampling error.

parison of parts a and b of Fig. 8 shows that parameter uncertainty flattens the persistence curves of the baseline runs, indicating that relatively intolerant species sometimes "draw" parameter values that promote late-successional persistence in the error analysis runs (Fig. 8b). Note that all species except WA are present in year 2000 of at least some error analysis runs, and that parameter uncertainty causes even Be and Hm to be excluded in a few runs (two for Be and six for Hm).

Our most complete information on patterns of dominance during succession is found in Table 4. Each element in the table gives the number of runs (B = baseline runs and E = error analysis runs) in which each species was one of the two most abundant species (hereafter labeled dominant) and/or one of the five most abundant species (hereafter labeled subdominant).

The information in Table 4 is summarized in Table 5. Table 5 was constructed specifically to expose the uncertainty in community level predictions of SORTIE caused by sampling uncertainty about parameter values. In the explanation that follows, consider only the left half of Table 5. This half reports results concerning which species are dominant. The right half reports results about subdominance, and the explanation applies to the right half of the table if the word "dominant" in what follows is simply replaced by the word "subdominant."

Let U_T be the "uncertainty threshold" analogous to

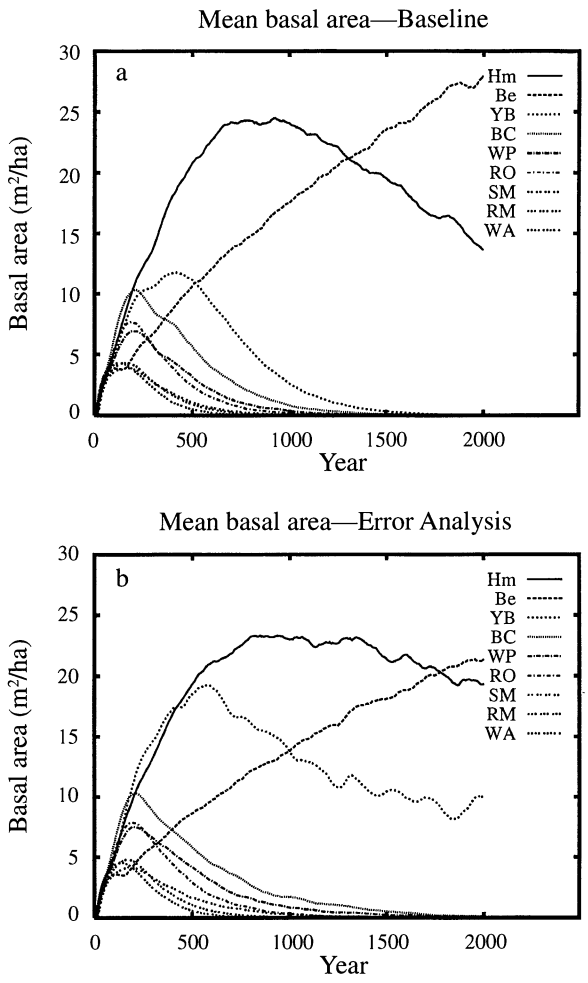

FIG. 7. Mean basal areas of each species produced by the (a) 100 baseline and (b) 100 error analysis runs. Note that the order of the species in the legend is the same as the order of the curves from top to bottom at approximately year 1100.

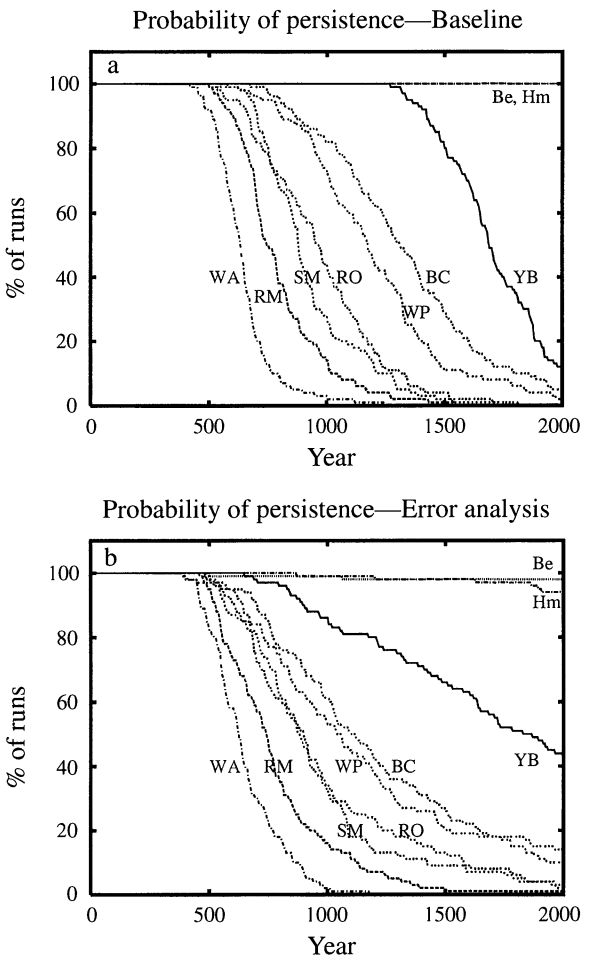

FIG. 8. Persistence of each species in the (a) 100 baseline and (b) 100 error analysis runs. The curve for a species gives the percentage of runs in which that species was still present (e.g., BC had not gone extinct by year 2000 in ≈5% of the baseline runs). The curves have shallower slopes in (b) than in (a) because of sampling uncertainty about the parameter estimates.

the significance level of a statistical test. The top half of the table describes results for $U_T = 25\%$, while the bottom half describes results for $U_T = 10\%$. An *N* in the table means that the species is dominant in less than U_T of the error analysis runs. Thus, an *N* indicates that SORTIE makes a reasonably strong prediction that the species is not dominant, despite the sampling uncertainty about parameter values. In contrast, a *Y* indicates that SORTIE makes a reasonably strong prediction that the species *is* dominant; a *Y* means that the species is dominant in more than $1 - U_T$ of the error analysis runs. The asterisks in Table 5 indicate that SORTIE does not make a strong prediction about dominance; the species is dominant in $\geq U_T$ and $\leq 1 - U_T$ of the error analysis runs. This community level uncertainty could be caused either by sampling uncertainty about parameter values or by the inherent stochasticity of the model. To separate these two sources of uncertainty, we add the subscript "+" to an asterisk if the species is dominant in $>1 - U_T$ of the *baseline runs,* and the superscript "−" if the species is dominant in $<U_T$ of the baseline runs. Thus, an asterisk without a superscript means that the inherent stochasticity of the model prevents a strong prediction, while a superscript means that sampling uncertainty about parameter values prevents a strong prediction.

The number of superscripted asterisks divided by the total number of strong predictions we could have made if sampling error had been zero (*N*'s + *Y*'s + superscripted asterisks) is a measure of how much predictive power we lose because of our uncertainty about parameter values. This ratio is 0.23 for predictions about dominants with an uncertainty threshold of 25%, 0.26 for predictions about subdominants with $U_T = 25\%$, 0.32 for dominants with $U_T = 10\%$, and 0.45 for subdominants with $U_T = 10\%$. Thus, we lose from one-quarter to one-half of our predictions because of sam-

TABLE 4. Results of error analysis and baseline runs. "E" indicates error analysis runs and "B" indicates baseline runs. "Top 2" indicates greatest two species in basal area. "Top 5" indicates greatest five species in basal area. The table entries

Species	Year 30				Year 60				Year 125				Year 250	
	Top 2		Top 5		Top 2		Top 5		Top 2		Top 5		Top 2	
	E	B	E	B	E	B	E	B	E	B	E	B	E	B
Be	0	0	7	0	1	0	19	10	1	0	6	6	5	0
He	30	2	95	100	33	28	83	81	40	47	95	100	64	94
SM	0	0	0	0	0	0	1	1	1	0	12	0	1	0
RM	0	0	25	0	3	0	31	16	2	1	28	8	0	0
YB	0	0	30	1	6	3	44	45	36	17	77	97	56	50
WP	21	0	78	100	19	15	74	78	21	1	74	89	15	2
RO	56	98	94	100	48	64	87	95	38	47	79	93	14	4
BC	64	100	99	100	62	73	91	98	57	87	93	98	45	50
WA	29	0	72	99	28	17	70	76	4	0	36	9	0	0

pling error. Finally, observe that the data in Table 4 may be used to construct tables like Table 5 for any value of U_T.

Table 5 contains three reasonably strong qualitative predictions about predicted patterns of dominance during succession. First, Be and Hm are predicted to be the late successional dominants, as evidenced by the *Y*'s in Table 5. Fig. 9 shows complete information about the dominance rank of Hm and Be in the error analysis and baseline runs. In this figure, curves labeled "1" indicate the number of runs in which a species was the most abundant species at each point in time, curves labeled "2" indicate that a species was among the top two most abundant species, curves labeled "3" indicate that a species was among the top three most abundant species and so on.

Note that Hm and Be were the two most abundant species late in succession in all baseline runs (Fig. 9a, b). Also, Be was among the top two in >90% of the error analysis runs late in succession and among the top three in >95% of error analysis runs (Fig. 9c). Moreover, early in succession, Be was among the top five species in <5% of error analysis runs (see years ≤20 in Fig. 9c). The case for Hm is marginally less strong (Fig. 9d). Hm was among the top two species in >90% of error analysis runs around year 500 and in 85–88% of error analysis runs between years 1500 and 2000. Also, Hm was among the top five species in >95% of error analysis runs late in succession, and surprisingly also very early in succession (first 50 yr; Fig. 9d). We attribute the early successional subdominance of Hm to its relatively high radial growth rate (Table 2), which under the uncrowded conditions early in succession can compensate for its squat architecture. Finally, although the baseline runs predict that Be will be more abundant than Hm by year 2000 (Fig. 9e), sampling uncertainty largely erases this prediction (Fig. 9f).

Our second qualitative prediction is that RO, BC, WA, RM, SM, and WP are neither dominant nor subdominant late in the runs (see the *N*'s late in succession in Table 5), but that the subset RO, BC, and WP collectively dominate communities early in succession (see the *Y*'s and *'s early in succession in Table 5). The case for high abundance rank early in succession is strongest for RO and BC. Fig. 10 shows that these species are predicted to be among the top three species early in succession in >95% of error analysis runs.

The relatively poor performance of RM and WA early in succession and of SM both late and early in succession deserve some comment. In a substantial fraction of error analysis runs, WA and RM were either dominant or subdominant early in succession (Table 4). Thus, we cannot conclude that WA and RM are predicted to be minor components of early successional forests. Rather, sampling error and the inherent stochasticity of the model prevent us from concluding that WA and RM are major components. Also, while SM is an important component of many late successional stands, especially in the midwestern states and more northern regions of the northeastern U.S., it is not a major component of the old growth in the vicinity of GMF (see *Results: Tests of SORTIE's dynamical predictions,* below). Finally, SM, RM, and WA are unusual in two respects. The radial growth functions of the maple species explain a far smaller fraction of the variance than the growth functions of any other species (see the R^2's in Table 2). As the sole dioecious species in SORTIE, WA has half the reproductive capacity of the other shade intolerants in the model. It is possible that females of dioecious species average twice the per capita seed production of hermaphrodites, but we currently have insufficient data to test this hypothesis (given the large interannual variation in seed production).

Our third qualitative prediction is that YB is a mid- to late-successional subdominant (see the *Y*'s from years 125 to 1000 in the upper right hand portion of Table 5). This conclusion is not as well supported as the previous two. Fig. 11 shows that YB is among the top three species in >90% of baseline runs between years 500 and 1000, and among the top five species in >90% of error analysis runs in some years between 400 and 700.

Sensitivity analysis

Sensitivity to G_3.—Changes in G_3 (annual growth of stem area for a canopy adult) had little impact on dy-

give the percentage of runs that each species was in each category. Obviously, extinct species were not eligible for either "Top 2" or "Top 5" status.

Year 250		Year 500				Year 1000				Year 2000			
Top 5		Top 2		Top 5		Top 2		Top 5		Top 2		Top 5	
E	B	E	B	E	B	E	B	E	B	E	B	E	B
45	46	33	47	97	100	78	100	97	100	91	100	97	100
98	100	87	100	99	100	82	100	99	100	88	100	94	100
20	6	1	0	25	6	0	0	23	11	0	0	2	0
17	3	0	0	14	3	0	0	12	3	0	0	1	0
86	100	55	47	89	98	34	0	80	99	19	0	40	12
76	72	9	0	61	73	1	0	42	56	0	0	8	2
66	75	2	0	44	22	0	0	28	23	0	0	2	0
82	97	13	6	67	96	5	0	50	76	0	0	14	5
10	1	0	0	4	2	0	0	1	0	0	0	0	0

namics. The three runs with high (126 cm^2) values of G_3 produced species compositions well within the range exhibited by the baseline runs, but predicted basal areas above the upper 97% curve in Fig. 6b. These basal areas reached peaks, ranging from 79 to 86 m^2/ha, that subsequently declined to values ranging from 53 to 57 m^2/ha by 2000 yr. In contrast, the low value of G_3 (63 cm^2) produced basal areas between the 25 and 75% limits in Fig. 6b, but predicted old growth communities in which Hm was consistently more abundant (factor of 3–4) than Be instead of the reverse (see Fig. 9e). All other aspects of community composition in the runs with low G_3 were indistinguishable from the baseline runs.

Sensitivity to initial diameter of seedlings.—Changes in the initial diameter of new recruits (to 1 and 4 mm) had no significant effects. All runs produced basal areas and community compositions well within the range of the baseline runs.

Sensitivity to initial densities.—All of the 27 runs in which one species was initiated at a 10-fold higher density than the others produced dramatic effects on community composition (Fig. 12). The species with the high initial density invariably remained the basal area dominant for a substantial period of time. White ash is SORTIE's least competitive species in old-growth (Fig. 7a), and yet remained the most dominant species through year 300 (Fig. 12a) when given an initial 10-fold numerical advantage. However, an initial advantage to any species except Be and Hm disappeared in the long term. Note that Be and Hm were the two most dominant species after year 1000 in all runs shown in Fig. 12. Similarly, although a doubling of total initial density (450 individuals/ha vs. 225 individuals/ha in

TABLE 5. Summary of error and baseline analyses. A) Y indicates >75% of error analysis runs, N indicates <25% of error analysis runs, * indicates ≤75% and ≥25% of both error analysis and baseline runs. *+ indicates ≥25% and ≤75% of error analysis runs but >75% of baseline runs, and *− indicates ≥25% and ≤75% of error analysis runs but <25% of baseline runs. B) same as A) but using thresholds of 90% and 10% instead of 75% and 25%.

	Year							Year						
Species	30	60	125	250	500	1000	2000	30	60	125	250	500	1000	2000
	Top two species in basal area							Top five species in basal area						
A)														
Be	N	N	N	N	*	Y	Y	N	N	N	*	Y	Y	Y
He	*−	*	*	*+	Y	Y	Y	Y	Y	Y	Y	Y	Y	Y
SM	N	N	N	N	N	N	N	N	N	N	N	*−	N	N
RM	N	N	N	N	N	N	N	*−	*−	*−	N	N	N	N
YB	N	N	*−	*	*	*−	N	*−	*	Y	Y	Y	Y	*−
WP	N	N	N	N	N	N	N	Y	*+	*+	Y	*	*	N
RO	*+	*	*	N	N	N	N	Y	Y	Y	*	*−	*−	N
BC	*+	*	*+	*	N	N	N	Y	Y	Y	Y	*+	*+	N
WA	*−	*−	N	N	N	N	N	*+	*	*−	N	N	N	N
B)														
Be	N	N	N	N	*	*+	Y	N	*	N	N	Y	Y	Y
He	*−	*	*	*+	*+	*+	*+	Y	*	Y	Y	Y	Y	Y
SM	N	N	N	N	N	N	N	N	N	*−	*−	*−	*	N
RM	N	N	N	N	N	N	N	*−	*	*−	*−	*−	*−	N
YB	N	N	*	*	*	*−	*−	*−	*	*+	*+	*+	*+	*
WP	*−	*	*−	*−	N	N	N	*+	*	*	*	*	*	N
RO	*+	*	*	*−	N	N	N	Y	*+	*+	*	*	*	N
BC	*+	*	*	*	*−	N	N	Y	Y	Y	*+	*+	*	*−
WA	*−	*	N	N	N	N	N	*+	*	*−	*−	N	N	N

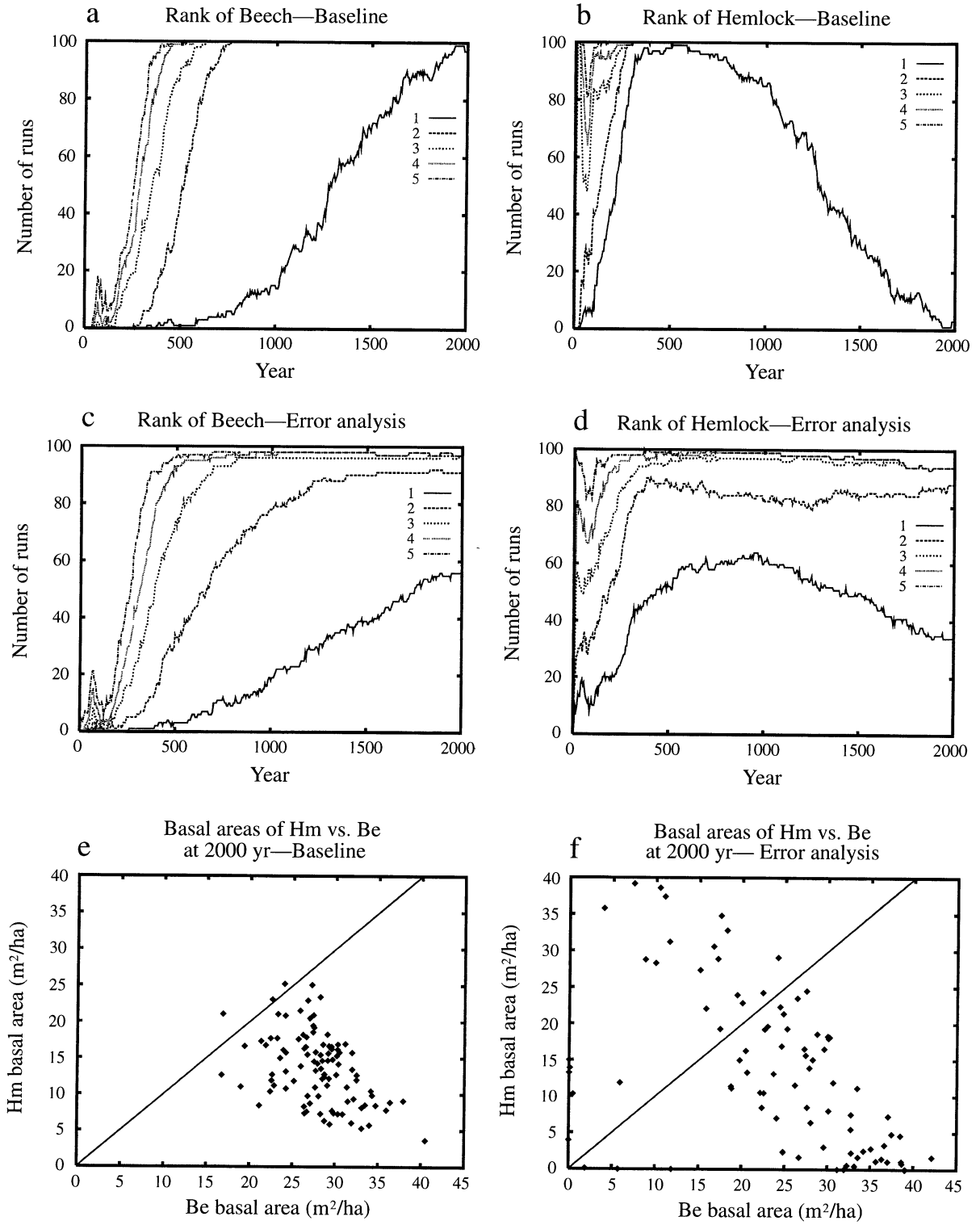

FIG. 9. Relative dominance of Be and Hm in the (a, b, e) baseline and (c, d, f) error analysis runs. The key in (a–d) is interpreted as follows. The curve labeled "1" shows the fraction of runs in which the species was the most abundant species present (greatest basal area). The curve labeled "2" shows the fraction in which the species was one of the two most abundant species present, and so on. For example, Be was the most abundant species at year 2000 in 98/100 baseline runs, but in only 56/100 error analysis runs. This difference is caused by sampling uncertainty about parameter values. (e) shows the basal areas of Hm and Be at year 2000 in the baseline runs. Note that Be is more abundant than Hm in 97/100 runs. (f) shows the corresponding plot for the error analysis runs. The wide scatter of the relative abundances in (f) shows that sampling error prevents a strong prediction that Be will dominate Hm late in succession.

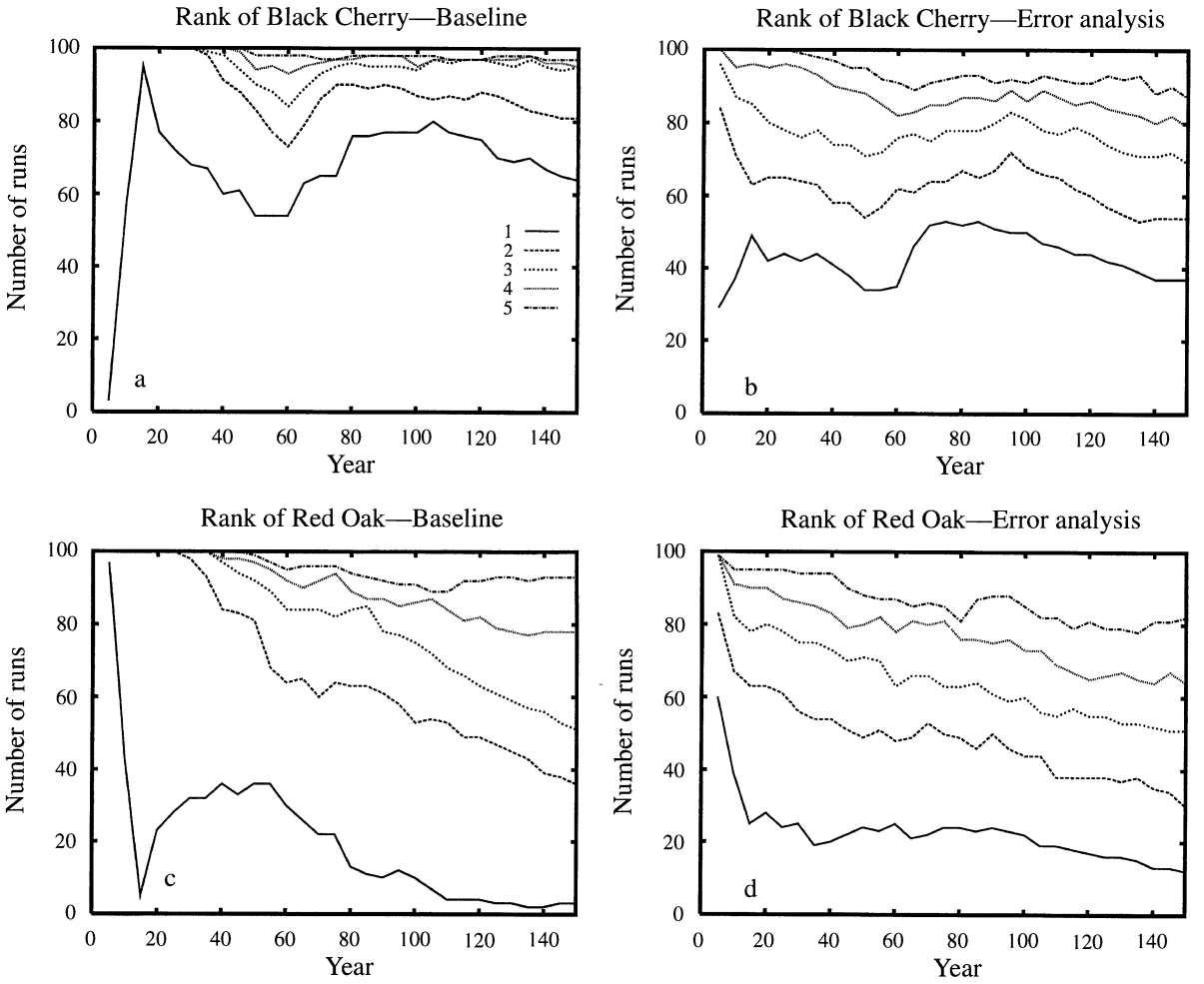

FIG. 10. Relative dominance of (a, b) BC and (c, d) RO in the (a, c) baseline and (b, d) error analysis runs. The key is interpreted as follows. The curve labeled "1" shows the fraction of runs in which the species was the most abundant species present (greatest basal area). The curve labeled "2" shows the fraction in which the species was one of the two most abundant species present, and so on. For example, BC was the most abundant species at year 15 in 96/100 baseline runs, but in only 49/100 error analysis runs. This difference is caused by sampling uncertainty about parameter values. The plots show only years 0–150 of the 2000-yr runs because they are intended to document the high abundances of RO and BC early in succession. Both species tend to be eliminated late in succession (see Fig. 8).

the baseline runs) produced initially higher total basal areas, these differences also disappeared during the course of succession (between year 100 and 500 depending on the species given the initial advantage).

The implication here is that second growth stands will be dominated by initial conditions for periods exceeding the age of most forest stands in northeastern North America. An understanding of community composition in these forests will require an understanding of the processes controlling initial composition (e.g., historical patterns of land use). Obviously, these processes are not included in SORTIE.

The runs in which we halved the initial densities of all species (12 individuals/ha) produced community compositions and total basal areas similar to baseline runs with the unsurprising exceptions of consistently lower basal areas for the first 50–100 yr (reflecting the lower initial densities) and marginally higher abundances of the shade intolerant species early in succession (reflecting the enhanced ability of these species to capitalize on unoccupied space, see the high-light growth rates and dispersal distances in Table 3).

In contrast, the runs with 10-fold higher initial densities of every species (250 individuals/ha of each species) revealed a significant flaw in SORTIE. Our mortality submodels are apparently unable to cause sufficient self-thinning of dense even-age stands of large saplings. For this reason, total basal area in runs with high initial densities climbed to unrealistically high levels early in succession, and fell to reasonable values only after 300–400 yr (see Fig. 13). All else being equal, the radial growth function (Eq. 3) and the growth-dependent mortality function (Eq. 6) specify mortality probabilities that decrease as sapling size in-

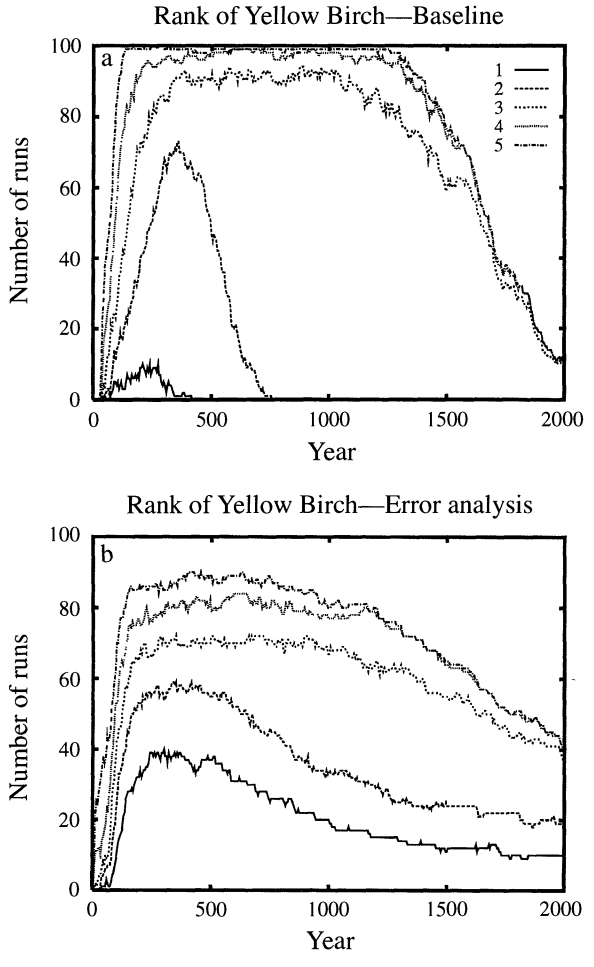

FIG. 11. Relative dominance of YB in the (a) baseline and (b) error analysis runs. The key is interpreted as follows. The curve labeled "1" shows the fraction of runs in which YB was the most abundant species present (greatest basal area). The curve labeled "2" shows the fraction in which the species was one of the two most abundant species present, and so on. For example, YB was among the top three most abundant species at year 500 in ≈90/100 baseline runs, but in only 70/100 error analysis runs. This difference is caused by sampling uncertainty about parameter values.

creases (because ring width increases with radius in (3)). These dependencies were included in the growth and mortality functions simply because they are in our data. However, the data include only saplings <10 cm dbh, and apparently do not capture processes that determine resource-dependent mortality of larger individuals. This problem was not apparent in the baseline and error analysis runs because initial densities were lower. Note however, that the peak in basal area early in succession in the baseline runs (Fig. 6b) is symptomatic of the problem. Also, the problem apparently does not affect seedlings produced by trees in the model because these have smaller initial size (0.2 cm dbh instead of 1 cm dbh for the saplings used to initiate a run), and because seedlings produced by trees grow under closed canopy or in relatively small gaps instead of the open conditions present at the beginning of a run. Note that the problem might be expected to surface in runs with high fecundity and large catastrophic disturbance. Finally, because of the high basal areas, understory light levels were low early in succession in the runs with high initial densities. This caused a more rapid successional dominance by the shade tolerant species Hm and Be.

Sensitivity to R_2.—Changes in fecundity (controlled by R_2) of all species simultaneously had no detectable effect on total basal area, but some effect on community composition. First, shade intolerant species were favored by decreasing the R_2's from 5:2 (all other species : Be) in the baseline runs to 2.5:1 (Fig. 14a). Fully six species were present in year 2000 of all three runs with R_2's of 2.5:1. Although Hm was the dominant species by a factor of 3 at the end of these runs, the most shade tolerant species, Be, was invariably a minor component (Fig. 14a). In contrast, increasing the R_2's to 10:4 or 20:8 produced community dynamics indistinguishable from the baseline runs (see the examples in Fig. 14b, c).

The stem densities predicted by SORTIE in the R_2 sensitivity analysis match well with observed densities of natural stands in the published literature. The total stem densities predicted by SORTIE, for all species >0.2 cm diameter at 10 cm height, varied as follows in the three replicate runs for the following R_2 ratios (other species : beech): 2.5:1 = 858–922 stems/ha; 5:2 = 1707–1825 stems/ha; 10:4 = 3410–3708 stems/ha; 20:8 = 8191–8403 stems/ha. These results are at year 2000, but the size density pattern produced by the model stabilized quickly (within 100–200 yr) with the typical inverse J-shaped size distribution pattern.

The results predicted for the R_2 ratios of 5:2 and 10:4 are most consistent with densities of comparable stands reported in the literature, relatively few of which provide complete size distributions (i.e., >0 cm dbh): Kelty (1984) reports, for one 87-yr-old stand at Great Mountain Forest in Connecticut, a total stem density for individuals >0 cm dbh of 1450 stems/ha; Potzger (1946), for a series of old-age northern hardwood stands in the Great Lakes area, reported densities (>0 cm stem diameter at 1 m) of 711–3505 stems/ha (mean = 1948, n = 17); Henry and Swan (1974) reporting on an old-age northern hardwood stand (in 1907) in New Hampshire, gave a density of 2125 stems/ha for all size classes.

It is possible to find reported stand densities outside these middle ranges predicted by SORTIE. For some undisturbed old-age stands dominated by very large stems, the reported densities can be quite low: for a cove forest in Tennessee (with seven of our species), the density reported by Clebsch and Busing (1989) for all individuals taller than 1.37 m was 863 stems/ha. For other stands, particularly younger stands or stands showing little effect of current or past deer browse, the

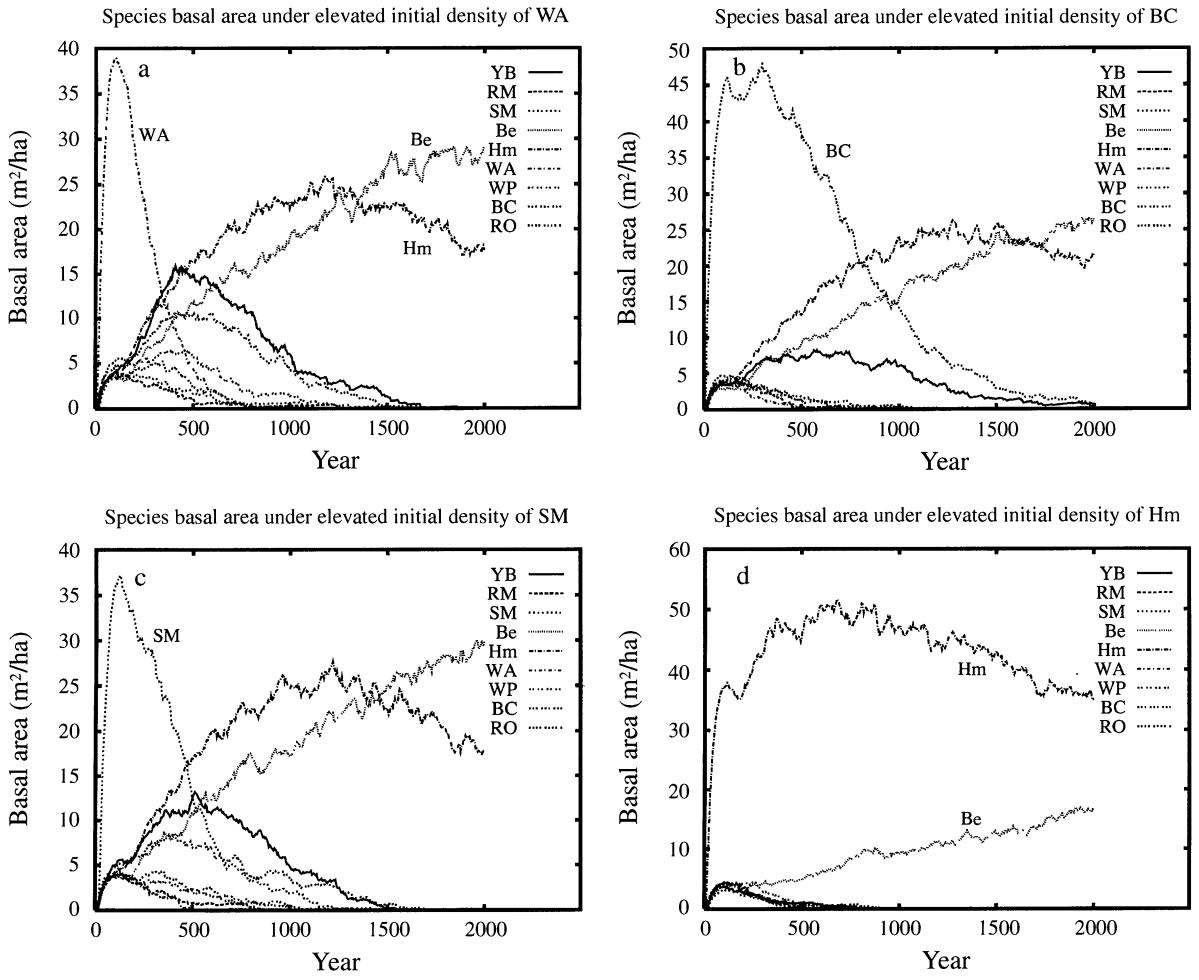

FIG. 12. Sensitivity of community dynamics to initial abundances. The initial abundance of a single species was set at 250 m²/ha, and all remaining species were initiated at a density of 25 m²/ha (per species). The species with the 10-fold higher initial abundance was WA in (a), BC in (b), SM in (c), and Hm in (d). Note the prolonged period of dominance by the species with the elevated initial abundance (compare to the baseline results in Fig. 7a). Each panel is a representative example of three replicate runs.

reported densities can be greater than what we predict: Kelty's (1984) 44-yr-old stand in central Massachusetts had a density of 4210 stems/ha for all individuals >0 cm dbh; one of Potzger's (1946) plots "earlier in secondary succession" had 5772 stems/ha; for an old-age northern hardwood stand in Vermont, Bormann and Buell (1964) reported densities (for all individuals >30.5 cm in height) of 4534 stems/ha; for three old-age northern hardwood stands in Wisconsin, with little apparent browsing, Stearns (1951) reported densities of 10 157–17 705 stems/ha for all sizes. In the last example, 90% of these were sugar maple seedlings and saplings <2.5 cm dbh.

This observed variation in reported stand densities undoubtedly reflects differences in stand age and dominance by smaller or larger size classes, the effects of browsing by deer (which depletes smaller size classes), sampling error associated with small plot sizes, species specific differences in patterns of size density relationships, etc. Nevertheless, the mean for the 25 plots is 3474 stems/ha, well within the mid-range of densities predicted by SORTIE. We therefore selected R_2's of 2:5 for most of the runs in the paper because larger R_2's of 10:4 would have required approximately twice the computer time.

In contrast to the limited effects of changing all species' R_2's simultaneously, we observed relatively large effects of elevating the R_2 of one species to either 8 (Be) or 20 (all others) and keeping all remaining species at 5:2. For all species except the three most dominant species late in succession in the baseline runs (Be, Hm, and YB), the effect was limited to a period of initial dominance by the species with the elevated fecundity (examples for RM and RO in Fig. 15a, b). If either Be, Hm (Fig. 15c), or YB (Fig. 15d) was given the fecundity advantage, then it became the most dominant species relatively early in succession and remained so through year 2000. However, neither Hm

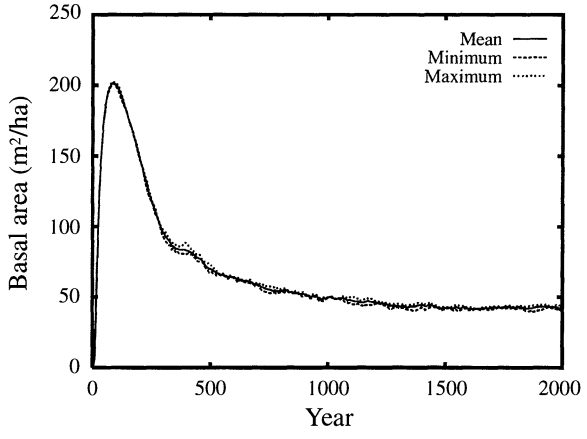

FIG. 13. Total basal area predicted by SORTIE if the initial abundance of each species was 250 m²/ha. Note the unrealistically high basal areas early in succession (compare to the baseline results and data in Fig. 6 a, b). The three curves show three replicate runs.

nor Be was driven extinct in any of the 27 runs. Note also that the basal areas predicted by runs dominated by YB (Fig. 15d) were well above basal areas in the baseline runs (Fig. 6b). The correspondence between dominance by YB and high basal area is supported by the error analysis. Those few error analysis runs dominated by YB (Fig. 11) were the same runs that produced extremely high basal areas (see Fig 6d). We suspect that YB-dominated communities achieve unrealistically high basal areas in SORTIE because YB trees cast less shade than Be or Hm trees and because YB is relatively fast-growing at low light levels (see Table 3).

The implication here is that interspecific differences among R_2's could matter if these differences were large enough. Again, we do not, at present, have sufficient data to span the range of temporal variation in estimates of the R_2's (e.g., due to masting). We thus cannot yet estimate average values of the R_2's with confidence from our field data.

We now turn to the sensitivity analysis for two groups of parameters (the R_1's and E's) also included in the error analysis. Recall that we expanded the sensitivity analysis to investigate R_1's and E's well outside their 95% confidence limits because of statistical concerns about the estimated sampling distributions of these parameters (see *Methods: Statistical concerns*).

Sensitivity to R_1.—Decreases in dispersal caused by doubling estimates of R_1 produced substantial changes. Basal areas were higher than in most baseline runs (compare Figs. 6b and 16). These increases in basal area were associated with an increase in the dominance of longer-dispersing shade intolerant species. For example, in one run WP was the most dominant species at 2000 yr and was three times more abundant than the second most dominant species. Fully six species were present at 2000 yr (WP, YB, BC, RO, Hm, and Be).

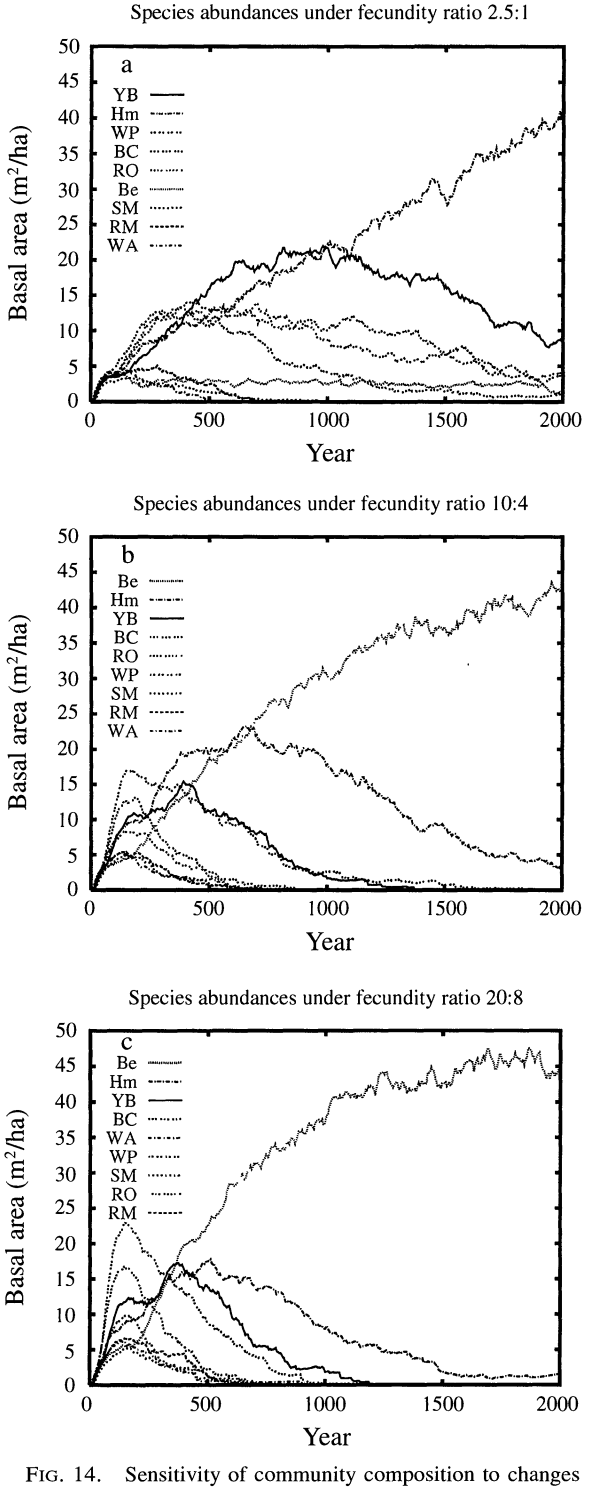

FIG. 14. Sensitivity of community composition to changes in the fecundity parameter R_2. R_2's were (a) 2.5:1 (all other species : Be), in (b) 10:4, and in (c) 20:8. Results for R_2's of 5:2 (the baseline runs) are shown in Fig. 7a. The order of the species in the legend corresponds to the order of the curves from top to bottom at year 750. Each panel is a representative example of three replicate runs.

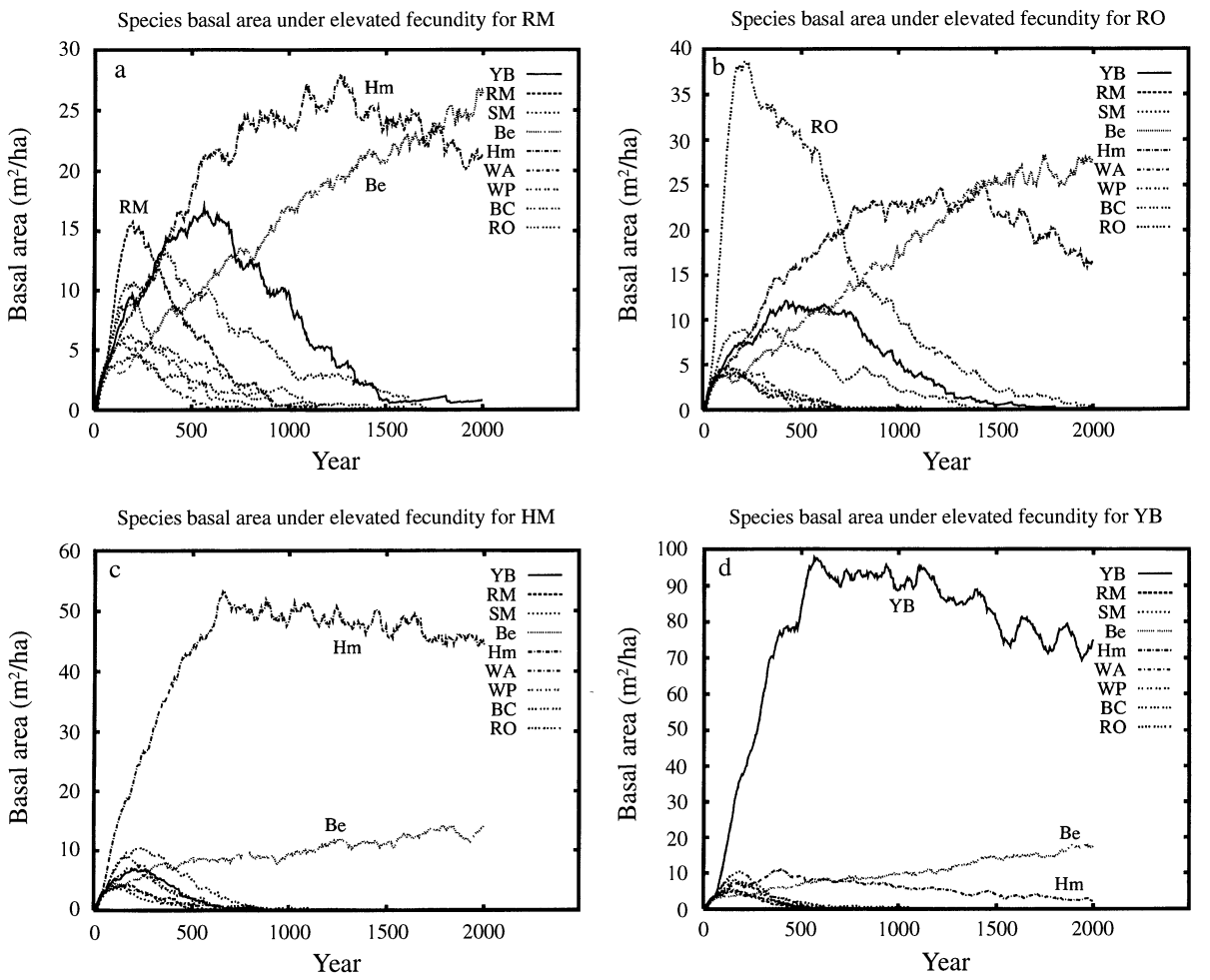

FIG. 15. Effects on community composition of quadrupling a single species' fecundity parameter (R_2). The R_2 of one species was set at 20:8 (all other species : Be) and all others were set at the baseline values 5:2. The species with elevated R_2 was RM in (a), RO in (b), Hm in (c), and YB in (d). Note the prolonged period of dominance by the species with the elevated R_2 (compare to the baseline runs in Fig. 7a). Each panel is a representative example of three replicate runs.

Effects were less dramatic in the other two runs, but species diversity at 2000 yr remained higher than in most baseline runs (four species in one run and five in the other). Apparently, Be and Hm cannot capitalize on available space in the model if their dispersal distances are significantly lower than the ranges predicted by our estimated sampling distributions. We suspect that the relatively light shade cast by shade intolerants is responsible for the elevated basal areas, just as in runs dominated by YB that were discussed previously (e.g., Fig. 15d).

Increases in dispersal distances caused by halving estimates of R_1 produced less dramatic effects. Basal areas were within the range produced by the central 50% of baseline runs. The only obvious change in community composition was that YB became extinct marginally more quickly than in most baseline runs—by year 1250 in all three runs and by year 1100 in one run (compare to the baseline results in Fig. 8a). Thus, doubling and halving the R_1's produced consistent effects. Artificially low dispersal distances caused a shift toward shade intolerants, while artificially high dispersal distances caused a shift toward shade tolerants.

Sensitivity to the E_t.—Reducing estimated crown opennesses (the e^{-E_t}) by 50 or 75% produced no substantial shifts in community composition (*data not presented*), but some decrease in basal area (compare Figs. 6b and 17a). Increasing crown opennesses by 50% also had no substantial effect on species composition, but caused both marked increases and sustained oscillations in basal area (Fig. 17b). We suspect that effects on community composition were negligible simply because changes in the density of canopy trees compensated for the changes in the amount of shade cast by each tree, thus making light levels in the understory similar across runs. We do not completely understand the sustained oscillations caused by artificially high opennesses. It is interesting, however, that sustained oscillations also occur in the few error analysis runs dominated by YB, a species with high openness relative

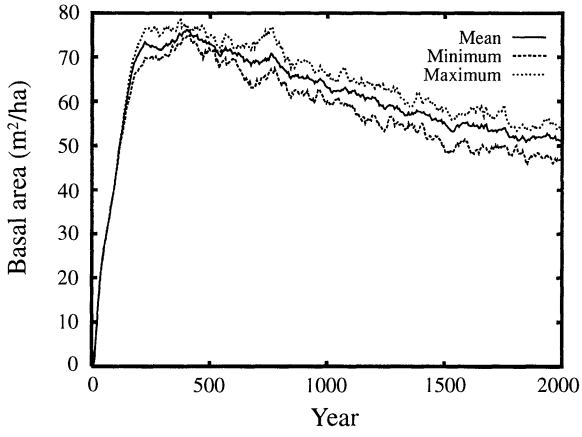

FIG. 16. Sensitivity of total basal area to increases in the estimated values of R_1 (the dispersal parameters). All species' R_1's were increased simultaneously well outside their 95% confidence limits (details in *Methods*). Note the generally higher basal areas than in the baseline runs (Fig. 6b). The three curves show three replicate runs.

to the usual late successional dominants Hm and Be (the upper 97% curve in Fig. 6d is "spiky" because of these runs).

Spatial distributions

Spatial aggregation and interspecific segregation of Hm and Be.—The spatial autocorrelation analysis of the 1-km² runs showed no significant clumping at scales >10 m for any species other than Be and Hm. Although spatial distributions of Hm and Be were initially random, significant ($P < 0.05$) positive autocorrelations at scales of 20 m developed by year 500. These clusters increased in size until year 1000 (significant autocorrelations up to 50 m) and then persisted without additional size increases through year 2000. Clumps tended to be dominated either by Hm or Be, but not both. Thus, spatial cross-correlations between Hm and Be were significantly negative up to 30 m (see Fig. 18). Moreover, the clumps of Hm and Be were largely stationary. We superimposed a 10 × 10 m grid on the modeled plots and recorded the dominant species in each grid cell at year 500, 1000, and 2000. Fully 95% of cells dominated by Be in year 500 remained so in year 2000. The corresponding number for Hm was 76%.

In summary, SORTIE predicts that competition and dispersal will cause a mosaic of stationary monodominant patches of Hm and Be to develop in old-growth even if the habitat is physically homogenous and spatial distributions are initially random. These species are the two shortest dispersing and most shade tolerant species in the model. The spatial distributions of the other species remain approximately random and are superimposed on this mosaic.

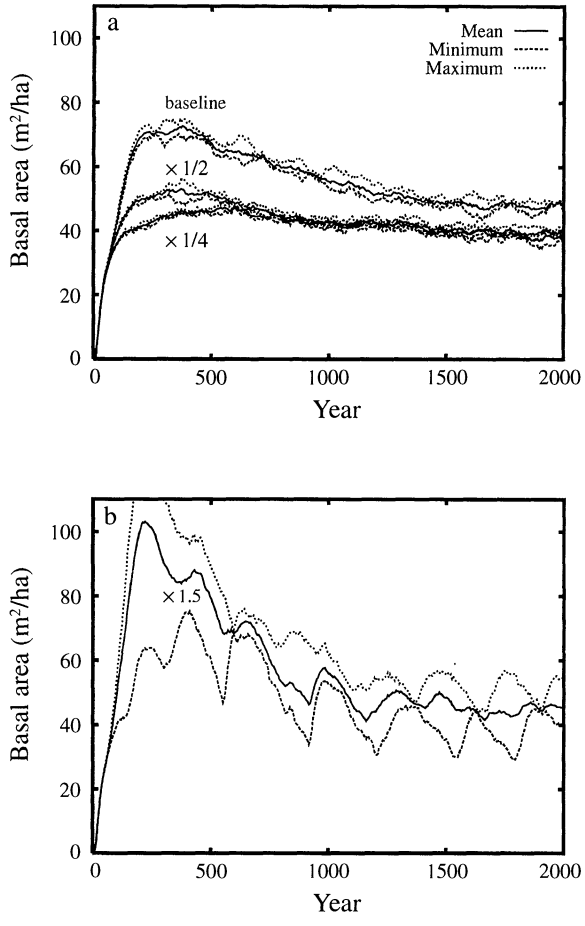

FIG. 17. Sensitivity of total basal area to changes in the crown openesses (the e^{-E_i}) of all species simultaneously. Estimated openesses were multiplied by ½ and ¼ in (a) and by 1.5 in (b). Three replicates are shown for each case. (a) also shows three replicates using the estimated openesses (labeled baseline). See Fig. 6b for results from the full 100 baseline runs.

Tests of SORTIE's dynamical predictions

In this section we test five predictions of the SORTIE model that were found to be most robust to sampling uncertainty in the error analysis. These include a system level prediction:

1) the successional increase of basal area shown in Fig. 6;

three predictions about community composition:

2) the dominance of Be and Hm and near absence of RO, BC, WA, RM, SM, and WP late in time,
3) the early dominance of RO, BC, and Hm,
4) the mid-to-late subdominance of YB;

and one prediction about spatial distributions:

5) the intraspecific clumping and interspecific spatial segregation of Be and Hm in old-growth.

Basal area.—We compiled a chronosequence of basal areas from natural stands located in or near GMF

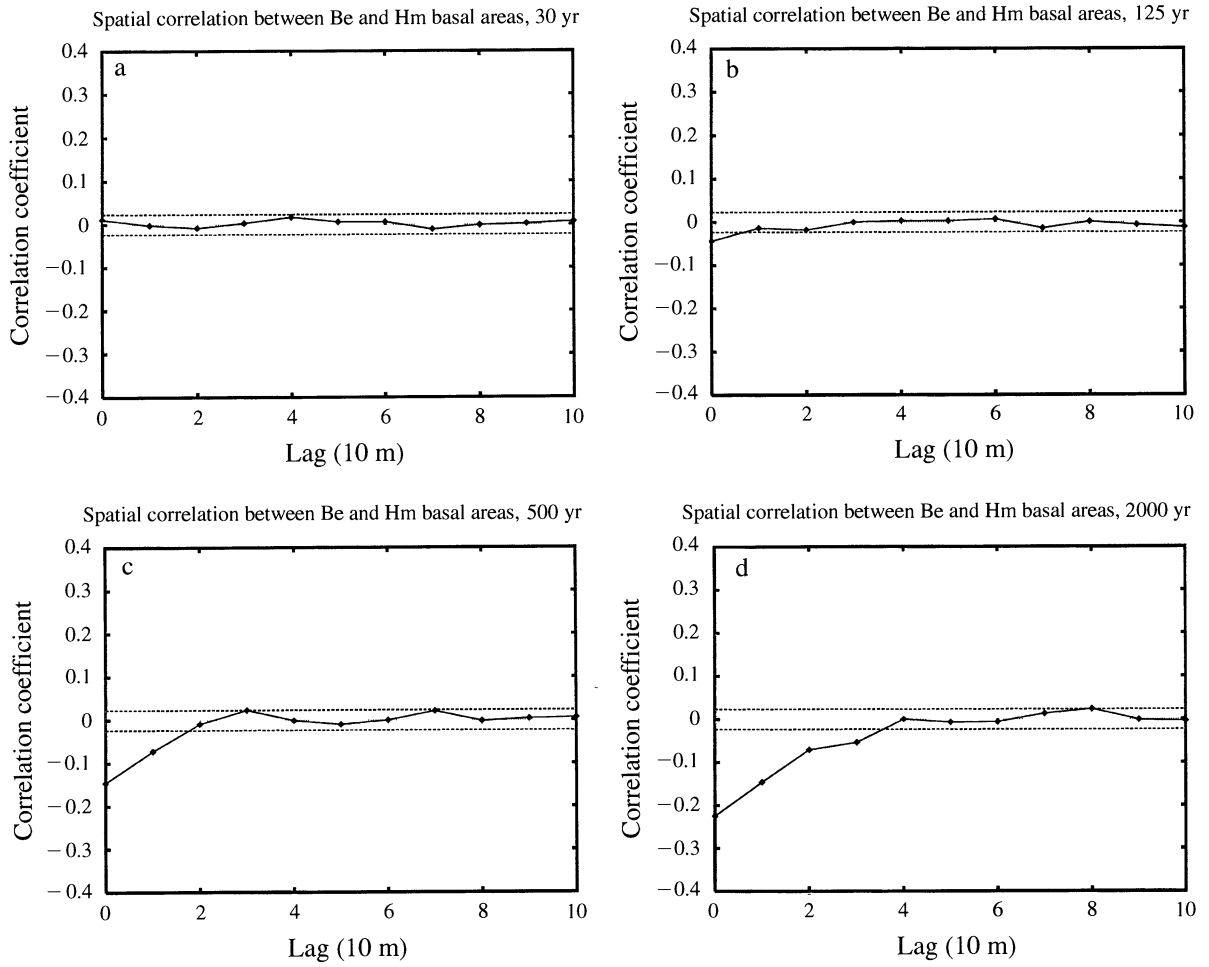

FIG. 18. Spatial cross correlations among Hm and Be showing the development of interspecific spatial segregation during succession. The dashed lines show the $P < 0.05$ significance thresholds. (a) corresponds to year 30, (b) to year 125, (c) to year 500, and (d) to year 2000. Note that negative cross correlation develops through time at progressively larger scales. The figure shows a representative example of three replicate 1-km^2 runs.

(shown by the diamonds in Fig. 6a, c). These come from the following sources: 50 yr (10 40–50 yr old stands in northwestern Connecticut and central Massachusetts; Stephens and Waggoner 1980, Kelty 1984, G. R. Stephens, *unpublished data*; the diamond gives the mean and the bars give the range), 65 and 95 yr (stands in GMF; Stephens and Hill 1971, G. R. Stephens, *unpublished data*), 135 yr (Catlin Woods near GMF in northwestern Connecticut; Kelty 1984), and 143 yr (Catlin Woods; G. R. Stephens, *unpublished data*). Observe that the agreement between the model and data is generally quite good. However, this correspondence must be evaluated in the context of the wide range exhibited by the 50-yr data; other successional ages probably exhibit similar variation in nature. In addition, the sensitivity analysis shows that basal areas predicted by the model early in succession depend strongly on initial densities, and we lack information about initial conditions in the natural stands.

We also compiled records of 30 old-growth or "virgin" stands in New York, Pennsylvania, New England, and the northern midwestern U.S. (Nichols 1913, Hough and Forbes 1943, Potzger 1946). The mean and range of basal area in these data is shown by the diamond and bars at year 2000 in Fig. 6b, d. Again, the agreement between the model and the data is quite close. Note that even the range in the data is close to the range exhibited by the baseline runs from years 400–2000. The late-successional agreement in Fig. 6b, d is probably a stronger validation of the model than the early-successional agreement in 6a, c, because effects of initial conditions almost certainly decrease with stand age.

Community composition.—Fig. 19 shows the average species composition for the 30 natural old-growth stands discussed, together with the average composition predicted by the baseline runs of SORTIE at years 500 and 1000. The corresponding inter-stand and 96% inter-run ranges are found in Table 6 and shown by the bars in Fig. 19. The natural old-growth stands were

TABLE 6. Predicted and actual community composition of old-growth stands. Table entries indicate percentage of total basal area. Baseline mean is the mean of the baseline runs; baseline 96% range is the range of central 96 of 100 baseline runs; error analysis 96% range is the range central 96 of 100 error analysis runs; stand mean is the mean reported for old-growth in the literature; and stand range is the range among stands reported in the literature.

	500 yr			1000 yr			Data	
Species	Baseline mean	Baseline 96% range	Error analysis 96% range	Baseline mean	Baseline 96% range	Error analysis 96% range	Stand mean	Stand range
Hm	37	27–46	6–62	52	35–66	1–87	32	10–40
Be	20	12–31	2–28	39	26–62	1–73	27	10–40
YB*	20	11–29	2–84	6	2–13	0–87	11	3–15
BC	10	2–20	0–34	2	0–8	0–29	3	0–5
WP	5	1–11	0–23	1	0–4	0–11	2	0–5
RO†	4	1–12	0–16	<1	0–2	0–7	8	0–10
SM	2	1–4	0–13	<1	0–1	0–6	13	10–20
RM	2	0–4	0–9	<1	0–1	0–1	2	0–4
WA	1	0–2	0–4	<1	0–<1	0–<1	2	0–3

* Includes black birch (YB and black birch not discriminated in most reports).
† Includes white oak (RO and white oak not discriminated in most reports).

overwhelmingly dominated by the species in SORTIE, with an average of only 6% of basal area consisting of other species.

The agreement between the model and data in Fig. 19 and Table 6 is obviously excellent with one exception. Sugar maple is significantly more abundant in old-growth stands in many regions of northeastern North America than in our baseline runs (average of 13% of basal area in the data and ≤2% in the model). There are at least two possible explanations for the uncompetitiveness of SM in SORTIE. First, the 96% upper bound for SM in the error analysis runs is equal to the mean of the data; ≈1 in 20 error analysis runs produced SM abundances of at least 13% in year 2000 (see Table 6). Thus, it is possible that SM's uncompetitiveness in the model is caused by sampling error. This view is supported by the low R^2 of the regression defining SM's radial growth submodel (Table 2). Second, the test data set covers a relatively wide geographic range. It is possible that SM is less competitive at our specific study sites at GMF than in some of the locations included in the test data set. For example, sugar maple survival at low light is much higher on nearby calcareous soils than on the sandy, acidic soils of GMF (Kobe et al. 1995). This difference results in significantly higher predicted abundance of sugar maple on calcareous soils (R. S. Kobe, *unpublished data*).

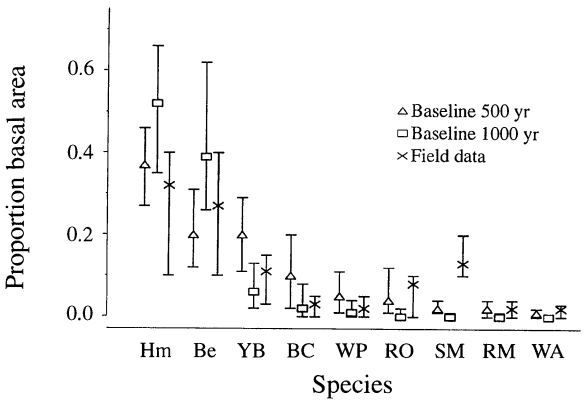

FIG. 19. Predicted and actual community composition in old growth (% of total basal area for each species). Diamonds give the means from the 100 baseline runs at yr 500 and squares give the means from yr 1000. 96% of baseline runs predicted values between the upper and lower bars projecting from each diamond or square. The crosses show the means from 30 natural transition oak–northern hardwoods forests reported as "virgin" or "old-growth" in the literature (citations in text). The bars projecting from the crosses show the range of values reported in the literature.

Table 7 contains the mean and range of community composition for the 10 40–50 yr-old natural stands in southern New England. Observe that the between-stand ranges in the final column are considerably wider than the ranges for old-growth forests in the final column of Table 6. We suspect that the early-successional ranges are large because of natural variation in the initial species composition (e.g., caused by the community composition of nearby seed sources and advanced regeneration present at the site). Again, SORTIE predicts that initial abundances have a strong influence on community composition early in succession (e.g., Fig. 12). Because we do not know the initial conditions for most of the natural stands in Table 6, it is pointless to compare these communities to the predictions of the baseline or error analysis runs. In Pacala et al. (1993), we showed that SORTIE was able to predict the community composition reported in two studies of species composition 40–50 yr after catastrophic disturbance (clear-cutting or hurricane damage) of old growth of known composition.

For obvious reasons, direct observations of long-term forest succession are rare. One of the best long-term data sets that is relevant to our study sites is the 60-yr record of change in canopy composition for four second-growth mixed hardwood stands in central Connecticut (Stephens and Waggoner 1980, Stephens and Ward 1992). The stands are at lower elevations than

TABLE 7. Actual community composition of 40–50 yr old stands. Values are percentage of total basal area (BA). Data from Stephens and Waggoner 1980, Kelty 1984, and G. R. Stephens, *unpublished.*

Species	Mean BA (%)	Between-stand range of BA (%)
Hemlock	24	0–49
Beech	10	0–75
Yellow birch*	13	0–57
Black cherry	5	0–59
White pine	18	0–100
Red oak†	17	0–50
Sugar maple	5	0–57
Red maple	6	0–37
White ash	1	0–1

* Includes black birch (yellow birch and black birch not discriminated in most reports).

† Includes white oak (red oak and white oak not discriminated in most reports).

Great Mountain Forest, and contain little hemlock (and instead have greater abundance of sugar maple and oaks); however, the current ages (≈100 yr) and disturbance histories (extensive logging during the 19th century, followed by little subsequent management) of the stands are comparable to our study sites. Between 1927 and 1987, red oak declined in relative density but increased in relative basal area as large oaks assumed dominance of the early successional canopy (Oliver 1978). Red maple (an early dominant) was already declining in both relative density and basal area by 1987. Sugar maple, yellow birch, and beech had all increased in relative basal area over the 60-yr period (Stephens and Ward 1992).

Spatial distributions in old growth.—The prediction that spatial distributions of Hm and Be are clumped and interspecifically segregated is supported by frequent observations of patchy distributions of late-successional tree populations (e.g., Jones 1945, Forcier 1975, Pigott 1975, Fox 1977, Frelich et al. 1993; but see Williamson 1975).

In addition, the prediction that clusters of Be or Hm persist for long periods of time in the same place is at least partly supported by a series of papers on the paleoecology of Hm–SM stands in upper Michigan (Davis et al. 1992, 1994, Frelich et al. 1993). Because this location lies outside the range of Be, Hm replaces Be as the most shade tolerant species present and SM replaces Hm as the second most shade tolerant species. Davis and her colleagues mapped the past spatial distribution of several stands by sampling buried pollen in small hollows located throughout the stands. Each hollow collects pollen from a relatively small area (e.g., 50% from within 30–50 m; Davis et al. 1994). The pollen data show that SM and Hm invaded the area ≈8000 and 3200 yr ago (respectively), and formed spatially segregated clusters (Davis et al. 1992, 1994). These clusters have remained in the same locations for 3000 yr and are now ≈100 m in diameter (e.g., significant spatial autocorrelations of 100 m for Hm and 120 m for SM in the site described in Frelich et al. 1993). Note that the clusters of shade tolerants produced in SORTIE by year 2000 are smaller (≤50 m) than the natural clusters in upper Michigan, a prediction also obtained by Frelich et al. (1993) using a simple spatially Markov model in which tree-by-tree replacement probabilities are dependent on the species occupancy of focal and neighboring spatial cells. Davis et al. (1994) suggest that the relatively rapid formation of large clusters evident in the pollen record (e.g., 200 years for Hm) was caused by climatic conditions present 3000 yr ago that facilitated patchy invasion (climatically induced amplification of effects of heterogeneous soils). Exploratory runs of the SORTIE model with patchy initial spatial distributions predict large stationary patches of Hm and Be, with late-successional patch size an increasing function of initial patch size.

Summary of tests.—Published data provide support for each of predictions 1–4 (in *Results: Tests*). Although these tests are by no means definitive given the variability in both the data and model output, it is at least clear that the published studies do not falsify any of the predictions (1–4). The strongest test of the model is probably its ability to generate the species composition and the spatial pattern in natural old-growth (predictions 2 and 4). We emphasize that we did not calibrate the model using any data from old-growth, nor tune the model to produce any community- or ecosystem-level phenomenon. Thus, the model would have produced unrealistic old-growth if our data on individual trees had omitted or failed to characterize critical processes that structure natural old-growth. The second strongest test is the excellent agreement between predicted and actual mean basal areas (prediction 1). However, our enthusiasm for this agreement is tempered by the large variability among natural stands and replicate runs, and by the unrealistically large early successional basal areas predicted with high initial abundances of saplings (e.g., Fig. 13). Finally, the support for predictions regarding community composition early in succession (prediction 3) is probably the weakest, given the extreme variability among natural early-successional stands, the lack of information about the initial conditions in these stands, and the large effect of initial abundances on the early-successional species composition produced by the model.

Causes of SORTIE's community level predictions

In this section we test some simple hypotheses that explain the community level predictions (2–5 in *Results: Tests*) in terms of species-specific attributes of individual plants. We do not attempt to explain predictions about total basal areas (prediction 1) simply because the sensitivity analysis has already shown that total basal area is controlled by a multitude factors,

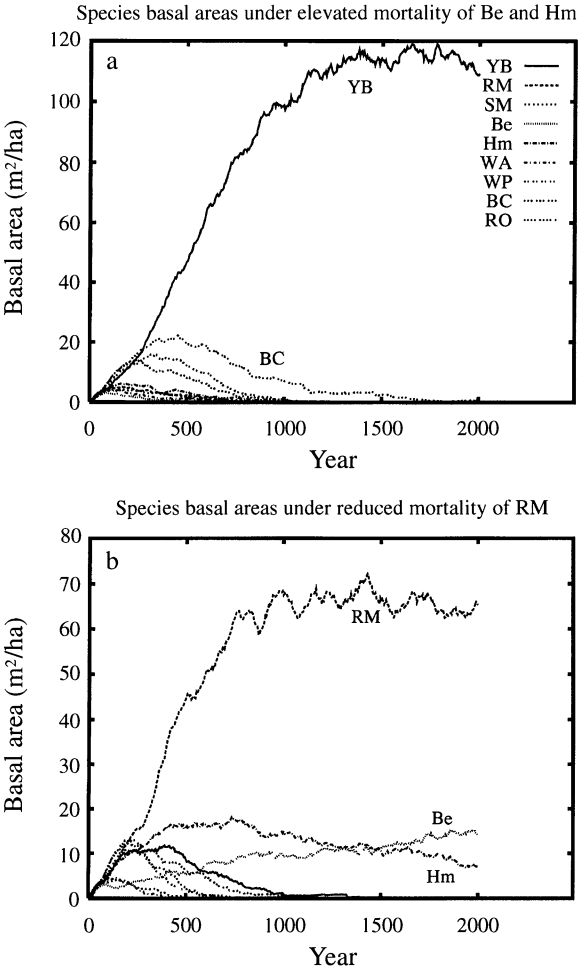

FIG. 20. (a) Effects of replacing the growth-dependent mortality function of Be and Hm by that of RM. Note that Be and Hm are the two least abundant species in the run, in contrast to the late-successional dominance of these species in the baseline runs (Fig. 7a). (b) Effects of replacing the growth-dependent mortality function of RM by that of Be. Note that RM becomes the late-successional dominant. Each panel is a representative example of three replicate runs.

including initial abundances, shade cast by an individual, dispersal, fecundity, and the response of growth and mortality to light.

First, the obvious hypothesis explaining the late-successional dominance of Hm and Be is that these species survive best at low light levels (Table 3). The high survivorship under low light is a consequence of Hm's and Be's unusual growth-dependent mortality functions (Fig. 3), because these species do not have unusually rapid growth at low light (see Table 3 and estimates of G_2 in Table 2). To test this hypothesis, we performed three replicate runs. In each, we replaced Hm's and Be's growth-dependent mortality function by RM's. Invariably, Hm and Be were minor components of the forest that ultimately became extinct (i.e., Fig. 20a). Moreover, if we replaced any other species' growth-dependent mortality submodel by Be's or Hm's, then that species became the late-successional dominant (see the example involving RM in Fig. 20b). The late-successional dominance of Hm and Be could not have been caused by the growth or dispersal functions because these species have unremarkable or disadvantageous growth and dispersal (Table 3). Also, although Hm and Be trees cast the most shade (Table 3), this attribute should most hinder Hm and Be saplings (all else being equal), whose low dispersal tends to place them beneath their mothers.

Second, we hypothesized that early successional dominance is determined primarily by rapid high-light growth. Red oak and BC have the most rapid growth in high light (Tables 2 and 3), and were the two most dominant species in year 30 of the baseline runs (among the top two species in 98% of runs for RO and 100% for BC, Table 4). This hypothesis is supported by runs in which we replaced RO's or BC's G_1 by Be's or RM's (three replicates of each). In all cases, RO and BC failed to become early successional dominants (i.e., Fig. 21). Moreover, Be and SM became early successional dominants if we gave them the high-light growth of BC. Finally, note that Hm is often a subdominant early in succession (see prediction 3) because its rapid radial growth in high light ensures rapid accumulation of basal area, despite a relatively poor ability to overtop caused by its low height–diameter ratio (see estimates of G_1 and H_2 in Table 2 and Column 3 in Table 3).

Even so, the causes of early successional dominance are less clear than the causes of late successional dominance. Red oak and BC also cast less shade and have greater mean dispersal distances than some of the other species. Both of these attributes should be advantageous before the canopy closes, but after the first trees begin to reproduce. Obviously, high dispersal facilitates colonization of vacant space and open crowns benefit offspring that fail to disperse far from their mother. Note that low-light growth rate could not be responsible for early-successional dominance because RO grows very slowly in low light (Table 3). To test the secondary importance of relatively high dispersal and low shade cast, we replaced RO's and BC's dispersal and crown characteristics, both alone and in combination, with Be's (three replicates of each). Although altering either attribute alone did not consistently and obviously reduce the early successional dominance of RO or BC, altering both simultaneously had significant effects. In all cases, RO and BC remained dominants in year 30 (before reproduction), but were driven extinct earlier than in 99% of the baseline runs (by year 630 for RO and 710 for BC; see Fig. 8a).

Third, we hypothesized that three unusual attributes of YB contribute to its mid- to late-successional subdominance. YB has the most rapid low-light height growth, the largest mean dispersal distance, and relatively rapid high-light height growth (Table 3). All of these attributes should facilitate gap phase persistence

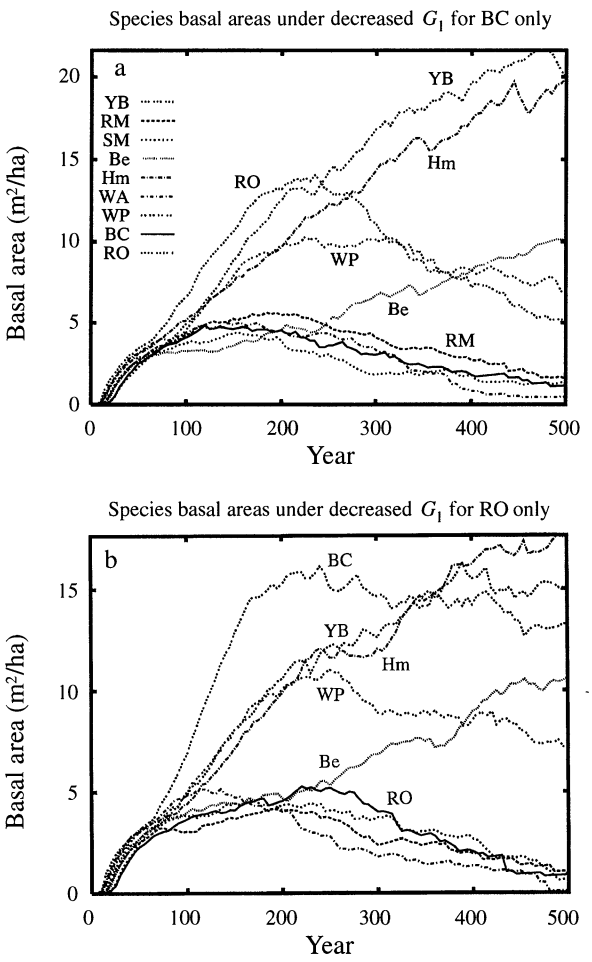

FIG. 21. Effects of replacing the high-light growth parameter (G_1) of BC or RO by that of SM. Note (a, solid line) BC or (b, solid line) RO loses its status as an early-successional dominant (compare to the baseline runs in Fig. 7a). Each panel shows a representative example of three replicate runs.

in old growth: long dispersal to locate gaps and rapid growth at all light levels to catch and surpass advance regeneration of more shade tolerant species. Note that the shade cast by YB should not provide it with any unusual advantages because it is intermediate (Table 3), and because the long dispersal of YB ensures that offspring virtually always disperse far from their mother (see Fig. 4). We performed runs in which we replaced YB's G_1, G_2 and R_1, both alone and in combination, with SM's G_1, RM's G_2, and Be's R_1 (three replicates of each). The results show that all three attributes contribute to YB's success as a gap phase species in old-growth. For example, Fig. 22 shows a series of runs in which we altered only G_2 (Fig. 22a), only G_2 and R_1 (Fig. 22b), and all three parameters (Fig. 22c). In runs in which we altered G_2, YB became extinct earlier than in any of the baseline runs (compare Figs. 22a and 8a). Altering both G_2 and R_1 produced peak abundances of YB below any of runs in which we al-

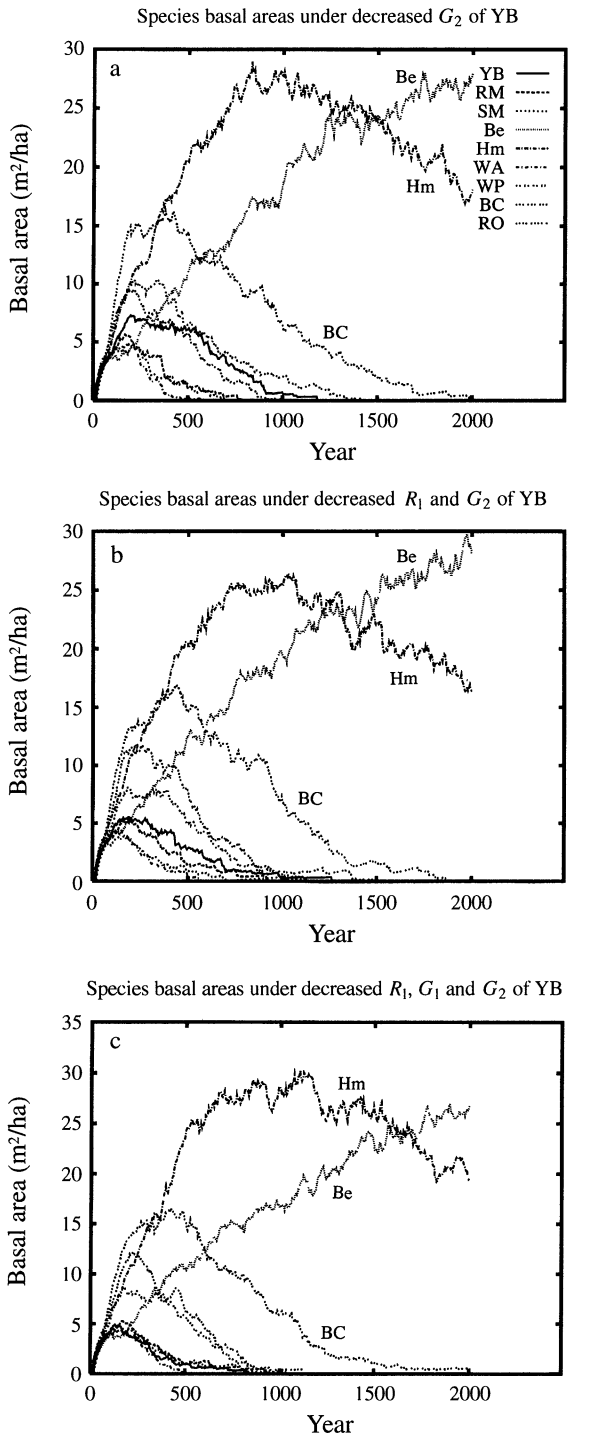

FIG. 22. (a) effects of reducing YB's low-light growth (YB's G_2 replaced by RM's); (b) effects of reducing YB's low-light growth and dispersal (YB's G_2 replaced by RM's and YB's R_1 replaced by Be's); (c) effects of reducing YB's low-light growth, dispersal, and high-light growth (YB's G_2 replaced by RM's, YB's R_1 replaced by Be's, and YB's G_1 replaced by SM's). Note that the abundances of YB (solid lines) are lower than in the baseline runs (Fig. 7a), and that YB progressively decreases in abundance from (a) to (c). Each panel shows a representative example from three replicate runs.

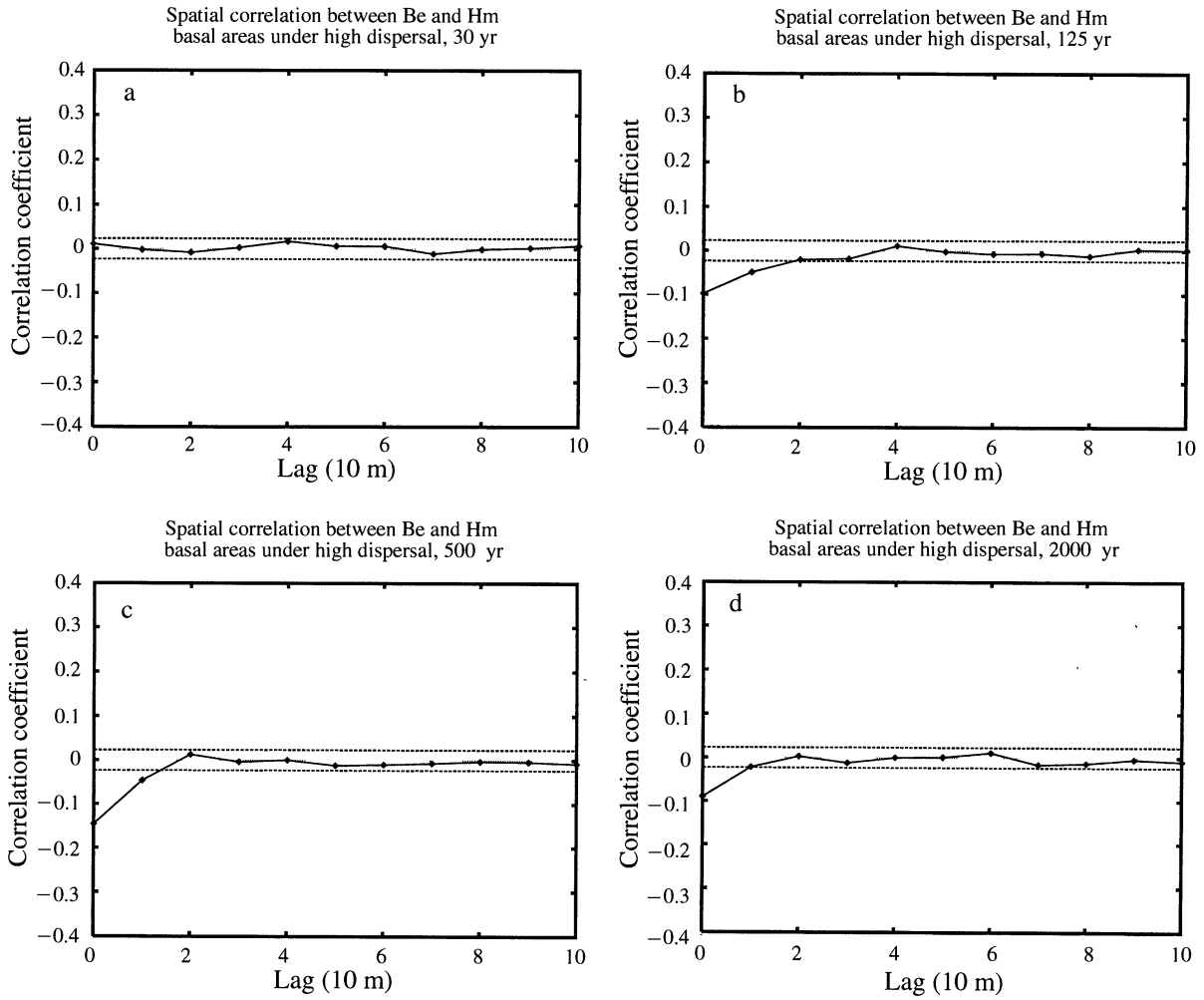

FIG. 23. Effects of increased dispersal of Hm and Be on the interspecific spatial segregation of these species. In the run shown, the R_1's of Hm and Be were replaced by WP's R_1. The solid lines show the spatial cross correlations among Hm and Be during succession ((a) year 30, (b) year 125, (c) year 500, and (d) year 2000). The dashed lines show the $P < 0.05$ significance thresholds. Note that negative cross correlation do not develop at large scales (unlike the results in Fig. 18). The figure shows a representative example of three replicate 1-km^2 runs.

tered only G_2 (compare Fig. 22a and b). Finally, altering all three parameters reduced peak abundances below any of the runs in which we altered only G_2 and R_1 (compare Fig. 22b and c).

Fourth, theoretical work with simple models of competition among neighbors shows that short dispersal causes the formation of clustered and interspecifically segregated spatial patterns (e.g., Pacala 1986, Durrett and Levin 1994). These spatial patterns promote coexistence by reducing the ratio of between- to within-species contacts, thereby reducing the strength of interspecific competition relative to intraspecific competition (Pacala 1986). Moreover, the rate of cluster growth is rapid initially, but then declines, and clusters tend to remain in the same place once they form (Durrett and Levin 1994). Because this is precisely what we observed for spatial distributions of Hm and Be in SORTIE, we hypothesized that short dispersal is responsible for the spatial patterns predicted in old-growth. We tested this hypothesis by replacing Be's and Hm's R_1 with WP's (three replicates). Spatial autocorrelation and cross-correlation analyses confirmed the hypothesis; in no case did significant spatial correlations develop at scales >10 m (e.g., compare Figs. 18 and 23).

To summarize, no single feature of SORTIE explains predictions 1–4. Rather, the community and system level dynamics of the model occur because of interspecific variation *collectively,* among the growth, mortality, resource, and dispersal submodels. In the *Discussion,* we offer a simple explanation for this diversity of causes.

DISCUSSION

Progress towards an explanatory and predictive theory of ecology has been hindered by a mismatch of scales: between those characterizing practical field ob-

servations, and those characterizing community, ecosystem, and landscape dynamics. We chose to formulate SORTIE at the level of the individual tree simply because it is comparatively easy to calibrate a mechanistic, individual-based model. The purpose of the model is to extrapolate from what is measurable to what we want to understand—from field data on individuals and resources to community dynamics and structure. In contrast, to calibrate a community level model like the Lotka-Volterra competition equations, one would have to measure the population growth of each species as a function of the abundance of every other species, and this is clearly impossible for large and long-lived organisms such as forest trees. We chose to base the model on measures of whole-organism performance instead of plant physiology, because the latter would have required that we characterize many more processes than the former.

In addition, Levin (1992) has argued that the goal in ecology (or in any science) is to understand how processes at one scale are translated into patterns at both that scale and others. SORTIE was designed to extrapolate across scales. Its purpose is not only to predict dynamics, but also to understand community level phenomena in terms of the biology of individuals. The principal disadvantage of modelling community dynamics at the individual level is the added complexity associated with predicting the fate of each and every individual. Because this complexity impedes understanding, a long-term goal of our study is to simplify SORTIE and to reduce it to a set of partial differential equations. Complexity also carries an additional risk. Because sampling error accompanies each parameter estimate, the total sampling error grows with the complexity of the model. These errors can interact nonadditively (Rastetter et al. 1991), and, if the model is too complex, can overwhelm the biological signal. On the other hand, omission of critical detail removes both sources of sampling error and critical aspects of the biological signal.

We thus formulated SORTIE to be as simple as possible given the constraints imposed by methodological limitations (the kinds and quantity of data we could collect), the number of tree species, and our judgement about the critical factors that govern dynamics. Even so, we were left with the possibility that the model would be so simple that it would fail to capture the governing processes or so complex that sampling error would overwhelm it.

Our results indicate that SORTIE finds a reasonable balance. Although the error analysis identifies some predictions that evaporate because of sampling error (e.g., Fig. 9f), other predictions appear to be robust (e.g., predictions 1–4 in *Results: Tests*). Although the sensitivity analysis reveals some omissions or flaws in the model (e.g., Fig. 13), the robust predictions are supported by test data from published studies (e.g., Figs. 6 and 19). Finally, although our attempts to understand SORTIE are only beginning, experiments with the model identify aspects of individual performance that cause its community- and system-level dynamics (e.g., Figs. 20–23).

Individual performance

Two separate lines of evidence provide support for the resource, growth, mortality, and recruitment submodels of SORTIE. First, as described in Canham et al. (1994), Kobe et al. (1995) and Ribbens et al. (1994), Pacala et. al (1995), and summarized in this paper, the submodels are defined by field data and supported by numerous statistical analyses and tests. Second, there are multiple interspecific trade-offs among aspects of performance predicted by the submodels (Fig. 5). These tradeoffs are critical to the realistic successional dynamics exhibited by the model. For example, by giving either a shade intolerant species the low-light mortality of a shade tolerant (e.g., Fig. 20b), or a shade tolerant the high-light growth of a shade intolerant, we create a superspecies that dominates throughout succession. It is difficult to imagine how a suite of measured trade-offs that create realistic successional dynamics could be artifacts of errors of estimation.

We suspect that the trade-offs in Fig. 5 occur in nature because of the concerted action of competition, evolution, and design constraints. Note that a simple two-dimensional surface would approximately touch the tops of all the bars in Fig. 5b (sloping down from background to foreground). Species inside this envelope (away from the reader and towards the intersection of the axes shown) would be competitively inferior, because they would grow more slowly and/or have lower survivorship than a species on the envelope. For example, a species located at the intersection of the axes shown in Fig. 5b (i.e., one requiring 165 yr to reach 3 m in height in 1% sun, 20 yr in 100% sun, and with a survivorship of 5% in 1% sun) would be competitively inferior to any species in SORTIE. Similarly, a species with WP's low light growth and survivorship that required 17 yr to reach 3 m height in full sun would be competitively inferior to WP. Thus, interspecific competition should "push" the community out towards the envelope by eliminating competitively inferior species. Note that natural selection would work the same way, by eliminating inferior genotypes through intraspecific competition. In contrast, species or genotypes outside the envelope (towards the reader and away from the intersection of the axes) would be competitively superior. For example, a species with YB's growth but a low-light survivorship of 95% would be competitively superior to YB.

We hypothesize that design constraints have prevented the evolution of these superspecies. A species simply cannot gain enough carbohydrate to allocate both to rapid growth and to functions that permit high understory survivorship (e.g., defenses; Kobe et al. 1995). In addition, species adapted to high-light en-

vironments generally fail to reach carbon compensation points under low light (Bazzaz 1979) because of the high respiratory costs associated with maintaining a photosynthetic apparatus of high capacity (Penning de Vries 1975).

Because dispersal, high-light growth, low-light survivorship, and shade cast by an individual are all collinear to at least a crude approximation (Fig. 5a), the two-dimensional envelope in three-space that we have been discussing is actually a two-dimensional envelope (approximately) in five-space. However, our arguments for the formation and maintenance of the envelope describing growth and survivorship probably do not extend to dispersal and shade cast. First, it is not obvious that design constraints prevent the evolution of increased dispersal distances, especially for shade tolerant species such as He (although they probably do for the clonally reproducing Be). Studies of evolutionary models have identified mechanisms that select for either short or long dispersal. Short dispersal is favored in stable and spatially heterogeneous environments to prevent dispersal of offspring into inhospitable regions (e.g., lakes; Levin et al. 1984, Cohen and Levin 1991, Ludwig and Levin 1991). Long dispersal is favored to avoid competition among siblings and, in temporally fluctuating environments, to permit repeated colonization of habitats that are transiently favorable (Hamilton and May 1977, Levin et al. 1984, Cohen and Levin 1991, Ludwig and Levin 1991). Dispersal distances of the species at GMF could be set by a balance between these selective forces, operating either on genotypes (evolution eliminates inferior genotypes) or species (competition eliminates inferior species). This process might explain the relatively short dispersal of shade tolerant species because shade tolerants are able to regenerate under closed canopy, and thus should experience less selection for long dispersal than shade intolerant species.

Second, we know of no simple design constraints that would prevent trees from producing additional or fewer leaves (e.g., by altering carbon allocation to reproduction), thereby changing the amount of shade cast by an individual. Changes in the number of leaves in a tree's crown would alter the rate of carbon gain (i.e., Horn 1971, Bazzaz 1979) in addition to the amount of shade cast. Because carbon gain controls rates of growth and survival (Givnish 1988), it is likely that patterns of selection on growth and survivorship cause interspecific variation in the amount of shade cast by individual trees (Horn 1971). Shade tolerant species typically have higher photosynthetic rates at low light levels and lower photosynthetic rates at high light levels than shade intolerant species (Bazzaz 1979). Because of reduced effects of self-shading on carbon gain, shade tolerants should carry more leaves and cast more shade than shade intolerants (as in Fig. 5a for the species at GMF). However, the situation is complicated further by the fact that the shade cast by an individual affects the competitive ability of offspring that fail to disperse from their mother's shadow. It is possible that kin selection acts directly on the amount of shade cast by an individual. Thus, the level of shade cast might represent the joint action of natural selection to optimize carbon gain and kin selection to improve the relative competitive ability of one's offspring. We know of no studies exploring the kin selection hypothesis.

Although the trade-offs in Fig. 5 are by no means perfect, there is reason to believe that they underestimate the crispness of the actual trade-offs in nature. For example, consider only the survivorship, shade cast, and high-light growth axes shown in Fig. 5a and suppose that the species in GMF were actually arrayed perfectly along a line in this three-dimensional space (e.g., the line from high shade cast, slow growth, and high survivorship to low shade cast, rapid growth, and low survivorship that would best fit the data in Fig. 5a). Sampling error would cause estimates of each species' position to fall off the line and create the kind of off-line scatter evident in Fig. 5a.

Community- and system-level dynamics

Tests of the model against data from published studies provide strong support for the successional dynamics predicted by SORTIE. The model predicts the approximate composition of old growth communities, the intraspecific clumping and interspecific spatial segregation of individuals in old-growth, and the successional progression of basal area. The model also appears to predict early-successional community composition, but this test is weakened by the lack of information about initial conditions in natural stands and the strong dependence of the model's early-successional predictions on initial abundances.

The model does not appear to predict the indefinite maintenance of species diversity, at least under the low levels of disturbance characterizing all runs in this paper (Fig. 7a). Is SORTIE capable of explaining the indefinite coexistence of tree species? This topic is sufficiently involved to warrant separate treatment; we are currently preparing two papers on the issue of very long-term (e.g., >10 000 yr) coexistence. We briefly outline two results from work in progress, because results such as Fig. 7a might otherwise create a false impression that SORTIE fails to capture the processes responsible for coexistence. First, runs with large-scale disturbance typical of natural stands (e.g., 1000-yr return time) predict the coexistence of six of the nine species. Second, we estimated the size and shape of the region in the *parameter space* of SORTIE that contains the estimates for the GMF species. Each axis of the parameter space gives the value of a different species-specific parameter and so each species is represented by a point in the space. The estimated region encompasses the nine GMF species as well as all possible "intermediates." If we select a large number of species spanning this region, we obtain some species

with parameter values very close to a GMF species, and others with intermediate parameter values. These intermediate species have performance measures between the values plotted in Fig. 5 (e.g., a species requiring 17 yr to reach 3 m in full sun and with a low light survivorship of 75% in Fig. 5a). In this way, we can generate species with interspecific differences and trade-offs like those in the GMF community. Runs with a large number of such hypothetical species predict the coexistence of >50 species for >10 000 yr. Moreover, the coexisting species exhibit a wide range of strategies, similar to the range shown in Fig. 5.

The error analysis shows that important community- and system-level predictions of the model (1–4 in *Results: Tests*) are reasonably robust to estimated levels of sampling error. Our data are not overwhelmed by the complexity of SORTIE. Still, the model is probably not too far from the limit of complexity where most predictions evaporate because of sampling uncertainty. Recall that we lose, because of sampling error, between one quarter and one half of the model's predictions about the identities of the top two and top five most abundant species during succession (Tables 4 and 5).

Of the uncertainties introduced by sampling error, perhaps the most serious involve the dynamics of YB. Because of sampling error, YB is the most dominant late-successional species in almost 10% of error analysis runs (Fig. 11). Moreover, these same runs produce the unrealistically high basal areas indicated by the top curve in Fig. 6d. Published data on old-growth stands (summarized in Fig. 19) show that YB is never the most dominant late-successional species in nature. Late-successional dominance by YB occurs in an error analysis run if YB happens to "draw" a high G_2 and M_2 and a low M_1. Then, YB is able to regenerate under closed canopy like Be and He.

This example illustrates the pitfalls of producing a complex model. If we had tried to calibrate SORTIE for a community containing considerably >nine species, but using the same amount of data per species, then we would have overestimated the low-light survivorship of some mid-tolerant species like YB with high probability (because of sampling error). Because of its relatively rapid high-light growth and long dispersal, this species would have displaced the actual old-growth species, and left us with a completely false prediction about the composition of old growth. Note that this same argument applies to any parameter-rich model, including parameter-rich models of species-poor communities (such as community level models formulated at the level of plant physiology). As the number of parameters grows, the likelihood increases that an unlucky parameter estimate will cause unreasonable large-scale behavior. In light of this problem, future efforts to calibrate models of species-rich communities should probably attempt to characterize the *distribution* of species in parameter space (perhaps by measuring a random sample of species), rather than to estimate parameters for every species.

It is important to understand that the error analysis is not complete. We lack sampling distributions for G_3, the initial diameter of new recruits, and the R_2's. Because SORTIE's dynamics show little sensitivity to changes in either G_3 or the initial diameter of new recruits, the omission of these parameters from the error analysis is probably not overly serious. In contrast, dynamics are sensitive to quadruplings of the R_2's, one species at a time (Fig. 15). This result confirms that species-specific patterns of seed production and preestablishment mortality could affect community composition. Actual interspecific differences among the R_2's might indeed exceed a factor of four. It is thus imperative that we complete ongoing research to produce field estimates of the R_2's. The sensitivity analysis also confirms the expected result that early-successional community composition depends strongly on the relative abundances of species present at the onset of succession (Fig. 12). SORTIE predicts significant effects of site history, at least for the first several hundred years of succession. Finally, the unrealistically large early-successional basal areas produced in sensitivity analysis runs with high initial densities expose flaws in the mortality submodels and perhaps in the growth submodels as well (Fig. 13). These runs demonstrate the limitations of our decision to focus the empirical studies of mortality and growth on saplings, and illustrate the need for additional data on subcanopy and canopy trees.

Tracing community dynamics to individual performance

Experiments with the model show that community level predictions of SORTIE can be traced to a variety of different aspects of individual performance. Old-growth dominance is determined primarily by the relationship between mortality and growth. Early-successional dominance is determined by high-light growth, and to a lesser extent, by dispersal and shade cast. YB's position as the primary gap phase species in mid- to late-successional stands is determined by its combination of relatively rapid high-light growth, unusually rapid low-light growth, and large dispersal. This diversity of causes is explained by the suite of trade-offs shown in Fig. 5. Again, we hypothesize that two factors have created the trade-offs: (1) the elimination of competitively inferior strategies by interspecific competition and/or evolution, and (2) the existence of design constraints. Note that all the submodels contribute to the observed trade-offs, with interspecific variation among growth, mortality, resource, and dispersal submodels each responsible for a facet of the pattern.

When we experimentally replace a submodel of one species with that of another, we create a new strategy which is either "inside" or "outside" the approxi-

mately two-dimensional envelope in the five-dimensional space shown in Fig. 5b. We thus create either a competitively inferior type, or a super-species that violates design constraints. For example, by replacing the growth-dependent mortality submodel of Be with that of RM, we move Be inside the envelope (by shortening Be's bar in Fig. 5b) and create a competitively inferior strategy (see Fig. 20a). By reducing RO's G_1 or increasing its shade cast and decreasing its R_1, we move the species inside the envelope and reduce its competitiveness (e.g., Fig 21b). By replacing Be's high-light growth with BC's, we create a super-species outside the envelope (by moving Be's bar down and to the right in Fig 5b). Finally, by decreasing YB's dispersal, G_2, or G_1, we create an inferior strategy inside the envelope (Fig. 22).

The trade-offs in Fig. 5 are relevant even to the result that spatial clustering of He and Be in old-growth is caused by short dispersal (Fig. 23). Trade-offs between dispersal distances and other facets of performance are partly responsible for the increased clustering late in succession, because attributes that cause late-successional dominance are associated with short dispersal. Also, if we experimentally increase the dispersal of either Hm or Be, then the long-dispersing species (which is outside the envelope) increases in dominance.

What are the dynamic implications of the two dimensions describing most of the interspecific variation in performance shown in Fig. 5? The axis defined by the approximate collinearity of shade cast, high-light growth, low-light survivorship, and dispersal (see Fig. 5a) is clearly associated with succession. The ordering of the species along this axis corresponds to a traditional ordering of shade tolerance and to a successional sequence. Experiments with SORTIE show that the trade-offs defining the axis are responsible for succession in the model.

The second dimension is more mysterious (Fig. 5b). Interspecific variation among low-light growth rates obviously defines part of this dimension, but patterns of growth-dependent mortality also contribute to it. For example, if all species shared the same growth-dependent mortality function, then YB would have much higher survivorship at low light than WP (because YB grows faster at low light), and SM would have higher survivorship than Be or Hm. Thus, the envelope defined by the strategies in Fig. 5 would slope strongly up from many to few years to reach 3 m in height at 1% sun, rather being level or sloping weakly down in this direction. A possible explanation for the observed tendency is a trade-off between growth and survival. Species such as YB or SM grow relatively quickly in low light but cannot survive slow growth, while species such as Hm, Be, and WP grow more slowly but are better at surviving slow growth (compare Figs. 2 and 3). Again, Kobe et al. (1995) hypothesize that differences in allocation create this pattern, with some species investing a relatively large fraction of photosynthate to new growth and others investing a relatively large fraction to storage or defenses. The "second dimension" in Fig. 5 clearly has dynamic consequences because YB's mid- to late-successional dominance in SORTIE depends on its rapid low-light growth. However, a full explanation of the dynamic implications of the relationship between survivorship and growth requires a separate theoretical study.

In summary, the large number of causes of SORTIE's community dynamics is considerably reduced if we view the problem in the appropriate way. Rather than separate explanations for each aspect of dynamics, we are left with only approximately two dimensions of strategic variation among species that appear to govern community composition throughout succession.

Relationship of SORTIE to the JABOWA-FORET family of forest models

Forest simulation models descended from JABOWA (Botkin et al. 1972) and FORET (Shugart and West 1977) are perhaps the most widely studied computer models in ecology (reviewed in Botkin 1992 and Shugart 1984). JABOWA-FORET models were designed specifically so that parameter values could be assigned using published information on such attributes as shade tolerance class, range limits, height and diameter of the largest individual of each species, and mode of regeneration. This feature has enabled the rapid development of JABOWA-FORET models for forests throughout the world, including some tropical rain forests with >100 species (e.g., Shugart et al. 1980). The models can be calibrated using published information because they assume detailed quantitative relationships between the published measures and the mechanisms governing individual performance.

Community- and ecosystem-level predictions of the models have been verified repeatedly. There is no doubt that the models can reproduce phenomena such as secondary succession, geographical patterns of zonation, and changes in species composition in response to past climate change (reviewed in Shugart 1984, Botkin 1992). However, in over 20 years, surprisingly few attempts have been made to verify the submodels of individual performance that cause the large-scale dynamics. This lack of attention to individual performance is explained partly by the use of JABOWA-FORET simulators, during the past decade, as "community modules" in ecosystem models (e.g., Pastor and Post 1988). Much of the code in modern JABOWA-FORET models is devoted to nutrient and hydrologic cycling, and some ecosystem level phenomena might be insensitive to the details of individual performance, providing that community dynamics are represented correctly. Indeed, one interpretation of modern JABOWA-FORET models is that they are designed primarily to produce realistic community dynamics for use in ecosystems studies, rather than to explain community dynamics per se.

Even so, a second use of these models in recent years

is to predict the responses of forest communities to climate change. If JABOWA-FORET models reproduce community dynamics for substantially incorrect reasons, then the predictions of such models must be questioned. Also, if the individual level mechanisms are incorrect, then existing models cannot be used to trace ecosystem- or community-level phenomena to their individual level causes.

In what follows, we outline the principal discrepancies between our findings and the assumptions of JABOWA-FORET models. We show that interspecific variation in individual performance at GMF is not accurately represented by JABOWA-FORET models. The points of disagreement involve the primary causes of successional dynamics in both SORTIE and JABOWA-FORET. Because JABOWA-FORET models are so diverse, individual examples undoubtedly contradict one or more aspects of this summary. In particular, the FORSKA model (Prentice and Leemans 1990, Leemans 1991, Prentice et al. 1993) contains growth and mortality submodels substantially unlike those in most JABOWA-FORET simulators.

Like SORTIE, JABOWA-FORET models forecast the fate of each individual tree throughout its life cycle using growth, mortality, recruitment, and resource submodels. Most examples are non-spatial, with trees occupying a single homogeneous cell that is typically the size of a large canopy adult. However, some recent examples link many such cells into a two-dimensional spatial lattice (e.g., the ZELIG model of Smith and Urban 1988 and Urban 1990).

In JABOWA-FORET models, individual trees have sigmoid growth under ideal conditions. Growth is reduced by shortages of available resources (light, water, and nutrients) and by unfavorable climate. To handle light limitation, each tree species is assigned to one of two or three shade tolerance classes on the basis of published tables (e.g., Baker 1949), and each class is assigned a single function relating radial growth to light availability. The function for the shade tolerant class typically increases rapidly with increasing light to a relatively low asymptote, while that for shade intolerants increases slowly to a high asymptote. In contrast, our growth data contain little, if any, evidence of this association between tolerance class and radial growth (see Fig. 2). Pacala et al. (1995) show that the estimated radial growth functions in SORTIE are generally not congruent with the functions assumed for the same species in JABOWA-FORET models. This discrepancy is important because the trade-off between growth rates at low and high light is a primary cause of the successional dynamics exhibited by JABOWA-FORET models.

Because of the lack of published data relating growth and mortality, JABOWA-FORET models simply assign the same growth-dependent mortality function to all species. In contrast, our data show enormous interspecific differences among the mortality submodels (Fig. 3). This represents probably the single greatest shortcoming of JABOWA-FORET models. Interspecific differences among the mortality-growth relationships determine which species dominate old growth at GMF (e.g., Fig. 20). The trade-off between high-light growth and low-light survivorship that largely drives succession at GMF (Figs. 20 and 21) is shaped more by interspecific variation among the mortality submodels than by variation among low-light growth rates. Again, if all species shared a single mortality function, then the two-dimensional envelope in Fig. 5b would slope strongly upward from many to few years to reach 3 m in height at 1% light. Yellow birch is the primary gap phase species in old growth largely because its disadvantageous growth-dependent mortality function is compensated for by unusually rapid low-light growth. Because JABOWA-FORET models omit interspecific variation among the mortality functions, they yield explanations of successional dynamics that disproportionately stress patterns of growth. Finally, predictions of JABOWA-FORET models about the responses of forests to novel conditions might be seriously flawed because of the omission of this critical source of interspecific variation.

For example, Bolker et al. (1995) developed a version of SORTIE that contains species-specific responses of sapling growth to increased atmospheric CO_2. These responses were estimated using growth chamber data on the nine species obtained by Bazzaz and Miao (1993) and Bazzaz et al. (1990). Previous studies with JABOWA-FORET models had predicted that shade tolerant species would increase in dominance under elevated CO_2 (Solomon 1986). Bolker et al. (1995) obtained the opposite prediction of increased dominance by shade intolerant species. The discrepancy between the two forecasts is apparently caused by the differences between the growth and mortality relationships assumed in JABOWA-FORET and those measured in SORTIE. Briefly, in SORTIE, the enhanced growth caused by elevated CO_2 permits shade intolerant species to survive in the understory. The ability to regenerate under closed canopy increases the relative competitive ability of the intolerant species, because the growth-dependent mortality functions of shade tolerant species ensure their survival in the understory even without enhanced CO_2. Thus, shade intolerant species receive a greater survivorship benefit than shade tolerant species, even if enhanced CO_2 increases equally the growth of shade intolerants and shade tolerants. This phenomenon is not as pronounced in JABOWA-FORET models because all species share the same growth-dependent mortality function. As a result, shade intolerant species receive greater benefit from enhanced CO_2 in the SORTIE model than in JABOWA-FORET models. The additional benefit to the shade intolerant species completely reverses the predicted effect of elevated CO_2 on community composition.

In most JABOWA-FORET models, new recruits are drawn at random from a list of species, rather than being produced by the modeled trees (as in SORTIE). An exception is provided by spatial descendents such as ZELIG (Urban 1990), in which some recruits are produced by the trees and others are drawn from a list of species. There is no dispersal in the non-spatial versions of JABOWA-FORET and spatial versions do not contain quantitative field estimates of dispersal like those in SORTIE.

In addition, recruitment in JABOWA-FORET models is controlled by numerous species-specific "switches" that simulate factors which prevent colonization and establishment (i.e., predation, absence of a seed source, unfavorable conditions for germination, etc.). The sensitivity of SORTIE's dynamics to species-specific changes in the R_2's (Fig. 15) suggest that these factors could have substantial effects if added to SORTIE. The switch simulating the lack of a seed source for new recruits deserves comment, because it supports the view that JABOWA-FORET simulators are designed primarily to produce realistic community dynamics in ecosystem level studies, rather than to explain the communities themselves. In the version of FORET included in the appendix of Shugart (1984), there are switches that stop recruitment at species-specific times during succession if no conspecific adults are present (the lines in the code referring to KTIME[J] at the center of page 232). Because the plot is only the size of a single adult, these switches inevitably stop the recruitment of each species near the operator-specified time at which it should disappear during succession. Obviously, the switches will enforce whatever successional sequence is specified in an input file (containing the times at which recruitment ceases). However, they do not provide an adequate explanation of natural succession.

JABOWA-FORET models employ a wide variety of submodels that predict the resources available to each tree. Consistent with an ecosystem emphasis, the water and nutrient submodels are highly developed (e.g., LINKAGES by Pastor and Post 1988), in contrast to the absence of nutrients and water in the version of SORTIE described here. In JABOWA-FORET models, light is typically handled by Beer's Law, with incident radiation coming from a single direction. Crown geometries range from simple (a single layer at the top of each stem, which is distributed uniformly across the modeled plot), to complex (multi-layered crowns; see Shugart 1984). The "fish-eye photography" used to calculate light availability in SORTIE was adopted because it predicts both tree growth and whole-season photosynthetically active radiation in the field. We do not yet know the community level implications of the differences between the light submodels in SORTIE and JABOWA-FORET.

The differences between the JABOWA-FORET and SORTIE models demonstrate the need to tighten the coupling between models and data. These differences are more than cosmetic; they are at the heart of the mechanisms that cause dynamics. To reach an explanatory and predictive theory, we must have models that extrapolate from what we can measure to what we need to understand. This paper shows that it is possible to estimate the processes controlling the dynamics of a reasonably diverse community. The resulting model is predictive and explanatory, although efforts to understand SORTIE are only just beginning. The most obvious needs for future development of SORTIE are to include effects of nutrients, water, and climate by investigating a wider range of physical conditions than those found at GMF, and to investigate the effects of herbivory and seed predation.

The most intriguing questions raised by this study involve the two stategic dimensions that apparently govern the model's dynamics (Fig. 5). Although one of the two dimensions obviously controls succession, we do not yet completely understand the implications of the other dimension. In nature, does this dimension govern patterns of diversity among species occurring at the same successional stage? Also, is the two-dimensional structure in Fig. 5 a general result common to other light-limited communities? If so, it might provide a basis for a general theory of forest dynamics.

Acknowledgments

We thank the Childs family for their generous hospitality and for the use of the facilities at Great Mountain Forest. We thank Diane Burbank, James Hill, Adrian Finzi, Linda Buttel, and numerous undergraduate assistants for their long hours in the field and laboratory. We thank Simon Levin for his intellectual input. Finally, we gratefully acknowledge the support of the National Science Foundation (BSR-8918616, DEB-9221097, DEB-9220620), National Aeronautics and Space Administration (NAGW-2088, NAGW-3471, NAGW-3703), and Department of Energy (DE-FG02–90ER60933 and DE-FG02–94ER61815).

Literature Cited

Anderson, R. M., and R. M. May. 1991. Infectious diseases of humans. Oxford University Press, Oxford, England.

Baker, F. S. 1949. A revised tolerance table. Journal of Forestry **47**:179–181.

Baker, R. H. 1968. Habitats and distribution. Pages 98–126 *in* J. A. King, editor. Biology of *Peromyscus* (Rodentia). American Society of Mammology, Special Publication Number 2, Stillwater, Oklahoma, USA.

Bazaaz, F. A. 1979. The physiological ecology of plant succession. Annual Review of Ecology and Systematics **10**: 351–372.

Bazzaz, F. A., J. S. Coleman, and S. R. Morse. 1990. Growth responses of 7 major co-occurring tree species of the northeastern United States to elevated CO_2. Canadian Journal of Forest Research **20**:1479–1484.

Bazzaz, F. A., and S. L. Miao. 1993. Successional status, seed size and responses of tree seedlings to CO_2, light and nutrients. Ecology **74**:104–112.

Bjorkbom, J. C. 1979. Seed production and advance regeneration in Allegheny hardwood forests. U.S. Department of Agriculture Forest Service Research Paper NE-435.

Bolker, B. M., S. W. Pacala, F. A. Bazzaz, C. D. Canham, and S. A. Levin. 1995. Species diversity and carbon di-

oxide fertilization of temperate forests. Global Change Biology, *in press.*

Bormann, F. H., and M. F. Buell. 1964. Old-age stand of hemlock-northern hardwood forest in central Vermont. Bulletin of the Torrey Botanical Club **91**:451–465.

Botkin, D. B. 1992. Forest dynamics: an ecological model. Oxford University Press, Oxford, England.

Botkin, D. B., J. F. Janak, and J. R. Wallis. 1972. Rationale, limitations, and assumptions of a northeastern forest simulator. International Business Machine Journal of Research and Development **16**:106–116.

Buchman, R. G. 1983. Survival predictions for major lake states tree species. U.S. Department of Agriculture Forest Service Research Paper NC-233.

Buchman, R. G., and E. L. Lentz. 1984. More lake states tree survival predictions. U.S. Department of Agriculture Forest Service Research Note NC-312.

Canham C. D. 1988*a*. Growth and architecture of shade-tolerant trees: response to canopy gaps. Ecology **69**:786–795.

———. 1988*b*. An index for understory light levels in and around canopy gaps. Ecology **69**:1634–1638.

Canham, C. D., J. S. Denslow, W. J. Platt, J. R. Runkle, T. A. Spies, and P. S. White. 1990. Light regimes beneath closed canopies and tree-fall gaps in temperate and tropical forests. Canadian Journal of Forest Research **20**:620–631.

Canham, C. D., A. C. Finzi, S. W. Pacala, and D. H. Burbank. 1994. Causes and consequences of resource heterogeneity in forests: interspecific variation in light transmission by canopy trees. Canadian Journal of Forest Research **24**:337–349.

Chapin, F. S., III, A. J. Bloom, C. B. Field, and R. H. Waring. 1987. Plant responses to multiple environmental factors. Bioscience **37**:49–57.

Clark, D. A., and D. B. Clark. 1992. Life history diversity of canopy and emergent trees in a neotropical rain forest. Ecological Monographs **62**:315–344.

Clebsch, E. E. C., and R. T. Busing. 1989. Secondary succession, gap dynamics, and community structure in a southern Appalachian cove forest. Ecology **70**:728–735.

Cliff, A. D., and J. K. Ord. 1981. Spatial processes: models and applications. Pioneer, London, England.

Clifford, P., S. Richardson, and D. Hemon. 1989. Assessing the significance of the correlation between two spatial processes. Biometrics **45**:123–134.

Cohen, D., and S. A. Levin. 1991. Dispersal in patchy environments: the effects of temporal and spatial structure. Theoretical Population Biology **39**:63–99.

Connell, J. H. 1971. On the role of natural enemies in preventing competitive exclusion in some marine animals and in rain forest trees. Pages 298–310 *in* B. J. den Boer and G. R. Gradwell, editors. Dynamics of populations. Centre for Agricultural Publishing and Documentation, Wageningen, The Netherlands.

———. 1980. Diversity and the coevolution of competitors, or the ghost of competition past. Oikos **35**:131–138.

Connor, E. F., and D. Simberloff. 1979. The assembly of species communities: chance or competition? Ecology **60**: 1132–1140.

Davis, M. B., S. Sugita, R. R. Calcote, J. B. Ferrari, and L. E. Frelich. 1994. Historical development of alternate communities in a hemlock–hardwood forest in northern Michigan, USA. Pages 19–39 *in* R. May, N. Webb, and P. Edwards, editors. Large-scale ecology and conservation biology. Blackwell, Oxford, England.

Davis, M. B., S. Sugita, R. R. Calcote, and L. Frelich. 1992. Effects of invasion by *Tsuga canadensis* on a North American forest ecosystem. Pages 34–44 *in* A. Teller, P. Mathy, and J. N. R. Jeffers, editors. Response of forest ecosystems to environmental changes. Elsevier Applied Science, New York, New York, USA and London, England.

Durrett, R., and S. A. Levin. 1994. Stochastic spatial models: a user's guide to ecological applications. Philosophical Transactions of the Royal Society of London B. **343**:329–350.

Forcier, L. K. 1975. Reproductive strategies and the co-occurrence of climax tree species. Science **189**:808–810.

Fox, J. F. 1977. Alternation and coexistence of tree species. American Naturalist **111**:69–89.

Frelich, L. E., R. R. Calcote, and M. B. Davis. 1993. Patch formation and maintenance in an old-growth hemlock-hardwood forest. Ecology **74**:513–527.

Givnish, T. J. 1988. Adaptation to sun and shade: a whole plant perspective. Australian Journal of Plant Physiology **15**:63–92.

Gleeson, S., and D. Tilman. 1992. Plant allocation and the multiple limitation hypothesis. American Naturalist **139**: 1322–1343.

Graber, R. E., and W. B. Leak. 1992. Seed fall in an old-growth northern hardwood forest. U.S. Department of Agriculture Forest Service Research Paper NE-663.

Gross, L. V. 1989. Plant physiological ecology: a theoretician's perspective. Pages 11–24 *in* J. Roughgarden, R. M. May, and S. A. Levin, editors. Perspectives in ecological theory. Princeton University Press, Princeton, New Jersey, USA.

Hamilton, D. A. 1986. A logistic model of mortality in thinned and unthinned mixed conifer stands of northern Idaho. Forest Science **32**:989–1000.

———. 1990. Extending the range of applicability of an individual tree mortality model. Canadian Journal of Forest Research **20**:1212–1218.

Hamilton, W. D., and R. M. May. 1977. Dispersal in stable habitats. Nature **269**:578–581.

Henry, J. D., and J. M. A. Swan. 1974. Reconstructing forest history from live and dead plant material—an approach to the study of forest succession in southwest New Hampshire. Ecology **55**:772–783.

Horn, H. S. 1971. The adaptive geometry of trees. Princeton University Press, Princeton, New Jersey, USA.

Hough, A. F., and R. D. Forbes. 1943. The ecology and silvics of forests in the high plateaus of Pennsylvania. Ecological Monographs **13**:301–320.

Inouye, R., and D. Tilman. 1988. Convergence and divergence along experimental nitrogen gradients. Ecology **69**: 995–1004.

Janzen, D. H. 1970. Herbivores and the number of tree species in tropical forests. American Naturalist **104**:501–528.

Jones, E. W. 1945. The structure and reproduction of the virgin forest of the North Temperate zone. New Phytologist **44**:130–148.

Kareiva, P. 1984. Predator–prey dynamics in spatially structured populations: manipulating dispersal in a coccinellid–aphid interaction. Lecture Notes in Biomathematics **54**: 368–389.

Kareiva, P., and M. Anderson. 1988. Spatial aspects of species interactions: the wedding of models and experiments. Pages 38–54 *in* A. Hastings, editor. Community ecology. Springer-Verlag, New York, New York, USA.

Kareiva, P., and G. Odell. 1987. Swarms of predators exhibit "prey taxis" if individual predators use restricted area search. American Naturalist **130**:233–270.

Kelty, M. J. 1984. The development of productivity of hemlock–hardwood forest in southern New England. Dissertation, Yale University, New Haven, Connecticut, USA.

———. 1986. Development patterns in two hemlock–hardwood stands in southern New England. Canadian Journal of Forest Research **10**:885–891.

Kendall, M. G., and A. Stuart. 1977. The advanced theory of statistics. Oxford University Press, Oxford, England.

Kobe, R. S., S. W. Pacala, J. A. Silander, Jr., and C. D. Canham. 1995. Juvenile tree survivorship as a component of shade tolerance. Ecological Applications **5**:517–532.

Landsberg, J. J. 1986. Physiological ecology of forest production. Academic Press, New York, New York, USA.

Leemans, R. 1991. Sensitivity analysis of a general forest succession model. Ecological Modelling **53**:247–262.

Levin, S. A. 1992. The problem of pattern and scale in ecology. Ecology **73**:1943–1967.

Levin, S. A., D. Cohen, and A. Hastings. 1984. Dispersal strategies in patchy environments. Theoretical Population Biology **19**:169–200.

Ludwig, D., and S. A. Levin. 1991. Evolutionary stability of plant communities and the maintenance of multiple dispersal types. Theoretical Population Biology **40**:285–307.

Matlack, G. R. 1989. Secondary dispersal of seed across snow in *Betula lenta,* a gap-colonizing tree species. Journal of Ecology **77**:853–869.

Monserud, R. A. 1976. Simulation of forest tree mortality. Forest Science **22**:438–444.

Mood, A. M., F. A. Graybill, and D. C. Boes. 1974. Introduction to the theory of statistics. McGraw-Hill, New York, New York, USA.

Mooney, H. A. 1991. Plant physiological ecology: determinants of progress. Functional Ecology **5**:127–135.

Nichols, G. E. 1913. The vegetation of Connecticut. II. Virgin forest. Torreya **13**:191–215.

Oliver, C. D. 1978. Development of northern red oak in mixed species stands in central New England. Yale University School of Forestry and Environmental Studies Bulletin Number 91.

Pacala, S. W. 1986. Neighborhood models of plant population dynamics. II. Multi-species models of annuals. Theoretical Population Biology **29**:262–292.

Pacala, S. W., C. D. Canham, and J. A. Silander, Jr. 1993. Forest models defined by field measurements: I. The design of a northeastern forest simulator. Canadian Journal of Forest Research **23**:1980–1988.

Pacala, S. W., C. D. Canham, J. A. Silander, Jr., and R. K. Kobe. 1995. Sapling growth as a function of resources in a north temperate forest. Canadian Journal of Forest Research **24**:2172–2183.

Pacala, S. W., and J. A. Silander, Jr. 1990. Field tests of neighborhood population dynamic models of two annual weed species. Ecological Monographs **60**:113–134.

Parton, W. J., D. S. Schimel, C. V. Cole, and D. S. Ojima. 1987. Analysis of factors controlling soil organic levels of grasslands in the Great Plains. Soil Science Society of America Journal **51**:1173–1179.

Parton, W. J., J. M. O. Scurlock, D. S. Ojima, T. G. Gilanov, R. J. Scholes, D. S. Schimel, T. Kirchner, J. C. Menaut, T. Seastetd, E. Garcia-Moya, A. Kamnalrut, and J. L. Kinyamario. 1993. Observation and modelling of biomass and soil organic matter dynamics for the grassland biome world-wide. Global Biogeochemical Cycles **7**:785–809.

Parton, W. J., J. W. B. Stewart, and C. V. Cole. 1988. Dynamics of C,N,P, and S in grassland soils: a model. Biogeochemistry **5**:109–131.

Pastor, J., and W. M. Post. 1988. Response of northern forest to CO_2-induced climate change. Nature **334**:55–58.

Penning de Vries, F. W. T. 1975. The cost of maintenance processes in cells. Annals of Botany **39**:77–92.

Phipps, R. L. 1967. Annual growth of suppressed chestnut oak and red maple, a basis for hydrological inference. U.S. Geological Survey Professional Paper 485-C.

Pigott, C. D. 1975. Natural regeneration of *Tilia cordata* in relation to forest-structure in the forest of Bialowieza, Poland. Philosophical Transactions of the Royal Society of London, B. Biological Sciences **270**:151–179.

Potter, C. S., V. T. Randerson, C. B. Field, P. A. Matson, P. M. Vitousek, H. A. Mooney, and S. A. Klooster. 1993. Terrestrial ecosystem production: a process model based on global satellite and surface data. Global Biogeochemical Cycles **7**:811–841.

Potzger, J. E. 1946. Phytosociology of the primeval forest in central-northern Wisconsin and upper Michigan, and a brief postglacial history of the lake forest formation. Ecological Monographs **16**:211–250.

Prentice, I. C., and R. Leemans. 1990. Pattern and process and dynamics of forest structure: a simulation approach. Journal of Ecology **78**:340–355.

Prentice, I. C., M. T. Sykes, and W. Cramer. 1993. A simulation model for the transient effects of climate change on forest landscapes. Ecological Modelling **65**:51–70.

Rastetter, E. B., A. W. King, B. J. Cosby, G. M. Hornberger, R. V. O'Neill, and J. E. Hobbie. 1991. Aggregating fine-scale ecological knowledge to model coarser-scale attributes of ecosystems. Ecological Applications **2**:55–70.

Rastetter, E. B., M. G. Ryan, G. R. Shauer, J. M. Melillo, K. U. Nadelhoffer, J. E. Hobbie, and J. D. Aber. 1991. A general model describing responses of the C and N cycles in terrestrial ecosystems to changes in CO_2, climate, and N-deposition. Tree Physiology **9**:101–126.

Ribbens, E., J. A. Silander, Jr., and S. W. Pacala. 1994. Recruitment in forests: calibrating models to predict patterns of tree seedling dispersal. Ecology **75**:1794–1804.

Rose, R. K., and E. C. Birney. 1985. Community ecology. Pages 310–339 *in* R. H. Tamarin, editor. Biology of new world *Microtus.* American Society of Mammalogy, Special Publication Number 8, Stillwater, Oklahoma, USA.

Roughgarden, J., S. Gaines, and S. Pacala. 1988. Supply side ecology: the role of physical transport processes. Pages 459–486 *in* P. Gillar and J. Gee, editors. Organization of communities past and present. Blackwell Scientific, London, England.

Roughgarden, J., W. Iwasa, and C. Baxter. 1985. Demographic theory for an open marine population with space-limited recruitment. Ecology **66**:54–67.

Runkle, J. R. 1985. Disturbance regimes in temperate forests. Pages 17–33 *in* S. T. A. Pickett, and P. S. White, editors. The ecology of natural disturbance and patch dynamics. Academic Press, Orlando, Florida, USA.

Shugart, H. H. 1984. A theory of forest dynamics. Springer-Verlag, New York, New York, USA.

Shugart, H. H., A. T. Mortlock, M. S. Hopkins, and I. P. Burgess. 1980. A computer simulation model of ecological succession in Australian subtropical rain forest. ORNL-M-7029. Oak Ridge National Laboratory, Oak Ridge, Tennessee, USA.

Shugart, H. H., and D. C. West. 1977. Development of an Appalachian deciduous forest model and its application to assessment of the impact of the chestnut blight. Journal of Environmental Management **5**:161–179.

Simberloff, D., and W. Boecklen. 1981. Santa Rosalia reconsidered: size ratios and competition. Evolution **35**: 1206–1228.

Smith, T. M., and D. L. Urban. 1988. Scale and resolution of forest structural pattern. Vegetatio **74**:143–150.

Solomon, A. M. 1986. Transient responses of forests to CO_2 induced climate change: simulation modeling experiments in eastern North America. Oecologia **68**:567–579.

Sork, V. L., J. Bramble, and O. Sexton. 1993. Ecology of mast-fruiting in three species of North American deciduous oaks. Ecology **74**:528–541.

Stearns, F. 1951. The composition of the sugar maple–hemlock–yellow birch association in northern Wisconsin. Ecology **32**:245–265.

Stephens, G. R., and D. E. Hill. 1971. Damage, drought, defoliation, and death in unmanaged Connecticut forests. Connecticut Agricultural Experiment Station New Haven, Bulletin 718.

Stephens, G. R., and P. E. Waggoner. 1980. A half century of natural transitions in mixed hardwood forests. Connecticut Agricultural Experiment Station New Haven, Bulletin 783.

Stephens, G. R., and J. S. Ward. 1992. Sixty years of natural change in unmanaged mixed hardwood forests. Connecticut Agricultural Experiment Station New Haven, Bulletin 902.

Strong, D. R., and D. Simberloff. 1981. Straining of gnats and swallowing ratios: character displacement. Evolution **35**:810–812.

Szymura, J. M., and N. H. Barton. 1986. Genetic analysis of a hybrid zone between the fire-bellied toads near Cracow in southern Poland. Evolution **40**:1141–1159.

Teck, R. M., and D. E. Hilt. 1991. Individual-tree diameter growth model for the northeastern United States. U.S. Department of Agriculture Forest Service Research Paper NE-649.

Tilman, D. 1993. Species richness of experimental productivity gradients: how important is colonization limitation? Ecology **74**:2179–2191.

———. 1987. Secondary succession and the pattern of plant dominance along experimental nitrogen gradients. Ecological Monographs **57**:189–214.

———. 1982. Resource competition and community structure. Monographs in Population Biology, Princeton University Press. Princeton, New Jersey, USA.

Tilman, D., and D. Wedin. 1991. Dynamics of nitrogen competition between successional grasses. Ecology **72**:1038–1049.

Urban, D. L. 1990. A versatile model to simulate forest pattern: a user's guide to ZELIG version 1.0. Environmental Sciences Department, University of Virginia, Charlottesville, Virginia, USA.

Wedin, D., and D. Tilman. 1990. Species effects on nitrogen cycling: a test with perennial grasses. Oecologia **84**:433–441.

Williamson, G. B. 1975. Pattern and seral composition in an old-growth beech–maple forest. Ecology **56**:727–731.